13. NEUTRINO MASS, MIXING, AND OSCILLATIONS

Updated May 2012 by K. Nakamura (Kavli IPMU (WPI), U. Tokyo, KEK) and S.T. Petcov (SISSA/INFN Trieste, Kavli IPMU (WPI), U. Tokyo, Bulgarian Academy of Sciences).

The experiments with solar, atmospheric, reactor and accelerator neutrinos have provided compelling evidences for oscillations of neutrinos caused by nonzero neutrino masses and neutrino mixing. The data imply the existence of 3-neutrino mixing in vacuum. We review the theory of neutrino oscillations, the phenomenology of neutrino mixing, the problem of the nature - Dirac or Majorana, of massive neutrinos, the issue of CP violation in the lepton sector, and the current data on the neutrino masses and mixing parameters. The open questions and the main goals of future research in the field of neutrino mixing and oscillations are outlined.

13.1. Introduction: Massive neutrinos and neutrino mixing

It is a well-established experimental fact that the neutrinos and antineutrinos which take part in the standard charged current (CC) and neutral current (NC) weak interaction are of three varieties (types) or flavours: electron, ν_e and $\bar{\nu}_e$, muon, ν_μ and $\bar{\nu}_\mu$, and tauon, ν_τ and $\bar{\nu}_\tau$. The notion of neutrino type or flavour is dynamical: ν_e is the neutrino which is produced with e^+, or produces an e^- in CC weak interaction processes; ν_μ is the neutrino which is produced with μ^+, or produces μ^-, *etc.* The flavour of a given neutrino is Lorentz invariant. Among the three different flavour neutrinos and antineutrinos, no two are identical. Correspondingly, the states which describe different flavour neutrinos must be orthogonal (within the precision of the current data): $\langle \nu_{l'} | \nu_l \rangle = \delta_{l'l}$, $\langle \bar{\nu}_{l'} | \bar{\nu}_l \rangle = \delta_{l'l}$, $\langle \bar{\nu}_{l'} | \nu_l \rangle = 0$.

It is also well-known from the existing data (all neutrino experiments were done so far with relativistic neutrinos or antineutrinos), that the flavour neutrinos ν_l (antineutrinos $\bar{\nu}_l$), are always produced in weak interaction processes in a state that is predominantly left-handed (LH) (right-handed (RH)). To account for this fact, ν_l and $\bar{\nu}_l$ are described in the Standard Model (SM) by a chiral LH flavour neutrino field $\nu_{lL}(x)$, $l = e, \mu, \tau$. For massless ν_l, the state of ν_l ($\bar{\nu}_l$) which the field $\nu_{lL}(x)$ annihilates (creates) is with helicity (-1/2) (helicity +1/2). If ν_l has a non-zero mass $m(\nu_l)$, the state of ν_l ($\bar{\nu}_l$) is a linear superposition of the helicity (-1/2) and (+1/2) states, but the helicity +1/2 state (helicity (-1/2) state) enters into the superposition with a coefficient $\propto m(\nu_l)/E$, E being the neutrino energy, and thus is strongly suppressed. Together with the LH charged lepton field $l_L(x)$, $\nu_{lL}(x)$ forms an $SU(2)_L$ doublet. In the absence of neutrino mixing and zero neutrino masses, $\nu_{lL}(x)$ and $l_L(x)$ can be assigned one unit of the additive lepton charge L_l and the three charges L_l, $l = e, \mu, \tau$, are conserved by the weak interaction.

At present there is no compelling evidence for the existence of states of relativistic neutrinos (antineutrinos), which are predominantly right-handed, ν_R (left-handed, $\bar{\nu}_L$). If RH neutrinos and LH antineutrinos exist, their interaction with matter should be much weaker than the weak interaction of the flavour LH neutrinos ν_l and RH antineutrinos $\bar{\nu}_l$, *i.e.*, ν_R ($\bar{\nu}_L$) should be "sterile" or "inert" neutrinos (antineutrinos) [1]. In the formalism of the Standard Model, the sterile ν_R and $\bar{\nu}_L$ can be described by $SU(2)_L$ singlet RH neutrino fields $\nu_R(x)$. In this case, ν_R and $\bar{\nu}_L$ will have no gauge interactions,

i.e., will not couple to the weak $W^{\pm}$ and Z^0 bosons. If present in an extension of the Standard Model, the RH neutrinos can play a crucial role i) in the generation of neutrino masses and mixing, ii) in understanding the remarkable disparity between the magnitudes of neutrino masses and the masses of the charged leptons and quarks, and iii) in the generation of the observed matter-antimatter asymmetry of the Universe (via the leptogenesis mechanism [2]) . In this scenario which is based on the see-saw theory [3], there is a link between the generation of neutrino masses and the generation of the baryon asymmetry of the Universe. The simplest hypothesis (based on symmetry considerations) is that to each LH flavour neutrino field $\nu_{lL}(x)$ there corresponds a RH neutrino field $\nu_{lR}(x)$, $l = e, \mu, \tau$, although schemes with less (more) than three RH neutrinos are also being considered.

The experiments with solar, atmospheric and reactor neutrinos [4–16] have provided compelling evidences for the existence of neutrino oscillations [17,18], transitions in flight between the different flavour neutrinos ν_e, ν_μ, ν_τ (antineutrinos $\bar{\nu}_e$, $\bar{\nu}_\mu$, $\bar{\nu}_\tau$), caused by nonzero neutrino masses and neutrino mixing.

The existence of flavour neutrino oscillations implies that if a neutrino of a given flavour, say ν_μ, with energy E is produced in some weak interaction process, at a sufficiently large distance L from the ν_μ source the probability to find a neutrino of a different flavour, say ν_τ, $P(\nu_\mu \rightarrow \nu_\tau; E, L)$, is different from zero. $P(\nu_\mu \rightarrow \nu_\tau; E, L)$ is called the $\nu_\mu \rightarrow \nu_\tau$ oscillation or transition probability. If $P(\nu_\mu \rightarrow \nu_\tau; E, L) \neq 0$, the probability that ν_μ will not change into a neutrino of a different flavour, *i.e.*, the "ν_μ survival probability" $P(\nu_\mu \rightarrow \nu_\mu; E, L)$, will be smaller than one. If only muon neutrinos ν_μ are detected in a given experiment and they take part in oscillations, one would observe a "disappearance" of muon neutrinos on the way from the ν_μ source to the detector. Disappearance of the solar ν_e, reactor $\bar{\nu}_e$ and of atmospheric ν_μ and $\bar{\nu}_\mu$ due to the oscillations have been observed respectively, in the solar neutrino [4–12], KamLAND [15,16] and Super-Kamokande [13,14] experiments. Strong evidences for disappearance of muon neutrinos due to oscillations were obtained also in the long-baseline accelerator neutrino experiments K2K [19] and MINOS [20,21]. As a consequence of the results of the experiments quoted above the existence of oscillations or transitions of the solar ν_e, atmospheric ν_μ and $\bar{\nu}_\mu$, accelerator ν_μ (at $L \sim 250$ km and $L \sim 730$ km) and reactor $\bar{\nu}_e$ (at $L \sim 180$ km), driven by nonzero neutrino masses and neutrino mixing, was firmly established. There are strong indications that the solar ν_e transitions are affected by the solar matter [22,23]. In June of 2011, the T2K [24] Collaboration reported indication of $\nu_\mu \rightarrow \nu_e$ oscillations, *i.e.*, "appearance" of ν_e in a beam of ν_μ at a significance of 2.5σ. Also MINOS [25] Collaboration obtained data consistent with $\nu_\mu \rightarrow \nu_e$ oscillations. In March and April, 2012, the Daya Bay [26] and RENO [27] experiments reported strong evidence for reactor $\bar{\nu}_e$ disappearance respectively at $L \sim 1.65$ km and $L \sim 1.38$ km and with statistical significance of 5.2σ and 4.9σ.

Oscillations of neutrinos are a consequence of the presence of flavour neutrino mixing, or lepton mixing, in vacuum. In the formalism of local quantum field theory, used to construct the Standard Model, this means that the LH flavour neutrino fields $\nu_{lL}(x)$, which enter into the expression for the lepton current in the CC weak interaction Lagrangian, are linear combinations of the fields of three (or more) neutrinos ν_j, having

masses $m_j \neq 0$:

$$\nu_{l\mathrm{L}}(x) = \sum_j U_{lj}\, \nu_{j\mathrm{L}}(x), \quad l = e, \mu, \tau, \tag{13.1}$$

where $\nu_{j\mathrm{L}}(x)$ is the LH component of the field of ν_j possessing a mass m_j and U is a unitary matrix - the neutrino mixing matrix [1,17,18]. The matrix U is often called the Pontecorvo-Maki-Nakagawa-Sakata (PMNS) or Maki-Nakagawa-Sakata (MNS) mixing matrix. Obviously, Eq. (13.1) implies that the individual lepton charges L_l, $l = e, \mu, \tau$, are not conserved.

All existing neutrino oscillation data, except for the LSND [28] and the MiniBooNE [29] results (see below), can be described assuming 3-flavour neutrino mixing in vacuum. The data on the invisible decay width of the Z^0-boson is compatible with only 3 light flavour neutrinos coupled to Z^0 [30]. The number of massive neutrinos ν_j, n, can, in general, be bigger than 3, $n > 3$, if, for instance, there exist sterile neutrinos and they mix with the flavour neutrinos. It follows from the existing data that at least 3 of the neutrinos ν_j, say ν_1, ν_2, ν_3, must be light, $m_{1,2,3} \lesssim 1$ eV, and must have different masses, $m_1 \neq m_2 \neq m_3$.

The short-baseline accelerator experiment LSND [28] observed a possible indication of $\bar\nu_\mu \to \bar\nu_e$ oscillations. Performing a $\bar\nu_\mu \to \bar\nu_e$ oscillation search, the MiniBooNE Collaboration reported a 1.5σ excess of $\bar\nu_e$ events [29], which is marginally consistent with the LSND indication of $\bar\nu_\mu \to \bar\nu_e$ oscillations. However, in the MiniBooNE experiment no indications of $\nu_\mu \to \nu_e$ oscillations were found so far [31]. Interpreting the LSND [28] and the MiniBooNE [29,31] results in terms of neutrino oscillations requires the introduction of at least two more light neutrinos with masses in the 1 eV range [32], and thus of two sterile neutrino fields which mix with the ν_e and ν_μ fields. However, further experimental investigations are definitely needed since the excess of $\bar\nu_e$ events observed in the MiniBooNE experiment has a relatively low statistical significance.

Hints (at $\sim 2.5\sigma$) for existence of additional light neutrinos beyond the three firmly established were obtained in the re-analysis [33] of the old short baseline (SBL) reactor $\bar\nu_e$ oscillation data using the results of a new and very detailed calculation of the reactor $\bar\nu_e$ fluxes [34]. The latter were found in Ref. 34 to be by approximately 3% larger than the fluxes calculated in Ref. 35 and widely used in the interpretation of the results of the SBL reactor $\bar\nu_e$ oscillation experiments. It should be added that the results for the reactor $\bar\nu_e$ fluxes have an uncertainty associated, *e.g.*, with the weak magnetism term contribution to the corresponding β-decay rates, which can be larger than the 3% difference between the "old" and "new" fluxes [36].

On the basis of the preceding discussion we can conclude that at present there are no compelling experimental evidences for the existence of more than 3 light neutrinos.

Being electrically neutral, the neutrinos with definite mass ν_j can be Dirac fermions or Majorana particles [37,38]. The first possibility is realised when there exists a lepton charge carried by the neutrinos ν_j, which is conserved by the particle interactions. This could be, *e.g.*, the total lepton charge $L = L_e + L_\mu + L_\tau$: $L(\nu_j) = 1$, $j = 1, 2, 3$. In this case the neutrino ν_j has a distinctive antiparticle $\bar\nu_j$: $\bar\nu_j$ differs from ν_j by the value of the lepton charge L it carries, $L(\bar\nu_j) = -1$. The massive neutrinos ν_j can be Majorana particles if no lepton charge is conserved (see, *e.g.*, Ref. 39). A massive Majorana particle

χ_j is identical with its antiparticle $\bar{\chi}_j$: $\chi_j \equiv \bar{\chi}_j$. On the basis of the existing neutrino data it is impossible to determine whether the massive neutrinos are Dirac or Majorana fermions.

In the case of n neutrino flavours and n massive neutrinos, the $n \times n$ unitary neutrino mixing matrix U can be parametrised by $n(n-1)/2$ Euler angles and $n(n+1)/2$ phases. If the massive neutrinos ν_j are Dirac particles, only $(n-1)(n-2)/2$ phases are physical and can be responsible for CP violation in the lepton sector. In this respect the neutrino (lepton) mixing with Dirac massive neutrinos is similar to the quark mixing. For $n = 3$ there is just one CP violating phase in U, which is usually called "the Dirac CP violating phase." CP invariance holds if (in a certain standard convention) U is real, $U^* = U$.

If, however, the massive neutrinos are Majorana fermions, $\nu_j \equiv \chi_j$, the neutrino mixing matrix U contains $n(n-1)/2$ CP violation phases [40,41], *i.e.*, by $(n-1)$ phases more than in the Dirac neutrino case: in contrast to Dirac fields, the massive Majorana neutrino fields cannot "absorb" phases. In this case U can be cast in the form [40]

$$U = VP \tag{13.2}$$

where the matrix V contains the $(n-1)(n-2)/2$ Dirac CP violation phases, while P is a diagonal matrix with the additional $(n-1)$ Majorana CP violation phases α_{21}, α_{31},..., α_{n1},

$$P = diag\left(1, e^{i\frac{\alpha_{21}}{2}}, e^{i\frac{\alpha_{31}}{2}}, ..., e^{i\frac{\alpha_{n1}}{2}}\right). \tag{13.3}$$

The Majorana phases will conserve CP if [42] $\alpha_{j1} = \pi q_j$, $q_j = 0, 1, 2$, $j = 2, 3, ..., n$. In this case $\exp[i(\alpha_{j1} - \alpha_{k1})] = \pm 1$ has a simple physical interpretation: this is the relative CP-parity of Majorana neutrinos χ_j and χ_k. The condition of CP invariance of the leptonic CC weak interaction in the case of mixing and massive Majorana neutrinos reads [39]:

$$U_{lj}^* = U_{lj}\,\rho_j\,, \quad \rho_j = \frac{1}{i}\eta_{CP}(\chi_j) = \pm 1\,, \tag{13.4}$$

where $\eta_{CP}(\chi_j) = i\rho_j = \pm i$ is the CP parity of the Majorana neutrino χ_j [42]. Thus, if CP invariance holds, the elements of U are either real or purely imaginary.

In the case of $n = 3$ there are altogether 3 CP violation phases - one Dirac and two Majorana. Even in the mixing involving only 2 massive Majorana neutrinos there is one physical CP violation Majorana phase. In contrast, the CC weak interaction is automatically CP-invariant in the case of mixing of two massive Dirac neutrinos or of two quarks.

13.2. Neutrino oscillations in vacuum

Neutrino oscillations are a quantum mechanical consequence of the existence of nonzero neutrino masses and neutrino (lepton) mixing, Eq. (13.1), and of the relatively small splitting between the neutrino masses. The neutrino mixing and oscillation phenomena are analogous to the $K^0 - \bar{K}^0$ and $B^0 - \bar{B}^0$ mixing and oscillations.

In what follows we will present a simplified version of the derivation of the expressions for the neutrino and antineutrino oscillation probabilities. The complete derivation would require the use of the wave packet formalism for the evolution of the massive neutrino states, or, alternatively, of the field-theoretical approach, in which one takes into account the processes of production, propagation and detection of neutrinos [43].

Suppose the flavour neutrino ν_l is produced in a CC weak interaction process and after a time T it is observed by a neutrino detector, located at a distance L from the neutrino source and capable of detecting also neutrinos $\nu_{l'}$, $l' \neq l$. We will consider the evolution of the neutrino state $|\nu_l\rangle$ in the frame in which the detector is at rest (laboratory frame). The oscillation probability, as we will see, is a Lorentz invariant quantity. If lepton mixing, Eq. (13.1), takes place and the masses m_j of all neutrinos ν_j are sufficiently small, the state of the neutrino ν_l, $|\nu_l\rangle$, will be a coherent superposition of the states $|\nu_j\rangle$ of neutrinos ν_j:

$$|\nu_l\rangle = \sum_j U_{lj}^* |\nu_j; \tilde{p}_j\rangle, \quad l = e, \mu, \tau, \tag{13.5}$$

where U is the neutrino mixing matrix and $\tilde{p}_j$ is the 4-momentum of ν_j [44].

We will consider the case of relativistic neutrinos ν_j, which corresponds to the conditions in both past and currently planned future neutrino oscillation experiments [46]. In this case the state $|\nu_j; \tilde{p}_j\rangle$ practically coincides with the helicity (-1) state $|\nu_j, L; \tilde{p}_j\rangle$ of the neutrino ν_j, the admixture of the helicity (+1) state $|\nu_j, R; \tilde{p}_j\rangle$ in $|\nu_j; \tilde{p}_j\rangle$ being suppressed due to the factor $\sim m_j/E_j$, where E_j is the energy of ν_j. If ν_j are Majorana particles, $\nu_j \equiv \chi_j$, due to the presence of the helicity (+1) state $|\chi_j, R; \tilde{p}_j\rangle$ in $|\chi_j; \tilde{p}_j\rangle$, the neutrino ν_l can produce an l^+ (instead of l^-) when it interacts with nucleons. The cross section of such a $|\Delta L_l| = 2$ process is suppressed by the factor $(m_j/E_j)^2$, which renders the process unobservable at present.

If the number n of massive neutrinos ν_j is bigger than 3 due to a mixing between the active flavour and sterile neutrinos, one will have additional relations similar to that in Eq. (13.5) for the state vectors of the (predominantly LH) sterile antineutrinos. In the case of just one RH sterile neutrino field $\nu_{sR}(x)$, for instance, we will have in addition to Eq. (13.5):

$$|\bar{\nu}_{sL}\rangle = \sum_{j=1}^{4} U_{sj}^* |\nu_j; \tilde{p}_j\rangle \cong \sum_{j=1}^{4} U_{sj}^* |\nu_j, L; \tilde{p}_j\rangle, \tag{13.6}$$

where the neutrino mixing matrix U is now a 4×4 unitary matrix.

For the state vector of RH flavour antineutrino $\bar{\nu}_l$, produced in a CC weak interaction

process we similarly get:

$$|\bar{\nu}_l\rangle = \sum_j U_{lj} |\bar{\nu}_j; \tilde{p}_j\rangle \cong \sum_{j=1} U_{lj} |\bar{\nu}_j, R; \tilde{p}_j\rangle, \quad l = e, \mu, \tau, \tag{13.7}$$

where $|\bar{\nu}_j, R; \tilde{p}_j\rangle$ is the helicity $(+1)$ state of the antineutrino $\bar{\nu}_j$ if ν_j are Dirac fermions, or the helicity $(+1)$ state of the neutrino $\nu_j \equiv \bar{\nu}_j \equiv \chi_j$ if the massive neutrinos are Majorana particles. Thus, in the latter case we have in Eq. (13.7): $|\bar{\nu}_j; \tilde{p}_j\rangle \cong |\nu_j, R; \tilde{p}_j\rangle \equiv |\chi_j, R; \tilde{p}_j\rangle$. The presence of the matrix U in Eq. (13.7) (and not of U^*) follows directly from Eq. (13.1).

We will assume in what follows that the spectrum of masses of neutrinos is not degenerate: $m_j \neq m_k$, $j \neq k$. Then the states $|\nu_j; \tilde{p}_j\rangle$ in the linear superposition in the r.h.s. of Eq. (13.5) will have, in general, different energies and different momenta, independently of whether they are produced in a decay or interaction process: $\tilde{p}_j \neq \tilde{p}_k$, or $E_j \neq E_k$, $\mathbf{p}_j \neq \mathbf{p}_k$, $j \neq k$, where $E_j = \sqrt{p_j^2 + m_j^2}$, $p_j \equiv |\mathbf{p}_j|$. The deviations of E_j and p_j from the values for a massless neutrino E and $p = E$ are proportional to m_j^2/E_0, E_0 being a characteristic energy of the process, and are extremely small. In the case of $\pi^+ \rightarrow \mu^+ + \nu_\mu$ decay at rest, for instance, we have: $E_j = E + m_j^2/(2m_\pi)$, $p_j = E - \xi m_j^2/(2E)$, where $E = (m_\pi/2)(1 - m_\mu^2/m_\pi^2) \cong 30$ MeV, $\xi = (1 + m_\mu^2/m_\pi^2)/2 \cong 0.8$, and m_μ and m_π are the μ^+ and π^+ masses. Taking $m_j = 1$ eV we find: $E_j \cong E(1 + 1.2 \times 10^{-16})$ and $p_j \cong E(1 - 4.4 \times 10^{-16})$.

Suppose that the neutrinos are observed via a CC weak interaction process and that in the detector's rest frame they are detected after time T after emission, after traveling a distance L. Then the amplitude of the probability that neutrino $\nu_{l'}$ will be observed if neutrino ν_l was produced by the neutrino source can be written as [43,45,47]:

$$A(\nu_l \rightarrow \nu_{l'}) = \sum_j U_{l'j} D_j U^\dagger_{jl}, \quad l, l' = e, \mu, \tau, \tag{13.8}$$

where $D_j = D_j(p_j; L, T)$ describes the propagation of ν_j between the source and the detector, $U^\dagger_{jl}$ and $U_{l'j}$ are the amplitudes to find ν_j in the initial and in the final flavour neutrino state, respectively. It follows from relativistic Quantum Mechanics considerations that [43,45]

$$D_j \equiv D_j(\tilde{p}_j; L, T) = e^{-i\tilde{p}_j(x_f - x_0)} = e^{-i(E_j T - p_j L)}, \quad p_j \equiv |\mathbf{p}_j|, \tag{13.9}$$

where [48] x_0 and x_f are the space-time coordinates of the points of neutrino production and detection, $T = (t_f - t_0)$ and $L = \mathbf{k}(\mathbf{x}_f - \mathbf{x}_0)$, $\mathbf{k}$ being the unit vector in the direction of neutrino momentum, $\mathbf{p}_j = \mathbf{k}p_j$. What is relevant for the calculation of the probability $P(\nu_l \rightarrow \nu_{l'}) = |A(\nu_l \rightarrow \nu_{l'})|^2$ is the interference factor $D_j D_k^*$ which depends on the phase

$$\delta\varphi_{jk} = (E_j - E_k)T - (p_j - p_k)L = (E_j - E_k)\left[T - \frac{E_j + E_k}{p_j + p_k} L\right]$$

$$+ \frac{m_j^2 - m_k^2}{p_j + p_k} L. \tag{13.10}$$

Some authors [49] have suggested that the distance traveled by the neutrinos L and the time interval T are related by $T = (E_j + E_k) L/(p_j + p_k) = L/\bar{v}$, $\bar{v} = (E_j/(E_j + E_k))v_j + (E_k/(E_j + E_k))v_k$ being the "average" velocity of ν_j and ν_k, where $v_{j,k} = p_{j,k}/E_{j,k}$. In this case the first term in the r.h.s. of Eq. (13.10) vanishes. The indicated relation has not emerged so far from any dynamical wave packet calculations. We arrive at the same conclusion concerning the term under discussion in Eq. (13.10) if one assumes [50] that $E_j = E_k = E_0$. Finally, it was proposed in Ref. 47 and Ref. 51 that the states of ν_j and $\bar{\nu}_j$ in Eq. (13.5) and Eq. (13.7) have the same 3-momentum, $p_j = p_k = p$. Under this condition the first term in the r.h.s. of Eq. (13.10) is negligible, being suppressed by the additional factor $(m_j^2 + m_k^2)/p^2$ since for relativistic neutrinos $L = T$ up to terms $\sim m_{j,k}^2/p^2$. We arrive at the same conclusion if $E_j \neq E_k$, $p_j \neq p_k$, $j \neq k$, and we take into account that neutrinos are relativistic and therefore, up to corrections $\sim m_{j,k}^2/E_{j,k}^2$, we have $L \cong T$ (see, *e.g.*, C. Giunti quoted in Ref. 43).

Although the cases considered above are physically quite different, they lead to the same result for the phase difference $\delta\varphi_{jk}$. Thus, we have:

$$\delta\varphi_{jk} \cong \frac{m_j^2 - m_k^2}{2p} L = 2\pi \frac{L}{L_{jk}^v} \operatorname{sgn}(m_j^2 - m_k^2)\,, \qquad (13.11)$$

where $p = (p_j + p_k)/2$ and

$$L_{jk}^v = 4\pi \frac{p}{|\Delta m_{jk}^2|} \cong 2.48 \ \text{m} \ \frac{p[MeV]}{|\Delta m_{jk}^2|[eV^2]} \qquad (13.12)$$

is the neutrino oscillation length associated with Δm_{jk}^2. We can safely neglect the dependence of p_j and p_k on the masses m_j and m_k and consider p to be the zero neutrino mass momentum, $p = E$. The phase difference $\delta\varphi_{jk}$, Eq. (13.11), is Lorentz-invariant.

Eq. (13.9) corresponds to a plane-wave description of the propagation of neutrinos ν_j. It accounts only for the movement of the center of the wave packet describing ν_j. In the wave packet treatment of the problem, the interference between the states of ν_j and ν_k is subject to a number of conditions [43], the localisation condition and the condition of overlapping of the wave packets of ν_j and ν_k at the detection point being the most important. For relativistic neutrinos, the localisation condition in space, for instance, reads: $\sigma_{xP}, \sigma_{xD} < L_{jk}^v/(2\pi)$, $\sigma_{xP(D)}$ being the spatial width of the production (detection) wave packet. Thus, the interference will not be suppressed if the spatial width of the neutrino wave packets determined by the neutrino production and detection processes is smaller than the corresponding oscillation length in vacuum. In order for the interference to be nonzero, the wave packets describing ν_j and ν_k should also overlap in the point of neutrino detection. This requires that the spatial separation between the two wave packets at the point of neutrinos detection, caused by the two wave packets having different group velocities $v_j \neq v_k$, satisfies $|(v_j - v_k)T| \ll \max(\sigma_{xP}, \sigma_{xD})$. If the interval of time T is not measured, T in the preceding condition must be replaced by the

distance L between the neutrino source and the detector (for further discussion see, *e.g.*, Refs. [43,45,47]) .

For the $\nu_l \to \nu_{l'}$ and $\bar{\nu}_l \to \bar{\nu}_{l'}$ oscillation probabilities we get from Eq. (13.8), Eq. (13.9), and Eq. (13.11):

$$P(\nu_l \to \nu_{l'}) = \sum_j |U_{l'j}|^2 |U_{lj}|^2 + 2 \sum_{j>k} |U_{l'j} U_{lj}^* U_{lk} U_{l'k}^*|$$
$$\cos(\frac{\Delta m_{jk}^2}{2p} L - \phi_{l'l;jk})\,, \tag{13.13}$$

$$P(\bar{\nu}_l \to \bar{\nu}_{l'}) = \sum_j |U_{l'j}|^2 |U_{lj}|^2 + 2 \sum_{j>k} |U_{l'j} U_{lj}^* U_{lk} U_{l'k}^*|$$
$$\cos(\frac{\Delta m_{jk}^2}{2p} L + \phi_{l'l;jk})\,, \tag{13.14}$$

where $l, l' = e, \mu, \tau$ and $\phi_{l'l;jk} = \arg\left(U_{l'j} U_{lj}^* U_{lk} U_{l'k}^* \right)$. It follows from Eq. (13.8) - Eq. (13.10) that in order for neutrino oscillations to occur, at least two neutrinos ν_j should not be degenerate in mass and lepton mixing should take place, $U \neq \mathbf{1}$. The neutrino oscillations effects can be large if we have

$$\frac{|\Delta m_{jk}^2|}{2p} L = 2\pi \frac{L}{L_{jk}^v} \gtrsim 1\,, \quad j \neq k\,. \tag{13.15}$$

at least for one Δm_{jk}^2. This condition has a simple physical interpretation: the neutrino oscillation length L_{jk}^v should be of the order of, or smaller, than source-detector distance L, otherwise the oscillations will not have time to develop before neutrinos reach the detector.

We see from Eq. (13.13) and Eq. (13.14) that $P(\nu_l \to \nu_{l'}) = P(\bar{\nu}_{l'} \to \bar{\nu}_l)$, $l, l' = e, \mu, \tau$. This is a consequence of CPT invariance. The conditions of CP and T invariance read [40,52,53]: $P(\nu_l \to \nu_{l'}) = P(\bar{\nu}_l \to \bar{\nu}_{l'})$, $l, l' = e, \mu, \tau$ (CP), $P(\nu_l \to \nu_{l'}) = P(\nu_{l'} \to \nu_l)$, $P(\bar{\nu}_l \to \bar{\nu}_{l'}) = P(\bar{\nu}_{l'} \to \bar{\nu}_l)$, $l, l' = e, \mu, \tau$ (T). In the case of CPT invariance, which we will assume to hold throughout this article, we get for the survival probabilities: $P(\nu_l \to \nu_l) = P(\bar{\nu}_l \to \bar{\nu}_l)$, $l, l' = e, \mu, \tau$. Thus, the study of the "disappearance" of ν_l and $\bar{\nu}_l$, caused by oscillations in vacuum, cannot be used to test whether CP invariance holds in the lepton sector. It follows from Eq. (13.13) and Eq. (13.14) that we can have CP violation effects in neutrino oscillations only if $\phi_{l'l;jk} \neq \pi q$, $q = 0, 1, 2$, *i.e.*, if $U_{l'j} U_{lj}^* U_{lk} U_{l'k}^*$, and therefore U itself, is not real. As a measure of CP and T violation in neutrino oscillations we can consider the asymmetries:

$$A_{\rm CP}^{(l'l)} \equiv P(\nu_l \to \nu_{l'}) - P(\bar{\nu}_l \to \bar{\nu}_{l'})\,, \quad A_{\rm T}^{(l'l)} \equiv P(\nu_l \to \nu_{l'}) - P(\nu_{l'} \to \nu_l)\,. \tag{13.16}$$
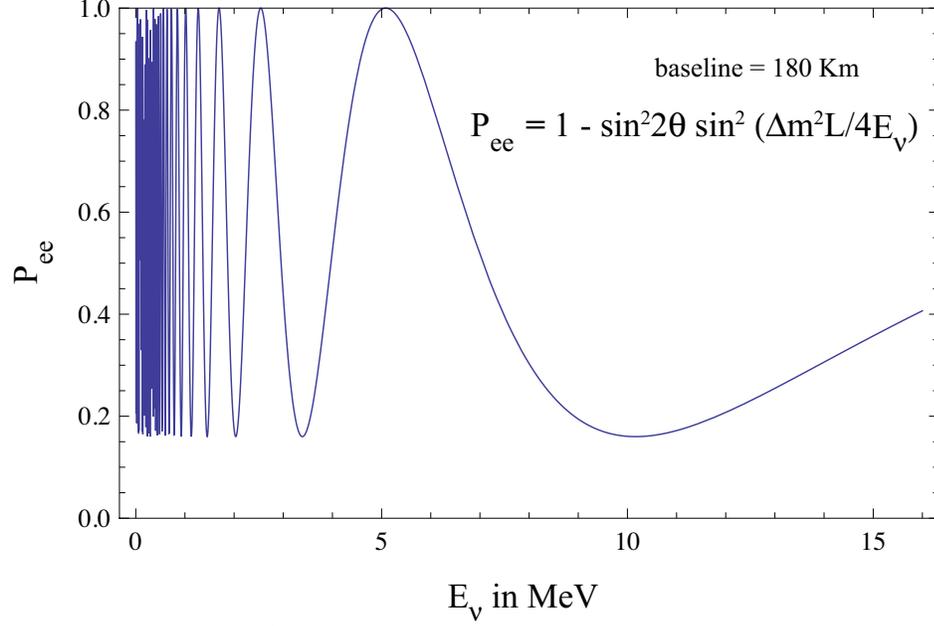
Figure 13.1: The ν_e ($\bar{\nu}_e$) survival probability $P(\nu_e \to \nu_e) = P(\bar{\nu}_e \to \bar{\nu}_e)$, Eq. (13.30), as a function of the neutrino energy for $L = 180$ km, $\Delta m^2 = 7.0 \times 10^{-5}$ eV^2 and $\sin^2 2\theta = 0.84$ (from Ref. 62).

CPT invariance implies: $A_{\rm CP}^{(l'l)} = -A_{\rm CP}^{(ll')}$, $A_{\rm T}^{(l'l)} = P(\bar{\nu}_{l'} \to \bar{\nu}_l) - P(\bar{\nu}_l \to \bar{\nu}_{l'}) = A_{\rm CP}^{(l'l)}$. It follows further directly from Eq. (13.13) and Eq. (13.14) that

$$A_{\rm CP}^{(l'l)} = 4 \sum_{j>k} {\rm Im}\left(U_{l'j}\, U_{lj}^*\, U_{lk}\, U_{l'k}^* \right) \sin \frac{\Delta m_{jk}^2}{2p} L\,, \quad l,l' = e,\mu,\tau\,. \tag{13.17}$$

Eq. (13.2) and Eq. (13.13) - Eq. (13.14) imply that $P(\nu_l \to \nu_{l'})$ and $P(\bar{\nu}_l \to \bar{\nu}_{l'})$ do not depend on the Majorana CP violation phases in the neutrino mixing matrix U [40]. Thus, the experiments investigating the $\nu_l \to \nu_{l'}$ and $\bar{\nu}_l \to \bar{\nu}_{l'}$ oscillations, $l,l' = e,\mu,\tau$, cannot provide information on the nature - Dirac or Majorana, of massive neutrinos. The same conclusions hold also when the $\nu_l \to \nu_{l'}$ and $\bar{\nu}_l \to \bar{\nu}_{l'}$ oscillations take place in matter [54]. In the case of $\nu_l \leftrightarrow \nu_{l'}$ and $\bar{\nu}_l \leftrightarrow \bar{\nu}_{l'}$ oscillations in vacuum, only the Dirac phase(s) in U can cause CP violating effects leading to $P(\nu_l \to \nu_{l'}) \neq P(\bar{\nu}_l \to \bar{\nu}_{l'})$, $l \neq l'$.

In the case of 3-neutrino mixing all different ${\rm Im}(U_{l'j}U_{lj}^*U_{lk}U_{l'k}^*) \neq 0$, $l' \neq l = e,\mu,\tau$, $j \neq k = 1,2,3$, coincide up to a sign as a consequence of the unitarity of U. Therefore one has [55]:

$$A_{\rm CP}^{(\mu e)} = -A_{\rm CP}^{(\tau e)} = A_{\rm CP}^{(\tau \mu)} =$$

$$4\, J_{\rm CP} \left(\sin \frac{\Delta m_{32}^2}{2p} L + \sin \frac{\Delta m_{21}^2}{2p} L + \sin \frac{\Delta m_{13}^2}{2p} L \right)\,, \tag{13.18}$$

where

$$J_{\rm CP} = {\rm Im}\left(U_{\mu 3}\, U_{e3}^*\, U_{e2}\, U_{\mu 2}^* \right)\,, \tag{13.19}$$

is the "rephasing invariant" associated with the Dirac CP violation phase in U. It is analogous to the rephasing invariant associated with the Dirac CP violating phase in the CKM quark mixing matrix [56]. It is clear from Eq. (13.18) that J_{CP} controls the magnitude of CP violation effects in neutrino oscillations in the case of 3-neutrino mixing. If $\sin(\Delta m_{ij}^2/(2p))L \cong 0$ for $(ij) = (32)$, or (21), or (13), we get $A_{CP}^{(l'l)} \cong 0$. Thus, if as a consequence of the production, propagation and/or detection of neutrinos, effectively oscillations due only to one non-zero neutrino mass squared difference take place, the CP violating effects will be strongly suppressed. In particular, we get $A_{CP}^{(l'l)} = 0$, unless all three $\Delta m_{ij}^2 \neq 0$, $(ij) = (32), (21), (13)$.

If the number of massive neutrinos n is equal to the number of neutrino flavours, $n = 3$, one has as a consequence of the unitarity of the neutrino mixing matrix: $\sum_{l'=e,\mu,\tau} P(\nu_l \to \nu_{l'}) = 1$, $l = e, \mu, \tau$, $\sum_{l=e,\mu,\tau} P(\nu_l \to \nu_{l'}) = 1$, $l' = e, \mu, \tau$. Similar "probability conservation" equations hold for $P(\bar{\nu}_l \to \bar{\nu}_{l'})$. If, however, the number of light massive neutrinos is bigger than the number of flavour neutrinos as a consequence, *e.g.*, of a flavour neutrino - sterile neutrino mixing, we would have $\sum_{l'=e,\mu,\tau} P(\nu_l \to \nu_{l'}) = 1 - P(\nu_l \to \bar{\nu}_{sL})$, $l = e, \mu, \tau$, where we have assumed the existence of just one sterile neutrino. Obviously, in this case $\sum_{l'=e,\mu,\tau} P(\nu_l \to \nu_{l'}) < 1$ if $P(\nu_l \to \bar{\nu}_{sL}) \neq 0$. The former inequality is used in the searches for oscillations between active and sterile neutrinos.

Consider next neutrino oscillations in the case of one neutrino mass squared difference "dominance": suppose that $|\Delta m_{j1}^2| \ll |\Delta m_{n1}^2|$, $j = 2, ..., (n-1)$, $|\Delta m_{n1}^2| L/(2p) \gtrsim 1$ and $|\Delta m_{j1}^2| L/(2p) \ll 1$, so that $\exp[i(\Delta m_{j1}^2 L/(2p)] \cong 1$, $j = 2, ..., (n-1)$. Under these conditions we obtain from Eq. (13.13) and Eq. (13.14), keeping only the oscillating terms involving Δm_{n1}^2:

$$P(\nu_{l(l')} \to \nu_{l'(l)}) \cong P(\bar{\nu}_{l(l')} \to \bar{\nu}_{l'(l)}) \cong \delta_{ll'} - 2|U_{ln}|^2 \left[\delta_{ll'} - |U_{l'n}|^2\right]$$

$$(1 - \cos \frac{\Delta m_{n1}^2}{2p} L). \tag{13.20}$$

It follows from the neutrino oscillation data (Sections 13.4 and 13.5) that in the case of 3-neutrino mixing, one of the two independent neutrino mass squared differences, say Δm_{21}^2, is much smaller in absolute value than the second one, Δm_{31}^2: $|\Delta m_{21}^2| \ll |\Delta m_{31}^2|$. The data imply:

$$|\Delta m_{21}^2| \cong 7.6 \times 10^{-5} \text{ eV}^2,$$
$$|\Delta m_{31}^2| \cong 2.4 \times 10^{-3} \text{ eV}^2,$$
$$|\Delta m_{21}^2|/|\Delta m_{31}^2| \cong 0.032. \tag{13.21}$$

Neglecting the effects due to Δm_{21}^2 we get from Eq. (13.20) by setting $n = 3$ and choosing, *e.g.*, i) $l = l' = e$ and ii) $l = e(\mu)$, $l' = \mu(e)$ [57]:

$$P(\nu_e \to \nu_e) = P(\bar{\nu}_e \to \bar{\nu}_e) \cong 1 - 2|U_{e3}|^2 \left(1 - |U_{e3}|^2\right) \left(1 - \cos \frac{\Delta m_{31}^2}{2p} L\right), \tag{13.22}$$

$$P(\nu_{\mu(e)} \to \nu_{e(\mu)}) \cong 2 |U_{\mu 3}|^2 |U_{e3}|^2 \left(1 - \cos \frac{\Delta m_{31}^2}{2p} L\right)$$

$$= \frac{|U_{\mu 3}|^2}{1 - |U_{e3}|^2} P^{2\nu} \left(|U_{e3}|^2, m_{31}^2\right), \tag{13.23}$$

Table 13.1: Sensitivity of different oscillation experiments.

Source	Type of ν	$\overline{E}$[MeV]	L[km]	$\min(\Delta m^2)$[eV^2]
Reactor	$\overline{\nu}_e$	~ 1	1	$\sim 10^{-3}$
Reactor	$\overline{\nu}_e$	~ 1	100	$\sim 10^{-5}$
Accelerator	$\nu_\mu, \overline{\nu}_\mu$	$\sim 10^3$	1	~ 1
Accelerator	$\nu_\mu, \overline{\nu}_\mu$	$\sim 10^3$	1000	$\sim 10^{-3}$
Atmospheric ν's	$\nu_{\mu,e}, \overline{\nu}_{\mu,e}$	$\sim 10^3$	10^4	$\sim 10^{-4}$
Sun	ν_e	~ 1	1.5×10^8	$\sim 10^{-11}$

and $P(\bar{\nu}_{\mu(e)} \to \bar{\nu}_{e(\mu)}) = P(\nu_{\mu(e)} \to \nu_{e(\mu)})$. Here $P^{2\nu}\left(|U_{e3}|^2, m_{31}^2\right)$ is the probability of the 2-neutrino transition $\nu_e \to (s_{23}\nu_\mu + c_{23}\nu_\tau)$ due to Δm_{31}^2 and a mixing with angle θ_{13}, where

$$\sin^2 \theta_{13} = |U_{e3}|^2, \ \ s_{23}^2 \equiv \sin^2 \theta_{23} = \frac{|U_{\mu 3}|^2}{1 - |U_{e3}|^2},$$

$$c_{23}^2 \equiv \cos^2 \theta_{23} = \frac{|U_{\tau 3}|^2}{1 - |U_{e3}|^2}. \tag{13.24}$$

Eq. (13.22) describes with a relatively high precision the oscillations of reactor $\bar{\nu}_e$ on a distance $L \sim 1$ km in the case of 3-neutrino mixing. It was used in the analysis of the data of the Chooz [58], Double Chooz [59], Daya Bay [26] and RENO [27] experiments. Eq. (13.20) with $n = 3$ and $l = l' = \mu$ describes with a relatively good precision the effects of oscillations of the accelerator ν_μ, seen in the K2K [19] and MINOS [20,21] experiments. The $\nu_\mu \to \nu_\tau$ oscillations, which the OPERA experiment [60,61] is aiming to detect, can be described by Eq. (13.20) with $n = 3$ and $l = \mu$, $l' = \tau$. Finally, the probability Eq. (13.23) describes with a good precision the $\nu_\mu \to \nu_e$ and $\bar{\nu}_\mu \to \bar{\nu}_e$ oscillations under the conditions of the K2K experiment.

In certain cases the dimensions of the neutrino source, ΔL, are not negligible in comparison with the oscillation length. Similarly, when analyzing neutrino oscillation data one has to include the energy resolution of the detector, ΔE, *etc.* in the analysis. As can be shown [39], if $2\pi\Delta L/L_{jk}^v \gg 1$, and/or $2\pi(L/L_{jk}^v)(\Delta E/E) \gg 1$, the oscillating terms in the neutrino oscillation probabilities will be strongly suppressed. In this case (as well as in the case of sufficiently large separation of the ν_j and ν_k wave packets at the

detection point) the interference terms in $P(\nu_l \to \nu_{l'})$ and $P(\bar{\nu}_{l'} \to \bar{\nu}_l)$ will be negligibly small and the neutrino flavour conversion will be determined by the average probabilities:

$$\bar{P}(\nu_l \to \nu_{l'}) = \bar{P}(\bar{\nu}_l \to \bar{\nu}_{l'}) \cong \sum_j |U_{l'j}|^2 \, |U_{lj}|^2 \,. \tag{13.25}$$

Suppose next that in the case of 3-neutrino mixing, $|\Delta m^2_{21}| \, L/(2p) \sim 1$, while at the same time $|\Delta m^2_{31(32)}| \, L/(2p) \gg 1$, and the oscillations due to Δm^2_{31} and Δm^2_{32} are strongly suppressed (averaged out) due to integration over the region of neutrino production, the energy resolution function, *etc.* In this case we get for the ν_e and $\bar{\nu}_e$ survival probabilities:

$$P(\nu_e \to \nu_e) = P(\bar{\nu}_e \to \bar{\nu}_e) \cong |U_{e3}|^4 + \left(1 - |U_{e3}|^2\right)^2 P^{2\nu}(\nu_e \to \nu_e)\,, \tag{13.26}$$

$$P^{2\nu}(\nu_e \to \nu_e) = P^{2\nu}(\bar{\nu}_e \to \bar{\nu}_e) \equiv P^{2\nu}_{ee}(\theta_{12}, \Delta m^2_{21})$$
$$= 1 - \frac{1}{2} \, \sin^2 2\theta_{12} \left(1 - \cos \frac{\Delta m^2_{21}}{2p} L\right) \tag{13.27}$$

being the ν_e and $\bar{\nu}_e$ survival probability in the case of 2-neutrino oscillations "driven" by the angle θ_{12} and Δm^2_{21}, with θ_{12} determined by

$$\cos^2 \theta_{12} = \frac{|U_{e1}|^2}{1 - |U_{e3}|^2}\,, \quad \sin^2 \theta_{12} = \frac{|U_{e2}|^2}{1 - |U_{e3}|^2}\,. \tag{13.28}$$

Eq. (13.26) with $P^{2\nu}(\bar{\nu}_e \to \bar{\nu}_e)$ given by Eq. (13.27) describes the effects of neutrino oscillations of reactor $\bar{\nu}_e$ observed by the KamLAND experiment.

In the case of 3-neutrino mixing with $0 < \Delta m^2_{21} < |\Delta m^2_{31(32)}|$ and $|U_{e3}|^2 = |\sin \theta_{13}|^2 \ll 1$ (see Section 13.6), one can identify Δm^2_{21} and θ_{12} as the neutrino mass squared difference and mixing angle responsible for the solar ν_e oscillations, and Δm^2_{31} and θ_{23} as those associated with the dominant atmospheric ν_μ and $\bar{\nu}_\mu$ oscillations. Thus, θ_{12} and θ_{23} are often called "solar" and "atmospheric" neutrino mixing angles and denoted as $\theta_{12} = \theta_\odot$ and $\theta_{23} = \theta_A$ (or θ_{atm}), while Δm^2_{21} and Δm^2_{31} are often referred to as the "solar" and "atmospheric" neutrino mass squared differences and denoted as $\Delta m^2_{21} \equiv \Delta m^2_\odot$ and $\Delta m^2_{31} \equiv \Delta m^2_A$ (or Δm^2_{atm}).

The data of ν-oscillations experiments is often analyzed assuming 2-neutrino mixing:

$$|\nu_l\rangle = |\nu_1\rangle \cos \theta + |\nu_2\rangle \sin \theta\,, \quad |\nu_x\rangle = -|\nu_1\rangle \sin \theta + |\nu_2\rangle \cos \theta\,, \tag{13.29}$$

where θ is the neutrino mixing angle in vacuum and ν_x is another flavour neutrino or sterile (anti-) neutrino, $x = l' \neq l$ or $\nu_x \equiv \bar{\nu}_{sL}$. In this case we have [51]:

$$P^{2\nu}(\nu_l \to \nu_l) = 1 - \frac{1}{2} \sin^2 2\theta \left(1 - \cos 2\pi \frac{L}{L^\nu}\right)\,,$$
$$P^{2\nu}(\nu_l \to \nu_x) = 1 - P^{2\nu}(\nu_l \to \nu_l)\,, \tag{13.30}$$

where $L^v = 4\pi p/\Delta m^2$, $\Delta m^2 = m_2^2 - m_1^2 > 0$. Combining the CPT invariance constraints with the probability conservation one obtains: $P(\nu_l \to \nu_x) = P(\bar{\nu}_l \to \bar{\nu}_x) = P(\nu_x \to \nu_l) = P(\bar{\nu}_x \to \bar{\nu}_l)$. These equalities and Eq. (13.30) with $l = \mu$ and $x = \tau$ were used, for instance, in the analysis of the Super-K atmospheric neutrino data [13], in which the first compelling evidence for oscillations of neutrinos was obtained. The probability $P^{2\nu}(\nu_l \to \nu_x)$, Eq. (13.30), depends on two factors: on $(1 - \cos 2\pi L/L^v)$, which exhibits oscillatory dependence on the distance L and on the neutrino energy $p = E$ (hence the name "neutrino oscillations"), and on $\sin^2 2\theta$, which determines the amplitude of the oscillations. In order to have $P^{2\nu}(\nu_l \to \nu_x) \cong 1$, two conditions have to be fulfilled: one should have $\sin^2 2\theta \cong 1$ and $L^v \lesssim 2\pi L$ with $\cos 2\pi L/L^v \cong -1$. If $L^v \gg 2\pi L$, the oscillations do not have enough time to develop on the way to the neutrino detector and $P(\nu_l \to \nu_x) \cong 0$. This is illustrated in Fig. 1 showing the dependence of the probability $P^{2\nu}(\nu_e \to \nu_e) = P^{2\nu}(\bar{\nu}_e \to \bar{\nu}_e)$ on the neutrino energy.

A given experiment searching for neutrino oscillations is specified, in particular, by the average energy of the neutrinos being studied, $\bar{E}$, and by the source-detector distance L. The requirement $L_{jk}^v \lesssim 2\pi L$ determines the minimal value of a generic neutrino mass squared difference $\Delta m^2 > 0$, to which the experiment is sensitive (figure of merit of the experiment): $\min(\Delta m^2) \sim 2\bar{E}/L$. Because of the interference nature of neutrino oscillations, experiments can probe, in general, rather small values of Δm^2 (see, *e.g.*, Ref. 47). Values of $\min(\Delta m^2)$, characterizing qualitatively the sensitivity of different experiments are given in Table 1. They correspond to the reactor experiments Chooz ($L \sim 1$ km) and KamLAND ($L \sim 100$ km), to accelerator experiments - past ($L \sim 1$ km), recent, current and future (K2K, MINOS, OPERA, T2K, NOνA [63]) , $L \sim (300 \div 1000)$ km), to the Super-Kamiokande experiment studying atmospheric neutrino oscillations, and to the solar neutrino experiments.

13.3.   Matter effects in neutrino oscillations

The presence of matter can change drastically the pattern of neutrino oscillations: neutrinos can interact with the particles forming the matter. Accordingly, the Hamiltonian of the neutrino system in matter H_m, differs from the Hamiltonian in vacuum H_0, $H_m = H_0 + H_{int}$, where H_{int} describes the interaction of neutrinos with the particles of matter. When, for instance, ν_e and ν_μ propagate in matter, they can scatter (due to H_{int}) on the electrons (e$^-$), protons (p) and neutrons (n) present in matter. The incoherent elastic and the quasi-elastic scattering, in which the states of the initial particles change in the process (destroying the coherence between the neutrino states), are not of interest - they have a negligible effect on the solar neutrino propagation in the Sun and on the solar, atmospheric and reactor neutrino propagation in the Earth [64]: even in the center of the Sun, where the matter density is relatively high (~ 150 g/cm^3), a ν_e with energy of 1 MeV has a mean free path with respect to the indicated scattering processes $\sim 10^{10}$ km. We recall that the solar radius is much smaller: R$_\odot = 6.96 \times 10^5$ km. The oscillating ν_e and ν_μ can scatter also elastically in the forward direction on the e$^-$, p and n, with the momenta and the spin states of the particles remaining unchanged. In such a process the coherence of the neutrino states is preserved.

The ν_e and ν_μ coherent elastic scattering on the particles of matter generates nontrivial indices of refraction of the ν_e and ν_μ in matter [22]: $\kappa(\nu_e) \neq 1$, $\kappa(\nu_\mu) \neq 1$. Most importantly, we have $\kappa(\nu_e) \neq \kappa(\nu_\mu)$. The difference $\kappa(\nu_e) - \kappa(\nu_\mu)$ is determined essentially by the difference of the real parts of the forward $\nu_e - e^-$ and $\nu_\mu - e^-$ elastic scattering amplitudes [22] Re $[\mathrm{F}_{\nu_e - e^-}(0)] -$ Re $[\mathrm{F}_{\nu_\mu - e^-}(0)]$: due to the flavour symmetry of the neutrino – quark (neutrino – nucleon) neutral current interaction, the forward $\nu_e - p, n$ and $\nu_\mu - p, n$ elastic scattering amplitudes are equal and therefore do not contribute to the difference of interest [65]. The imaginary parts of the forward scattering amplitudes (responsible, in particular, for decoherence effects) are proportional to the corresponding total scattering cross-sections and in the case of interest are negligible in comparison with the real parts. The real parts of the amplitudes $\mathrm{F}_{\nu_e - e^-}(0)$ and $\mathrm{F}_{\nu_\mu - e^-}(0)$ can be calculated in the Standard Model. To leading order in the Fermi constant G_F, only the term in $\mathrm{F}_{\nu_e - e^-}(0)$ due to the diagram with exchange of a virtual $W^\pm$-boson contributes to $\mathrm{F}_{\nu_e - e^-}(0) - \mathrm{F}_{\nu_\mu - e^-}(0)$. One finds the following result for $\kappa(\nu_e) - \kappa(\nu_\mu)$ in the rest frame of the scatters [22,67,68]:

$$\kappa(\nu_e) - \kappa(\nu_\mu) = \frac{2\pi}{p^2} \left(\mathrm{Re} \ [\mathrm{F}_{\nu_e - e^-}(0)] - \mathrm{Re} \ [\mathrm{F}_{\nu_\mu - e^-}(0)] \right)$$

$$= -\frac{1}{p}\sqrt{2}G_F N_e \ , \tag{13.31}$$

where N_e is the electron number density in matter. Given $\kappa(\nu_e) - \kappa(\nu_\mu)$, the system of evolution equations describing the $\nu_e \leftrightarrow \nu_\mu$ oscillations in matter reads [22]:

$$i\frac{d}{dt}\begin{pmatrix} A_e(t, t_0) \\ A_\mu(t, t_0) \end{pmatrix} = \begin{pmatrix} -\epsilon(t) & \epsilon' \\ \epsilon' & \epsilon(t) \end{pmatrix} \begin{pmatrix} A_e(t, t_0) \\ A_\mu(t, t_0) \end{pmatrix} \tag{13.32}$$

where $A_e(t, t_0)$ $(A_\mu(t, t_0))$ is the amplitude of the probability to find ν_e (ν_μ) at time t of the evolution of the system if at time $t_0 \leq t$ the neutrino ν_e or ν_μ has been produced and

$$\epsilon(t) = \frac{1}{2} \ [\frac{\Delta m^2}{2E}\cos 2\theta - \sqrt{2}G_F N_e(t)], \ \ \epsilon' = \frac{\Delta m^2}{4E}\sin 2\theta. \tag{13.33}$$

The term $\sqrt{2}G_F N_e(t)$ in $\epsilon(t)$ accounts for the effects of matter on neutrino oscillations. The system of evolution equations describing the oscillations of antineutrinos $\bar{\nu}_e \leftrightarrow \bar{\nu}_\mu$ in matter has exactly the same form except for the matter term in $\epsilon(t)$ which changes sign. The effect of matter in neutrino oscillations is usually called the Mikheyev, Smirnov, Wolfenstein (or MSW) effect.

Consider first the case of $\nu_e \leftrightarrow \nu_\mu$ oscillations in matter with constant density: $N_e(t) = N_e = $ const. Due to the interaction term H_{int} in H_m, the eigenstates of the Hamiltonian of the neutrino system in vacuum, $|\nu_{1,2}\rangle$ are not eigenstates of H_m. For the eigenstates $|\nu_{1,2}^m\rangle$ of H_m, which diagonalize the evolution matrix in the r.h.s. of the system Eq. (13.32) we have:

$$|\nu_e\rangle = |\nu_1^m\rangle \cos\theta_m + |\nu_2^m\rangle \sin\theta_m \ , \ \ \ |\nu_\mu\rangle = -|\nu_1^m\rangle \sin\theta_m + |\nu_2^m\rangle \cos\theta_m \ . \tag{13.34}$$

Here θ_m is the neutrino mixing angle in matter [22],

$$\sin 2\theta_m = \frac{\tan 2\theta}{\sqrt{(1 - \frac{N_e}{N_e^{res}})^2 + \tan^2 2\theta}}, \quad \cos 2\theta_m = \frac{1 - N_e/N_e^{res}}{\sqrt{(1 - \frac{N_e}{N_e^{res}})^2 + \tan^2 2\theta}}, \quad (13.35)$$

where the quantity

$$N_e^{res} = \frac{\Delta m^2 \cos 2\theta}{2E\sqrt{2}G_F} \cong 6.56 \times 10^6 \frac{\Delta m^2[\text{eV}^2]}{E[\text{MeV}]} \cos 2\theta \, \text{cm}^{-3} \, \text{N}_\text{A} \,, \quad (13.36)$$

is called (for $\Delta m^2 \cos 2\theta > 0$) "resonance density" [23,67], N_A being Avogadro's number. The "adiabatic" states $|\nu_{1,2}^m\rangle$ have energies $E_{1,2}^m$ whose difference is given by

$$E_2^m - E_1^m = \frac{\Delta m^2}{2E} \left((1 - \frac{N_e}{N_e^{res}})^2 \cos^2 2\theta + \sin^2 2\theta\right)^{\frac{1}{2}} \equiv \frac{\Delta M^2}{2E} \,. \quad (13.37)$$

The probability of $\nu_e \to \nu_\mu$ transition in matter with $N_e = const.$ has the form [22,67]

$$P_m^{2\nu}(\nu_e \to \nu_\mu) = |A_\mu(t)|^2 = \frac{1}{2} \sin^2 2\theta_m \, [1 - \cos 2\pi \frac{L}{L_m}]$$

$$L_m = 2\pi/(E_2^m - E_1^m) \,, \quad (13.38)$$

where L_m is the oscillation length in matter. As Eq. (13.35) indicates, the dependence of $\sin^2 2\theta_m$ on N_e has a resonance character [23]. Indeed, if $\Delta m^2 \cos 2\theta > 0$, for any $\sin^2 2\theta \neq 0$ there exists a value of N_e given by N_e^{res}, such that when $N_e = N_e^{res}$ we have $\sin^2 2\theta_m = 1$ independently of the value of $\sin^2 2\theta < 1$. This implies that the presence of matter can lead to a strong enhancement of the oscillation probability $P_m^{2\nu}(\nu_e \to \nu_\mu)$ even when the $\nu_e \leftrightarrow \nu_\mu$ oscillations in vacuum are suppressed due to a small value of $\sin^2 2\theta$. For obvious reasons

$$N_e = N_e^{res} \equiv \frac{\Delta m^2 \cos 2\theta}{2E\sqrt{2}G_F} \,, \quad (13.39)$$

is called the "resonance condition" [23,67], while the energy at which Eq. (13.39) holds for given N_e and $\Delta m^2 \cos 2\theta$, is referred to as the "resonance energy", E^{res}. The oscillation length at resonance is given by [23] $L_m^{res} = L^v/\sin 2\theta$, while the width in N_e of the resonance at half height reads $\Delta N_e^{res} = 2N_e^{res} \tan 2\theta$. Thus, if the mixing angle in vacuum is small, the resonance is narrow, $\Delta N_e^{res} \ll N_e^{res}$, and $L_m^{res} \gg L^v$. The energy difference $E_2^m - E_1^m$ has a minimum at the resonance: $(E_2^m - E_1^m)^{res} = \min \, (E_2^m - E_1^m) = (\Delta m^2/(2E)) \sin 2\theta$.

It is instructive to consider two limiting cases. If $N_e \ll N_e^{res}$, we have from Eq. (13.35) and Eq. (13.37), $\theta_m \cong \theta$, $\text{L}_\text{m} \cong \text{L}^\text{v}$ and neutrinos oscillate practically as in vacuum. In the limit $N_e \gg N_e^{res}$, $N_e^{res} \tan^2 2\theta$, one finds $\theta_m \cong \pi/2$ ($\cos 2\theta_m \cong -1$) and the presence of matter suppresses the $\nu_e \leftrightarrow \nu_\mu$ oscillations. In this case $|\nu_e\rangle \cong |\nu_2^m\rangle$, $|\nu_\mu\rangle = -|\nu_1^m\rangle$,

i.e., ν_e practically coincides with the heavier matter-eigenstate, while ν_μ coincides with the lighter one.

Since the neutral current weak interaction of neutrinos in the Standard Model is flavour symmetric, the formulae and results we have obtained are valid for the case of $\nu_e - \nu_\tau$ mixing and $\nu_e \leftrightarrow \nu_\tau$ oscillations in matter as well. The case of $\nu_\mu - \nu_\tau$ mixing, however, is different: to a relatively good precision we have [69] $\kappa(\nu_\mu) \cong \kappa(\nu_\tau)$ and the $\nu_\mu \leftrightarrow \nu_\tau$ oscillations in the matter of the Earth and the Sun proceed practically as in vacuum [70].

The analogs of Eq. (13.35) to Eq. (13.38) for oscillations of antineutrinos, $\bar{\nu}_e \leftrightarrow \bar{\nu}_\mu$, in matter can formally be obtained by replacing N_e with $(-N_e)$ in the indicated equations. It should be clear that depending on the sign of $\Delta m^2 \cos 2\theta$, the presence of matter can lead to resonance enhancement either of the $\nu_e \leftrightarrow \nu_\mu$ or of the $\bar{\nu}_e \leftrightarrow \bar{\nu}_\mu$ oscillations, but not of both types of oscillations [67]. For $\Delta m^2 \cos 2\theta < 0$, for instance, the matter can only suppress the $\nu_e \to \nu_\mu$ oscillations, while it can enhance the $\bar{\nu}_e \to \bar{\nu}_\mu$ transitions. This disparity between the behavior of neutrinos and that of antineutrinos is a consequence of the fact that the matter in the Sun or in the Earth we are interested in is not charge-symmetric (it contains e^-, p and n, but does not contain their antiparticles) and therefore the oscillations in matter are neither CP- nor CPT-invariant [54]. Thus, even in the case of 2-neutrino mixing and oscillations we have, *e.g.*, $P_m^{2\nu}(\nu_e \to \nu_{\mu(\tau)}) \neq P_m^{2\nu}(\bar{\nu}_e \to \bar{\nu}_{\mu(\tau)})$.

The matter effects in the $\nu_e \leftrightarrow \nu_{\mu(\tau)}$ $(\bar{\nu}_e \leftrightarrow \bar{\nu}_{\mu(\tau)})$ oscillations will be invariant with respect to the operation of time reversal if the N_e distribution along the neutrino path is symmetric with respect to this operation [55,71]. The latter condition is fulfilled (to a good approximation) for the N_e distribution along a path of a neutrino crossing the Earth [72].

13.3.1. *Effects of Earth matter on oscillations of neutrinos* :

The formalism we have developed can be applied, *e.g.*, to the study of matter effects in the $\nu_e \leftrightarrow \nu_{\mu(\tau)}$ $(\nu_{\mu(\tau)} \leftrightarrow \nu_e)$ and $\bar{\nu}_e \leftrightarrow \bar{\nu}_{\mu(\tau)}$ $(\bar{\nu}_{\mu(\tau)} \leftrightarrow \bar{\nu}_e)$ oscillations of neutrinos which traverse the Earth [73]. Indeed, the Earth density distribution in the existing Earth models [72] is assumed to be spherically symmetric and there are two major density structures - the core and the mantle, and a certain number of substructures (shells or layers). The Earth radius is $R_\oplus = 6371$ km; the Earth core has a radius of $R_c = 3486$ km, so the Earth mantle depth is 2885 km. For a spherically symmetric Earth density distribution, the neutrino trajectory in the Earth is specified by the value of the nadir angle θ_n of the trajectory. For $\theta_n \leq 33.17^o$, or path lengths $L \geq 10660$ km, neutrinos cross the Earth core. The path length for neutrinos which cross only the Earth mantle is given by $L = 2R_\oplus \cos \theta_n$. If neutrinos cross the Earth core, the lengths of the paths in the mantle, $2L^{\mathrm{man}}$, and in the core, L^{core}, are determined by: $L^{\mathrm{man}} = R_\oplus \cos \theta_n - (R_c^2 - R_\oplus^2 \sin^2 \theta_n)^{\frac{1}{2}}$, $L^{\mathrm{core}} = 2(R_c^2 - R_\oplus^2 \sin^2 \theta_n)^{\frac{1}{2}}$. The mean electron number densities in the mantle and in the core according to the PREM model read [72]: $\bar{N}_e^{man} \cong 2.2$ cm^{-3} N$_A$, $\bar{N}_e^c \cong 5.4$ cm^{-3} N$_A$. Thus, we have $\bar{N}_e^c \cong 2.5$ $\bar{N}_e^{man}$. The change of N_e from the mantle to the core can well be approximated by a step function [72]. The electron number density N_e changes relatively little around the

indicated mean values along the trajectories of neutrinos which cross a substantial part of the Earth mantle, or the mantle and the core, and the two-layer constant density approximation, $N_e^{man} = const. = \tilde{N}_e^{man}$, $N_e^c = const. = \tilde{N}_e^c$, $\tilde{N}_e^{man}$ and $\tilde{N}_e^c$ being the mean densities along the given neutrino path in the Earth, was shown to be sufficiently accurate in what concerns the calculation of neutrino oscillation probabilities [55,75,76] (and references quoted in [75,76]) in a large number of specific cases. This is related to the fact that the relatively small changes of density along the path of the neutrinos in the mantle (or in the core) take place over path lengths which are typically considerably smaller than the corresponding oscillation length in matter.

In the case of 3-neutrino mixing and for neutrino energies of $E \gtrsim 2$ GeV, the effects due to Δm_{21}^2 ($|\Delta m_{21}^2| \ll |\Delta m_{31}^2|$, see Eq. (13.21)) in the neutrino oscillation probabilities are sub-dominant and to leading order can be neglected: the corresponding resonance density $|N_{e21}^{res}| \lesssim 0.25 \ cm^{-3} \ N_A \ll \bar{N}_e^{man,c}$ and the Earth matter strongly suppresses the oscillations due to Δm_{21}^2. For oscillations in vacuum this approximation is valid as long as the leading order contribution due to Δm_{31}^2 in the relevant probabilities is bigger than approximately 10^{-3}. In this case the 3-neutrino $\nu_e \rightarrow \nu_{\mu(\tau)}$ ($\bar{\nu}_e \rightarrow \bar{\nu}_{\mu(\tau)}$) and $\nu_{\mu(\tau)} \rightarrow \nu_e$ ($\bar{\nu}_{\mu(\tau)} \rightarrow \bar{\nu}_e$) transition probabilities for neutrinos traversing the Earth, reduce effectively to a 2-neutrino transition probability (see, *e.g.*, Refs. [76–78]) , with Δm_{31}^2 and θ_{13} playing the role of the relevant 2-neutrino vacuum oscillation parameters. As will be discussed in Sections 13.6 and 13.7, the value of $\sin^2 2\theta_{13}$ has been determined recently with a rather high precision in the Daya Bay [26] and RENO [27] experiments. The best fit values found in the two experiments read, respectively, $\sin^2 2\theta_{13} = 0.092$ and 0.113, while the 3σ allowed range reported in [26] is $0.04 \lesssim \sin^2 2\theta_{13} \lesssim 0.14$. The 3-neutrino oscillation probabilities of the atmospheric and accelerator $\nu_{e,\mu}$ having energy E and crossing the Earth along a trajectory characterized by a nadir angle θ_n, for instance, have the following form:

$$P_m^{3\nu}(\nu_e \rightarrow \nu_e) \cong 1 - P_m^{2\nu}, \tag{13.40}$$

$$P_m^{3\nu}(\nu_e \rightarrow \nu_\mu) \cong P_m^{3\nu}(\nu_\mu \rightarrow \nu_e) \cong s_{23}^2 \ P_m^{2\nu}, \qquad P_m^{3\nu}(\nu_e \rightarrow \nu_\tau) \cong c_{23}^2 \ P_m^{2\nu}, \tag{13.41}$$

$$P_m^{3\nu}(\nu_\mu \rightarrow \nu_\mu) \cong 1 - s_{23}^4 \ P_m^{2\nu} - 2c_{23}^2 s_{23}^2 \ \left[1 - Re \ (e^{-i\kappa} A_m^{2\nu}(\nu' \rightarrow \nu'))\right], \tag{13.42}$$

$$P_m^{3\nu}(\nu_\mu \rightarrow \nu_\tau) = 1 - P_m^{3\nu}(\nu_\mu \rightarrow \nu_\mu) - P_m^{3\nu}(\nu_\mu \rightarrow \nu_e). \tag{13.43}$$

Here $P_m^{2\nu} \equiv P_m^{2\nu}(\Delta m_{31}^2, \theta_{13}; E, \theta_n)$ is the probability of the 2-neutrino $\nu_e \rightarrow \nu' \equiv (s_{23}\nu_\mu + c_{23}\nu_\tau)$ oscillations in the Earth, and κ and $A_m^{2\nu}(\nu' \rightarrow \nu') \equiv A_m^{2\nu}$ are known phase and 2-neutrino transition probability amplitude (see, *e.g.*, Refs. [76,77]). We note that Eq. (13.40) to Eq. (13.42) are based only on the assumptions that $|N_{e21}^{res}|$ is much smaller than the densities in the Earth mantle and core and that $|\Delta m_{21}^2| \ll |\Delta m_{31}^2|$, and does not rely on the constant density approximation. Similar results are valid for the corresponding antineutrino oscillation probabilities: one has just to replace $P_m^{2\nu}$, κ and $A_m^{2\nu}$ in the expressions given above with the corresponding quantities for antineutrinos (the latter are obtained from those for neutrinos by changing the sign in front of N_e). Obviously, we have: $P(\nu_{e(\mu)} \rightarrow \nu_{\mu(e)}), P(\bar{\nu}_{e(\mu)} \rightarrow \bar{\nu}_{\mu(e)}) \leq \sin^2 \theta_{23}$, and $P(\nu_e \rightarrow \nu_\tau), P(\bar{\nu}_e \rightarrow \bar{\nu}_\tau) \leq \cos^2 \theta_{23}$. The one Δm^2 dominance approximation and correspondingly Eq. (13.40) to Eq. (13.43)

were used by the Super-Kamiokande Collaboration in their 2006 neutrino oscillation analysis of the multi-GeV atmospheric neutrino data [79].

In the case of neutrinos crossing only the Earth mantle and in the constant density approximation, $P_m^{2\nu}$ is given by the r.h.s. of Eq. (13.38) with θ and Δm^2 replaced by θ_{13} and Δm_{31}^2, while for κ and $A_m^{2\nu}$ we have (see, *e.g.*, Ref. 76):

$$\kappa \cong \frac{1}{2}[\frac{\Delta m_{31}^2}{2E}\ L + \sqrt{2}G_F \bar{N}_e^{man}L - \frac{\Delta M^2 L}{2E}],$$

$$A_m^{2\nu} = 1 + (e^{-i\frac{\Delta M^2 L}{2E}} - 1)\cos^2\theta_m' \ , \tag{13.44}$$

where ΔM^2 is defined in Eq. (13.37) (with $\theta = \theta_{13}$ and $\Delta m^2 = \Delta m_{31}^2$), θ_m' is the mixing angle in the mantle which coincides in vacuum with θ_{13} (Eq. (13.35) with $N_e = \bar{N}_e^{man}$ and $\theta = \theta_{13}$), and $L = 2R_\oplus \cos\theta_n$ is the distance the neutrino travels in the mantle.

It follows from Eq. (13.40) and Eq. (13.41) that for $\Delta m_{31}^2 \cos 2\theta_{13} > 0$, the oscillation effects of interest, *e.g.*, in the $\nu_{e(\mu)} \to \nu_{\mu(e)}$ and $\nu_e \to \nu_\tau$ transitions will be maximal if $P_m^{2\nu} \cong 1$, *i.e.*, if Eq. (13.39) leading to $\sin^2 2\theta_m \cong 1$ is fulfilled, and ii) $\cos(\Delta M^2 L/(2E)) \cong -1$. Given the value of $\bar{N}_e^{man}$, the first condition determines the neutrino's energy, while the second determines the path length L, for which one can have $P_m^{2\nu} \cong 1$. For $\Delta m_{31}^2 \cong 2.4 \times 10^{-3}$ eV^2, $\sin^2 2\theta_{13} \lesssim 0.14$ and $\bar{N}_e^{man} \cong 2.2$ N$_A$cm^{-3}, one finds that $E_{res} \cong 7.2$ GeV and $L \cong 2370/\sin 2\theta_{13}$ km $\gtrsim 6267.3$ km. Since for neutrinos crossing only the mantle $L \lesssim 10660$ km, the second condition can be satisfied only if $\sin\theta_{13} \gtrsim 0.11$, which falls in the range of the experimentally allowed values of $\sin\theta_{13}$. Thus, for $\Delta m_{31}^2 > 0$, the Earth matter effects can amplify $P_m^{2\nu}$, and therefore $P(\nu_{e(\mu)} \to \nu_{\mu(e)})$ and $P(\nu_e \to \nu_\tau)$, maximally when the neutrinos cross only the mantle for $E \sim 7$ GeV and $L \gtrsim 5400$ km, or $\cos\theta_n \gtrsim 0.43$, provided $\sin\theta_{13} \gtrsim 0.1$. If $\Delta m_{31}^2 < 0$ the same considerations apply for the corresponding antineutrino oscillation probabilities $\bar{P}_m^{2\nu} = \bar{P}_m^{2\nu}(\bar{\nu}_e \to (s_{23}\bar{\nu}_\mu + c_{23}\bar{\nu}_\tau))$ and correspondingly for $P(\bar{\nu}_{e(\mu)} \to \bar{\nu}_{\mu(e)})$ and $P(\bar{\nu}_e \to \bar{\nu}_\tau)$. For $\Delta m_{31}^2 > 0$, the $\bar{\nu}_{e(\mu)} \to \bar{\nu}_{\mu(e)}$ and $\bar{\nu}_e \to \bar{\nu}_\tau$ oscillations are suppressed by the Earth matter, while if $\Delta m_{31}^2 < 0$, the same conclusion holds for the $\nu_{e(\mu)} \to \nu_{\mu(e)}$ and $\nu_e \to \nu_\tau$, oscillations.

In the case of neutrinos crossing the Earth core, new resonance-like effects become possible in the $\nu_\mu \to \nu_e$ and $\nu_e \to \nu_{\mu(\tau)}$ (or $\bar{\nu}_\mu \to \bar{\nu}_e$ and $\bar{\nu}_e \to \bar{\nu}_{\mu(\tau)}$) transitions [75–77,80–82]. For $\sin^2\theta_{13} \lesssim 0.05$ and $\Delta m_{31}^2 > 0$, we can have [81] $P_m^{2\nu}(\Delta m_{31}^2, \theta_{13}) \cong 1$, and correspondingly maximal $P_m^{3\nu}(\nu_e \to \nu_\mu) = P_m^{3\nu}(\nu_\mu \to \nu_e) \cong s_{23}^2$, only due to the effect of maximal constructive interference between the amplitudes of the $\nu_e \to \nu'$ transitions in the Earth mantle and in the Earth core. The effect differs from the MSW one and the enhancement happens in the case of interest at a value of the energy between the MSW resonance energies corresponding to the density in the mantle and that of the core, or at a value of the resonance density N_e^{res} which lies between the values of N_e in the mantle and in the core [75]. In Refs. [75,76] the enhancement was called "neutrino oscillation length resonance", while in Refs. [77,80] the term "parametric resonance" for the same effect was used [83]. The *mantle-core*

enhancement effect is caused by the existence (for a given neutrino trajectory through the Earth core) of points of resonance-like maximal neutrino conversion, $P_m^{2\nu}(\Delta m_{31}^2, \theta_{13}) = 1$, in the corresponding space of neutrino oscillation parameters [81]. For $\Delta m_{31}^2 < 0$ the mantle-core enhancement can take place for the antineutrino transitions, $\bar{\nu}_\mu \to \bar{\nu}_e$ and $\bar{\nu}_e \to \bar{\nu}_{\mu(\tau)}$.

A rather complete set of values of $\Delta m_{31}^2/E > 0$ and $\sin^2 2\theta_{13}$ for which $P_m^{2\nu}(\Delta m_{31}^2, \theta_{13}) = 1$ was found in Ref. 81. The location of these points in the $\Delta m_{31}^2/E - \sin^2 2\theta_{13}$ plane determines the regions in the plane where $P_m^{2\nu}(\Delta m_{31}^2, \theta_{13})$ is large, $P_m^{2\nu}(\Delta m_{31}^2, \theta_{13}) \gtrsim 0.5$. These regions vary slowly with the nadir angle, being remarkably wide in the nadir angle and rather wide in the neutrino energy [81], so that the transitions of interest can produce noticeable effects in the measured observables. For $\sin^2 \theta_{13} \lesssim 0.05$, there are two sets of values of $(\Delta m_{31}^2/E, \sin^2 \theta_{13})$ for which $P_m^{2\nu}(\Delta m_{31}^2, \theta_{13}) = 1$, and thus two regions in $\Delta m_{31}^2/E - \sin^2 2\theta_{13}$ plane where $P_m^{2\nu}(\Delta m_{31}^2, \theta_{13}) \gtrsim 0.5$. For $\Delta m_{31}^2 = 2.4 \times 10^{-3}$ eV^2 and nadir angle, *e.g.*, $\theta_n=0$ (Earth center crossing neutrinos), we have $P_m^{2\nu}(\Delta m_{31}^2, \theta_{13}) = 1$ at $(E, \sin^2 2\theta_{13}) =$(3.3 GeV,0.034) and (5.0 GeV,0.15). At the same time for $E =$3.3 GeV (5.0 Gev), the probability $P_m^{2\nu}(\Delta m_{31}^2, \theta_{13}) \gtrsim 0.5$ for the values of $\sin^2 2\theta_{13}$ from the interval $0.02 \lesssim \sin^2 2\theta_{13} \lesssim 0.10$ $(0.04 \lesssim \sin^2 2\theta_{13} \lesssim 0.26)$. Similar results hold for neutrinos crossing the Earth core along the trajectories with $\theta_n \neq 0$ (for further details see the last article in Ref. 81; see also the last article in Ref. 82).

The mantle-core enhancement of $P_m^{2\nu}$ (or $\bar{P}_m^{2\nu}$) is relevant, in particular, for the searches of sub-dominant $\nu_{e(\mu)} \to \nu_{\mu(e)}$ (or $\bar{\nu}_{e(\mu)} \to \bar{\nu}_{\mu(e)}$) oscillations of atmospheric neutrinos having energies $E \gtrsim 2$ GeV and crossing the Earth core on the way to the detector (see Ref. 75 to Ref. 82 and the references quoted therein). The effects of Earth matter on the oscillations of atmospheric and accelerator neutrinos have not been observed so far. At present there are no compelling evidences for oscillations of the atmospheric ν_e and/or $\bar{\nu}_e$.

The expression for the probability of the $\nu_e \to \nu_\mu$ oscillations taking place in the Earth mantle in the case of 3-neutrino mixing, in which both neutrino mass squared differences Δm_{21}^2 and Δm_{31}^2 contribute and the CP violation effects due to the Dirac phase in the neutrino mixing matrix are taken into account, has the following form in the constant density approximation and keeping terms up to second order in the two small parameters $|\alpha| \equiv |\Delta m_{21}^2|/|\Delta m_{31}^2| \ll 1$ and $\sin^2 \theta_{13} \ll 1$ [84]:

$$P_m^{3\nu\ man}(\nu_e \to \nu_\mu) \cong P_0 + P_{\sin\delta} + P_{\cos\delta} + P_3\,. \tag{13.45}$$

Here

$$P_0 = \sin^2 \theta_{23} \frac{\sin^2 2\theta_{13}}{(A-1)^2} \sin^2[(A-1)\Delta]$$

$$P_3 = \alpha^2 \cos^2 \theta_{23} \frac{\sin^2 2\theta_{12}}{A^2} \sin^2(A\Delta)\,, \tag{13.46}$$

$$P_{\sin\delta} = \alpha \frac{8 J_{CP}}{A(1-A)} (\sin\Delta)(\sin A\Delta)(\sin[(1-A)\Delta])\,, \tag{13.47}$$

$$P_{\cos\delta} = \alpha \; \frac{8 \, J_{CP} \, \cot\delta}{A(1-A)} \, (\cos\Delta) \, (\sin A\Delta) \, (\sin[(1-A)\Delta]) \;, \tag{13.48}$$

where

$$\alpha = \frac{\Delta m_{21}^2}{\Delta m_{31}^2}, \quad \Delta = \frac{\Delta m_{31}^2 \, L}{4E}, \quad A = \sqrt{2} G_{\rm F} N_e^{man} \frac{2E}{\Delta m_{31}^2}, \tag{13.49}$$

and $\cot\delta = J_{CP}^{-1}\text{Re}(U_{\mu3}U_{e3}^*U_{e2}U_{\mu2}^*)$, $J_{CP} = \text{Im}(U_{\mu3}U_{e3}^*U_{e2}U_{\mu2}^*)$. The analytic expression for $P_m^{3\nu \; man}(\nu_e \to \nu_\mu)$ given above is valid for [84] neutrino path lengths in the mantle $(L \le 10660 \text{ km})$ satisfying $L \lesssim 10560 \text{ km} \; E[\text{GeV}] \, (7.6 \times 10^{-5} \text{ eV}^2/\Delta m_{21}^2)$, and energies $E \gtrsim 0.34 \text{ GeV}(\Delta m_{21}^2/7.6 \times 10^{-5} \text{ eV}^2) \, (1.4 \text{ cm}^{-3} N_A/N_e^{man})$. The expression for the $\bar\nu_e \to \bar\nu_\mu$ oscillation probability can be obtained formally from that for $P_m^{3\nu \; man}(\nu_e \to \nu_\mu)$ by making the changes $A \to -A$ and $J_{CP} \to -J_{CP}$, with $J_{CP} \cot\delta \equiv \text{Re}(U_{\mu3}U_{e3}^*U_{e2}U_{\mu2}^*)$ remaining unchanged. The term $P_{\sin\delta}$ in $P_m^{3\nu \; man}(\nu_e \to \nu_\mu)$ would be equal to zero if the Dirac phase in the neutrino mixing matrix U possesses a CP-conserving value. Even in this case, however, we have $A_{CP}^{(\mu e) \; man} \equiv (P_m^{3\nu \; man}(\nu_e \to \nu_\mu) - P_m^{3\nu \; man}(\bar\nu_e \to \bar\nu_\mu)) \neq 0$ due to the effects of the Earth matter. It will be important to experimentally disentangle the effects of the Earth matter and of J_{CP} in $A_{CP}^{(\mu e) \; man}$: this will allow to get information about the Dirac CP violation phase in U. In the vacuum limit of $N_e^{man} = 0$ $(A = 0)$ we have $A_{CP}^{(\mu e) \; man} = A_{CP}^{(\mu e)}$ (see Eq. (13.18)) and only the term $P_{\sin\delta}$ contributes to the asymmetry $A_{CP}^{(\mu e)}$.

13.3.2. *Oscillations of solar neutrinos* :

Consider next the oscillations of solar ν_e while they propagate from the central part of the Sun, where they are produced, to the surface of the Sun [23,74](see also Ref. 22 and, *e.g.*, Ref. 85) Details concerning the production, spectrum, magnitude and particularities of the solar neutrino flux, the methods of detection of solar neutrinos, description of solar neutrino experiments and of the data they provided will be discussed in the next section (see also Ref. 86). The electron number density N_e changes considerably along the neutrino path in the Sun: it decreases monotonically from the value of $\sim 100 \text{ cm}^{-3} \; N_A$ in the center of the Sun to 0 at the surface of the Sun. According to the contemporary solar models (see, *e.g.*, Ref. [86,87]), N_e decreases approximately exponentially in the radial direction towards the surface of the Sun:

$$N_e(t) = N_e(t_0) \exp\left\{-\frac{t-t_0}{r_0}\right\} \;, \tag{13.50}$$

where $(t - t_0) \cong d$ is the distance traveled by the neutrino in the Sun, $N_e(t_0)$ is the electron number density at the point of ν_e production in the Sun, r_0 is the scale-height of the change of $N_e(t)$ and one has [86,87] $r_0 \sim 0.1 R_\odot$.

Consider the case of 2-neutrino mixing, Eq. (13.34). Obviously, if N_e changes with t (or equivalently with the distance) along the neutrino trajectory, the matter-eigenstates, their energies, the mixing angle and the oscillation length in matter, become, through their dependence on N_e, also functions of t: $|\nu_{1,2}^m\rangle = |\nu_{1,2}^m(t)\rangle$, $E_{1,2}^m = E_{1,2}^m(t)$, $\theta_m = \theta_m(t)$ and

$L_m = L_m(t)$. It is not difficult to understand qualitatively the possible behavior of the neutrino system when solar neutrinos propagate from the center to the surface of the Sun if one realizes that one is dealing effectively with a two-level system whose Hamiltonian depends on time and admits "jumps" from one level to the other (see Eq. (13.32)). Consider the case of $\Delta m^2 \cos 2\theta > 0$. Let us assume first for simplicity that the electron number density at the point of a solar ν_e production in the Sun is much bigger than the resonance density, $N_e(t_0) \gg N_e^{res}$. Actually, this is one of the cases relevant to the solar neutrinos. In this case we have $\theta_m(t_0) \cong \pi/2$ and the state of the electron neutrino in the initial moment of the evolution of the system practically coincides with the heavier of the two matter-eigenstates:

$$|\nu_e\rangle \; \cong \; |\nu_2^m(t_0)\rangle \,. \tag{13.51}$$

Thus, at t_0 the neutrino system is in a state corresponding to the "level" with energy $E_2^m(t_0)$. When neutrinos propagate to the surface of the Sun they cross a layer of matter in which $N_e = N_e^{res}$: in this layer the difference between the energies of the two "levels" $(E_2^m(t) - E_1^m(t))$ has a minimal value on the neutrino trajectory (Eq. (13.37) and Eq. (13.39)). Correspondingly, the evolution of the neutrino system can proceed basically in two ways. First, the system can stay on the "level" with energy $E_2^m(t)$, *i.e.*, can continue to be in the state $|\nu_2^m(t)\rangle$ up to the final moment t_s, when the neutrino reaches the surface of the Sun. At the surface of the Sun $N_e(t_s) = 0$ and therefore $\theta_m(t_s) = \theta$, $|\nu_{1,2}^m(t_s)\rangle \equiv |\nu_{1,2}\rangle$ and $E_{1,2}^m(t_s) = E_{1,2}$. Thus, in this case the state describing the neutrino system at t_0 will evolve continuously into the state $|\nu_2\rangle$ at the surface of the Sun. Using Eq. (13.29) with $l = e$ and $x = \mu$, it is easy to obtain the probabilities to find ν_e and ν_μ at the surface of the Sun:

$$P(\nu_e \to \nu_e; t_s, t_0) \cong |\langle \nu_e|\nu_2\rangle|^2 = \sin^2\theta$$
$$P(\nu_e \to \nu_\mu; t_s, t_0) \cong |\langle \nu_\mu|\nu_2\rangle|^2 = \cos^2\theta \,. \tag{13.52}$$

It is clear that under the assumption made and if $\sin^2\theta \ll 1$, practically a total $\nu_e \to \nu_\mu$ conversion is possible. This type of evolution of the neutrino system and the $\nu_e \to \nu_\mu$ transitions taking place during the evolution, are called [23] "adiabatic." They are characterized by the fact that the probability of the "jump" from the upper "level" (having energy $E_2^m(t)$) to the lower "level" (with energy $E_1^m(t)$), P', or equivalently the probability of the $\nu_2^m(t_0) \to \nu_1^m(t_s)$ transition, $P' \equiv P'(\nu_2^m(t_0) \to \nu_1^m(t_s))$, on the whole neutrino trajectory is negligible:

$$P' \equiv P'(\nu_2^m(t_0) \to \nu_1^m(t_s)) \cong 0 \; : \; adiabatic \; transitions \,. \tag{13.53}$$

The second possibility is realized if in the resonance region, where the two "levels" approach each other closest the system "jumps" from the upper "level" to the lower "level" and after that continues to be in the state $|\nu_1^m(t)\rangle$ until the neutrino reaches the surface of the Sun. Evidently, now we have $P' \equiv P'(\nu_2^m(t_0) \to \nu_1^m(t_s)) \sim 1$. In this case the neutrino system ends up in the state $|\nu_1^m(t_s)\rangle \equiv |\nu_1\rangle$ at the surface of the Sun and

$$P(\nu_e \to \nu_e; t_s, t_0) \cong |\langle \nu_e|\nu_1\rangle|^2 = \cos^2\theta$$
$$P(\nu_e \to \nu_\mu; t_s, t_0) \cong |\langle \nu_\mu|\nu_1\rangle|^2 = \sin^2\theta \,. \tag{13.54}$$

Obviously, if $\sin^2\theta \ll 1$, practically no transitions of the solar ν_e into ν_μ will occur. The considered regime of evolution of the neutrino system and the corresponding $\nu_e \to \nu_\mu$ transitions are usually referred to as "extremely nonadiabatic."

Clearly, the value of the "jump" probability P' plays a crucial role in the the $\nu_e \to \nu_\mu$ transitions: it fixes the type of the transition and determines to a large extent the $\nu_e \to \nu_\mu$ transition probability [74,88,89]. We have considered above two limiting cases. Obviously, there exists a whole spectrum of possibilities since P' can have any value from 0 to $\cos^2\theta$ [90,91]. In general, the transitions are called "nonadiabatic" if P' is non-negligible.

Numerical studies have shown [23] that solar neutrinos can undergo both adiabatic and nonadiabatic $\nu_e \to \nu_\mu$ transitions in the Sun and the matter effects can be substantial in the solar neutrino oscillations for 10^{-8} eV$^2 \lesssim \Delta m^2 \lesssim 10^{-4}$ eV^2, $10^{-4} \lesssim \sin^2 2\theta < 1.0$.

The condition of adiabaticity of the solar ν_e transitions in Sun can be written as [74,88]

$$\gamma(t) \equiv \sqrt{2}G_F \frac{(N_e^{res})^2}{|\dot{N}_e(t)|} \tan^2 2\theta \left(1 + \tan^{-2} 2\theta_m(t)\right)^{\frac{3}{2}} \gg 1$$

$$\text{adiabatic transitions}, \tag{13.55}$$

while if $\gamma(t) \lesssim 1$ the transitions are nonadiabatic (see also Ref. 91), where $\dot{N}_e(t) \equiv \frac{d}{dt}N_e(t)$. Condition in Eq. (13.55) implies that the $\nu_e \to \nu_{\mu(\tau)}$ transitions in the Sun will be adiabatic if $N_e(t)$ changes sufficiently slowly along the neutrino path. In order for the transitions to be adiabatic, condition in Eq. (13.55) has to be fulfilled at any point of the neutrino's path in the Sun.

Actually, the system of evolution equations Eq. (13.32) can be solved exactly for N_e changing exponentially, Eq. (13.50), along the neutrino path in the Sun [90,92]. More specifically, the system in Eq. (13.32) is equivalent to one second order differential equation (with appropriate initial conditions). The latter can be shown [93] to coincide in form, in the case of N_e given by Eq. (13.50), with the Schroedinger equation for the radial part of the nonrelativistic wave function of the Hydrogen atom [94]. On the basis of the exact solution, which is expressed in terms of confluent hypergeometric functions, it was possible to derive a complete, simple and very accurate analytic description of the matter-enhanced transitions of solar neutrinos in the Sun for any values of Δm^2 and θ [22,90,91,95,96] (see also Refs. [23,74,89,97,98]).

The probability that a ν_e, produced at time t_0 in the central part of the Sun, will not transform into $\nu_{\mu(\tau)}$ on its way to the surface of the Sun (reached at time t_s) is given by

$$P_\odot^{2\nu}(\nu_e \to \nu_e; t_s, t_0) = \bar{P}_\odot^{2\nu}(\nu_e \to \nu_e; t_s, t_0) + \ Oscillating \ terms. \tag{13.56}$$

Here

$$\bar{P}_\odot^{2\nu}(\nu_e \to \nu_e; t_s, t_0) \equiv \bar{P}_\odot = \frac{1}{2} + \left(\frac{1}{2} - P'\right)\cos 2\theta_m(t_0) \cos 2\theta \ , \tag{13.57}$$

is the average survival probability for ν_e having energy $E \cong p$ [89], where

$$P' = \frac{\exp\left[-2\pi r_0 \frac{\Delta m^2}{2E} \sin^2\theta\right] - \exp\left[-2\pi r_0 \frac{\Delta m^2}{2E}\right]}{1 - \exp\left[-2\pi r_0 \frac{\Delta m^2}{2E}\right]}, \tag{13.58}$$

is [90] the "jump" probability for exponentially varying N_e, and $\theta_m(t_0)$ is the mixing angle in matter at the point of ν_e production [97]. The expression for $\bar{P}_\odot^{2\nu}(\nu_e \to \nu_e; t_s, t_0)$ with P' given by Eq. (13.58) is valid for $\Delta m^2 > 0$, but for both signs of $\cos 2\theta \neq 0$ [90,98]; it is valid for any given value of the distance along the neutrino trajectory and does not take into account the finite dimensions of the region of ν_e production in the Sun. This can be done by integrating over the different neutrino paths, *i.e.*, over the region of ν_e production.

The oscillating terms in the probability $P_\odot^{2\nu}(\nu_e \to \nu_e; t_s, t_0)$ [95,93] were shown [96] to be strongly suppressed for $\Delta m^2 \gtrsim 10^{-7}$ eV^2 by the various averagings one has to perform when analyzing the solar neutrino data. The current solar neutrino and KamLAND data suggest that $\Delta m^2 \cong 7.6 \times 10^{-5}$ eV^2. For $\Delta m^2 \gtrsim 10^{-7}$ eV^2, the averaging over the region of neutrino production in the Sun *etc.* renders negligible all interference terms which appear in the probability of ν_e survival due to the $\nu_e \leftrightarrow \nu_{\mu(\tau)}$ oscillations in vacuum taking place on the way of the neutrinos from the surface of the Sun to the surface of the Earth. Thus, the probability that ν_e will remain ν_e while it travels from the central part of the Sun to the surface of the Earth is effectively equal to the probability of survival of the ν_e while it propagates from the central part to the surface of the Sun and is given by the average probability $\bar{P}_\odot(\nu_e \to \nu_e; t_s, t_0)$ (determined by Eq. (13.57) and Eq. (13.58)).

If the solar ν_e transitions are adiabatic ($P' \cong 0$) and $\cos 2\theta_m(t_0) \cong -1$ (*i.e.*, $N_e(t_0)/|N_e^{res}| \gg 1, |\tan 2\theta|$, the ν_e are born "above" (in N_e) the resonance region), one has [23]

$$\bar{P}^{2\nu}(\nu_e \to \nu_e; t_s, t_0) \cong \frac{1}{2} - \frac{1}{2}\cos 2\theta. \tag{13.59}$$

The regime under discussion is realised for $\sin^2 2\theta \cong 0.8$ (suggested by the data, Section 13.4), if $E/\Delta m^2$ lies approximately in the range $(2 \times 10^4 - 3 \times 10^7)$ MeV/eV^2 (see Ref. 91). This result is relevant for the interpretation of the Super-Kamiokande and SNO solar neutrino data. We see that depending on the sign of $\cos 2\theta \neq 0$, $\bar{P}^{2\nu}(\nu_e \to \nu_e)$ is either bigger or smaller than $1/2$. It follows from the solar neutrino data that in the range of validity (in $E/\Delta m^2$) of Eq. (13.59) we have $\bar{P}^{2\nu}(\nu_e \to \nu_e) \cong 0.3$. Thus, the possibility of $\cos 2\theta \leq 0$ is ruled out by the data. Given the choice $\Delta m^2 > 0$ we made, the data imply that $\Delta m^2 \cos 2\theta > 0$.

If $E/\Delta m^2$ is sufficiently small so that $N_e(t_0)/|N_e^{res}| \ll 1$, we have $P' \cong 0$, $\theta_m(t_0) \cong \theta$ and the oscillations take place in the Sun as in vacuum [23]:

$$\bar{P}^{2\nu}(\nu_e \to \nu_e; t_s, t_0) \cong 1 - \frac{1}{2}\sin^2 2\theta, \tag{13.60}$$

which is the average two-neutrino vacuum oscillation probability. This expression describes with good precision the transitions of the solar *pp* neutrinos (Section 13.4).

The extremely nonadiabatic ν_e transitions in the Sun, characterised by $\gamma(t) \ll 1$, are also described by the average vacuum oscillation probability (Eq. (13.60)) (for $\Delta m^2 \cos 2\theta > 0$ in this case we have (see *e.g.*, Refs. [90,91]) $\cos 2\theta_m(t_0) \cong -1$ and $P' \cong \cos^2 \theta$).

   The probability of ν_e survival in the case 3-neutrino mixing takes a simple form for $|\Delta m_{31}^2| \cong 2.4 \times 10^{-3}$ eV$^2 \gg |\Delta m_{21}^2|$. Indeed, for the energies of solar neutrinos $E \lesssim 10$ MeV, N^{res} corresponding to $|\Delta m_{31}^2|$ satisfies $N_{e31}^{res} \gtrsim 10^3$ cm^{-3} N$_A$ and is by a factor of 10 bigger than N_e in the center of the Sun. As a consequence, the oscillations due to Δm_{31}^2 proceed as in vacuum. The oscillation length associated with $|\Delta m_{31}^2|$ satisfies $L_{31}^v \lesssim 10$ km $\ll \Delta R$, ΔR being the dimension of the region of ν_e production in the Sun. We have for the different components of the solar ν_e flux [86] $\Delta R \cong (0.04 - 0.20) R_\odot$. Therefore the averaging over ΔR strongly suppresses the oscillations due to Δm_{31}^2 and we get [78,99]:

$$P_\odot^{3\nu} \cong \sin^4 \theta_{13} + \cos^4 \theta_{13} \ P_\odot^{2\nu}(\Delta m_{21}^2, \theta_{12}; N_e \cos^2 \theta_{13}) , \qquad (13.61)$$

where $P_\odot^{2\nu}(\Delta m_{21}^2, \theta_{12}; N_e \cos^2 \theta_{13})$ is given by Eq. (13.56) to Eq. (13.58) in which $\Delta m^2 = \Delta m_{21}^2$, $\theta = \theta_{12}$ and the solar e^- number density N_e is replaced by $N_e \cos^2 \theta_{13}$. Thus, the solar ν_e transitions observed by the Super-Kamiokande and SNO experiments are described approximately by:

$$P_\odot^{3\nu} \cong \sin^4 \theta_{13} + \cos^4 \theta_{13} \ \sin^2 \theta_{12} . \qquad (13.62)$$

The data show that $P_\odot^{3\nu} \cong 0.3$, which is a strong evidence for matter effects in the solar ν_e transitions [100] since in the case of oscillations in vacuum $P_\odot^{3\nu} \cong \sin^4 \theta_{13} + (1 - 0.5 \sin^2 2\theta_{12}) \cos^4 \theta_{13} \gtrsim 0.49$, where we have used $\sin^2 \theta_{13} \lesssim 0.040$ and $\sin^2 2\theta_{12} \lesssim 0.93$ (see Section 13.7).

13.4.   Measurements of $\Delta m_\odot^2$ and $\theta_\odot$

13.4.1.   *Solar neutrino observations* :

   Observation of solar neutrinos directly addresses the theory of stellar structure and evolution, which is the basis of the standard solar model (SSM). The Sun as a well-defined neutrino source also provides extremely important opportunities to investigate nontrivial neutrino properties such as nonzero mass and mixing, because of the wide range of matter density and the great distance from the Sun to the Earth.

   The solar neutrinos are produced by some of the fusion reactions in the pp chain or CNO cycle. The combined effect of these reactions is written as
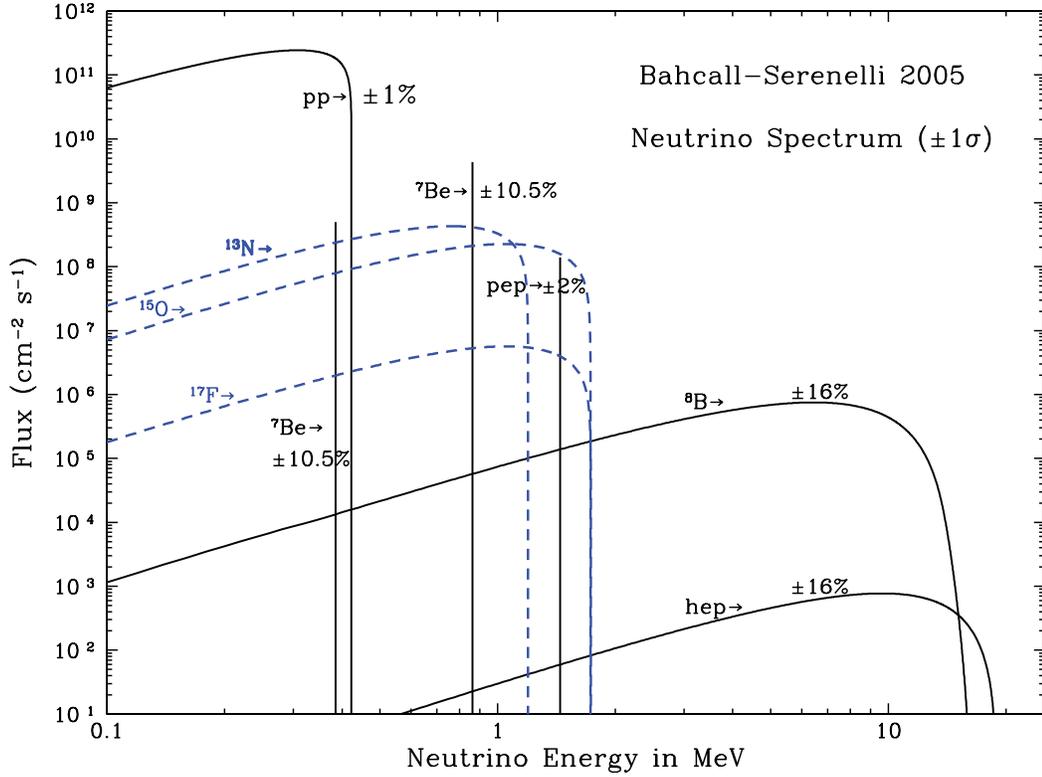
$$4p \rightarrow {}^4\text{He} + 2e^+ + 2\nu_e. \qquad (13.63)$$

Figure 13.2: The solar neutrino spectrum predicted by the BS05(OP) standard solar model [101]. The neutrino fluxes are given in units of $cm^{-2}s^{-1}MeV^{-1}$ for continuous spectra and $cm^{-2}s^{-1}$ for line spectra. The numbers associated with the neutrino sources show theoretical errors of the fluxes. This figure is taken from the late John Bahcall's web site, `http://www.sns.ias.edu/~jnb/`.

Positrons annihilate with electrons. Therefore, when considering the solar thermal energy generation, a relevant expression is

$$4p + 2e^- \rightarrow {}^4\text{He} + 2\nu_e + 26.73 \text{ MeV} - E_\nu \; , \tag{13.64}$$

where E_ν represents the energy taken away by neutrinos, with an average value being $\langle E_\nu \rangle \sim 0.6$ MeV. There have been efforts to calculate solar neutrino fluxes from these reactions on the basis of SSM. A variety of input information is needed in the evolutionary calculations. The most elaborate SSM calculations have been developed by Bahcall and his collaborators, who define their SSM as the solar model which is constructed with the best available physics and input data. Therefore, their SSM calculations have been rather frequently updated. SSM's labelled as BS05(OP) [101], BSB06(GS) and BSB06(AGS) [87], and BPS08(GS) and BPS08(AGS) [102] represent some of recent model calculations. Here, "OP" means that newly calculated radiative opacities from the "Opacity Project" are used. The later models are also calculated with OP opacities. "GS" and "AGS" refer to old and new determinations of solar abundances of heavy elements. There are significant differences between the old, higher heavy element abundances (GS)

and the new, lower heavy element abundances (AGS). The models with GS are consistent with helioseismological data, but the models with AGS are not.

The prediction of the BPS08(GS) model for the fluxes from neutrino-producing reactions is given in Table 13.2. Fig. 13.2 shows the solar-neutrino spectra calculated with the BS05(OP) model which is similar to the BPS08(GS) model. Here we note that in Ref. 103 the authors point out that electron capture on ^{13}N, ^{15}O, and ^{17}F produces line spectra of neutrinos, which have not been considered in the SSM calculations quoted above.

In 2011, a new SSM calculations [104] have been presented by A.M. Serenelli, W.C. Haxton, and C. Peña-Garay, by adopting the newly analyzed nuclear fusion cross sections. Their high metalicity SSM is labelled as SHP11(GS). For the same solar abundances as used in Ref. 101 and Ref. 87, the most significant change is a decrease of ^{8}B flux by $\sim 5\%$.

Table 13.2:   Neutrino-producing reactions in the Sun (first column) and their abbreviations (second column). The neutrino fluxes predicted by the BPS08(GS) model [102] are listed in the third column.

Reaction	Abbr.	Flux $(\mathrm{cm}^{-2}\ \mathrm{s}^{-1})$
$pp \rightarrow d\,e^+\,\nu$	pp	$5.97(1 \pm 0.006) \times 10^{10}$
$pe^-p \rightarrow d\,\nu$	pep	$1.41(1 \pm 0.011) \times 10^{8}$
$^{3}\mathrm{He}\,p \rightarrow\ ^{4}\mathrm{He}\,e^+\nu$	hep	$7.90(1 \pm 0.15) \times 10^{3}$
$^{7}\mathrm{Be}\,e^- \rightarrow\ ^{7}\mathrm{Li}\,\nu + (\gamma)$	$^{7}\mathrm{Be}$	$5.07(1 \pm 0.06) \times 10^{9}$
$^{8}\mathrm{B} \rightarrow\ ^{8}\mathrm{Be}^*\,e^+\nu$	$^{8}\mathrm{B}$	$5.94(1 \pm 0.11) \times 10^{6}$
$^{13}\mathrm{N} \rightarrow\ ^{13}\mathrm{C}\,e^+\nu$	$^{13}\mathrm{N}$	$2.88(1 \pm 0.15) \times 10^{8}$
$^{15}\mathrm{O} \rightarrow\ ^{15}\mathrm{N}\,e^+\nu$	$^{15}\mathrm{O}$	$2.15(1^{+0.17}_{-0.16}) \times 10^{8}$
$^{17}\mathrm{F} \rightarrow\ ^{17}\mathrm{O}\,e^+\nu$	$^{17}\mathrm{F}$	$5.82(1^{+0.19}_{-0.17}) \times 10^{6}$

So far, solar neutrinos have been observed by chlorine (Homestake) and gallium (SAGE, GALLEX, and GNO) radiochemical detectors and water Cherenkov detectors using light water (Kamiokande and Super-Kamiokande) and heavy water (SNO). Recently, a liquid scintillation detector (Borexino) successfully observed low energy solar neutrinos.

A pioneering solar neutrino experiment by Davis and collaborators at Homestake using the ^{37}Cl - ^{37}Ar method proposed by Pontecorvo [105] started in the late 1960's. This experiment exploited ν_e absorption on ^{37}Cl nuclei followed by the produced ^{37}Ar decay through orbital e^- capture,

$$\nu_e +^{37}\mathrm{Cl} \rightarrow\ ^{37}\mathrm{Ar} + e^- \quad (\text{threshold }\ 814\ \text{keV}). \tag{13.65}$$

The ^{37}Ar atoms produced are radioactive, with a half life ($\tau_{1/2}$) of 34.8 days. After an exposure of the detector for two to three times $\tau_{1/2}$, the reaction products were chemically

extracted and introduced into a low-background proportional counter, where they were counted for a sufficiently long period to determine the exponentially decaying signal and a constant background. Solar-model calculations predict that the dominant contribution in the chlorine experiment came from ^{8}B neutrinos, but ^{7}Be, *pep*, ^{13}N, and ^{15}O neutrinos also contributed (for notations, refer to Table 13.2).

From the very beginning of the solar-neutrino observation [106], it was recognized that the observed flux was significantly smaller than the SSM prediction, provided nothing happens to the electron neutrinos after they are created in the solar interior. This deficit has been called "the solar-neutrino problem."

Table 13.3: Results from radiochemical solar-neutrino experiments. The predictions of a recent standard solar model BPS08(GS) are also shown. The first and the second errors in the experimental results are the statistical and systematic errors, respectively. SNU (Solar Neutrino Unit) is defined as 10^{-36} neutrino captures per atom per second.

	^{37}Cl→^{37}Ar (SNU)	^{71}Ga→^{71}Ge (SNU)
Homestake [4]	$2.56 \pm 0.16 \pm 0.16$	–
GALLEX [8]	–	$77.5 \pm 6.2^{+4.3}_{-4.7}$
GALLEX-Reanalysis [107]	–	$73.4^{+6.1+3.7}_{-6.0-4.1}$
GNO [9]	–	$62.9^{+5.5}_{-5.3} \pm 2.5$
GNO+GALLEX [9]	–	$69.3 \pm 4.1 \pm 3.6$
GNO+GALLEX-Reanalysis [107]	–	$67.6^{+4.0+3.2}_{-4.0-3.2}$
SAGE [6]	–	$65.4^{+3.1+2.6}_{-3.0-2.8}$
SSM [BPS08(GS)] [102]	$8.46^{+0.87}_{-0.88}$	$127.9^{+8.1}_{-8.2}$

Gallium experiments (GALLEX and GNO at Gran Sasso in Italy and SAGE at Baksan in Russia) utilize the reaction

$$\nu_e + {}^{71}\text{Ga} \rightarrow {}^{71}\text{Ge} + e^- \quad (\text{threshold } 233 \text{ keV}). \tag{13.66}$$

They are sensitive to the most abundant *pp* solar neutrinos. The solar-model calculations predict that more than 80% of the capture rate in gallium is due to low energy *pp* and ^{7}Be solar neutrinos with the *pp* rate being about twice the ^{7}Be rate. SAGE reported the first results in 1991 [108]. They observed the capture rate to be $20^{+15}_{-20} \pm 32$ SNU, or a

90% confidence-level upper limit of 79 SNU. In 1992, GALLEX reported the observed capture rate of $83 \pm 19 \pm 8$ SNU [7]. It was the first evidence for low-energy solar-neutrino observation. Later, SAGE observed similar flux [109] to GALLEX. The latest SAGE results are published in Ref. 6. The GALLEX Collaboration finished observations in early 1997 [8,107]. Since April, 1998, a newly defined collaboration, GNO (Gallium Neutrino Observatory) continued the observations until April 2003. The GNO results are published in Ref. 9. The GNO + GALLEX joint analysis results are also presented in Ref. 9 and Ref. 107. The results from radiochemical solar neutrino experiments are shown in Table 13.3.

In 1987, the Kamiokande experiment in Japan succeeded in real-time solar neutrino observation, utilizing νe scattering,

$$\nu_x + e^- \rightarrow \nu_x + e^- , \tag{13.67}$$

in a large water-Cherenkov detector. This experiment takes advantage of the directional correlation between the incoming neutrino and the recoil electron. This feature greatly helps the clear separation of the solar-neutrino signal from the background. The Kamiokande result gave the first direct evidence that neutrinos come from the direction of the Sun [110]. Later, the high-statistics Super-Kamiokande experiment [111–114] with a 50-kton water Cherenkov detector replaced the Kamiokande experiment. Due to the high thresholds (7 MeV in Kamiokande and 5 MeV at present in Super-Kamiokande) the experiments observe pure ^{8}B solar neutrinos. It should be noted that the reaction (Eq. (13.67)) is sensitive to all active neutrinos, $x = e$, μ, and τ. However, the sensitivity to ν_μ and ν_τ is much smaller than the sensitivity to ν_e, $\sigma(\nu_{\mu,\tau}e) \approx 0.16\,\sigma(\nu_e e)$.

In 1999, a new real time solar-neutrino experiment, SNO (Sudbury Neutrino Observatory), in Canada started observation. This experiment used 1000 tons of ultra-pure heavy water (D_2O) contained in a spherical acrylic vessel, surrounded by an ultra-pure H_2O shield. SNO measured ^{8}B solar neutrinos via the charged-current (CC) and neutral-current (NC) reactions

$$\nu_e + d \rightarrow e^- + p + p \qquad \text{(CC)}, \tag{13.68}$$

and

$$\nu_x + d \rightarrow \nu_x + p + n \qquad \text{(NC)}, \tag{13.69}$$

as well as νe scattering, (Eq. (13.67)). The CC reaction, (Eq. (13.68)), is sensitive only to ν_e, while the NC reaction, (Eq. (13.69)), is sensitive to all active neutrinos. This is a key feature to solve the solar neutrino problem. If it is caused by flavour transitions such as neutrino oscillations, the solar neutrino fluxes measured by CC and NC reactions would show a significant difference.

The Q-value of the CC reaction is -1.4 MeV and the e^- energy is strongly correlated with the ν_e energy. Thus, the CC reaction provides an accurate measure of the shape of the ^{8}B neutrino spectrum. The contributions from the CC reaction and νe scattering can be distinguished by using different $\cos\theta$ distributions, where θ is the angle of the

e^- momentum with respect to the Sun-Earth axis. While the νe scattering events have a strong forward peak, CC events have an approximate angular distribution of $1 - 1/3$ $\cos\theta$.

The neutrino energy threshold of the NC reaction is 2.2 MeV. In the pure D_2O [11,12], the signal of the NC reaction was neutron capture in deuterium, producing a 6.25-MeV γ-ray. In this case, the capture efficiency was low and the deposited energy was close to the detection threshold of 5 MeV. In order to enhance both the capture efficiency and the total γ-ray energy (8.6 MeV), 2 tons of NaCl were added to the heavy water in the second phase of the experiment [115]. Subsequently NaCl was removed and an array of ^{3}He neutron counters were installed for the third phase measurement [116]. These neutron counters provided independent NC measurement with different systematics from that of the second phase, and thus strengthened the reliability of the NC measurement. The SNO experiment completed data acquisition in 2006. Recently, the SNO group presented the results of Phase I and Phase II joint analysis [117] as well as the results of a combined analysis of all three phases [118].

Table 13.4 shows the ^{8}B solar neutrino results from real time experiments. The standard solar model predictions are also shown. Table 13.4 includes the results from the SNO group's recent joint analysis of the SNO Phase I and Phase II data with the analysis threshold as low as 3.5 MeV (effective electron kinetic energy) and significantly improved systematic uncertainties [117]. Also, the recent result from a combined analysis of all three phases [118] is included. It is seen from these tables that the results from all the solar-neutrino experiments, except SNO's NC result, indicate significantly less flux than expected from the solar-model predictions.

Another real time solar neutrino experiment, Borexino at Gran Sasso in Italy, started solar neutrino observation in 2007. This experiment measures solar neutrinos via νe scattering in 300 tons of ultra-pure liquid scintillator. With a detection threshold as low as 250 keV, the flux of monochromatic 0.862 MeV ^{7}Be solar neutrinos has been directly observed for the first time (see Table 13.5). The observed energy spectrum shows the characteristic Compton-edge over the background [119,120]. Borexino also reported an observation of null day-night asymmetry of the ^{7}Be neutrino flux, $A_{dn} = 2(R_N - R_D)/(R_N + R_D) = 0.001 \pm 0.012 \pm 0.007$ [121], where R_N and R_D are the night and day count rates of ^{7}Be neutrinos.

Further, Borexino measured the flux of monochromatic 1.44 MeV *pep* solar neutrinos [122]. The absence of the *pep* solar neutrino signal is disfavored at 98% CL. The *pep* solar neutrino flux measured *via* νe scattering (calculated from the measured interaction rate and the expected one with the assumption of no neutrino oscillations and the SHP11(GS) SSM [104], both given in [122]) is shown in Table 13.6 and compared with the SSM predictions. Also, an upper limit of the "unoscillated" CNO solar neutrino flux is determined [122] as $< 7.7 \times 10^8$ cm^{-2}s^{-1} (95% CL) by assuming the MSW large mixing angle solution with $\Delta m_\odot^2 = (7.6 \pm 0.2) \times 10^{-5}$ eV^2 and $\tan^2\theta_\odot = 0.47^{+0.05}_{-0.04}$ and the SHP11(GS) SSM prediction [104] for the *pep* ν flux.

Borexino also measured ^{8}B solar neutrinos with an energy threshold of 3 MeV [123]. Measurements of low energy solar neutrinos are important not only to test the SSM further, but also to study the MSW effect over the energy region spanning from sub-MeV

Table 13.4: ^{8}B solar neutrino results from real time experiments. The predictions of BPS08(GS) and SHP11(GS) standard solar models are also shown. The first and the second errors in the experimental results are the statistical and systematic errors, respectively.

	Reaction	^{8}B ν flux $(10^6 \text{cm}^{-2}\text{s}^{-1})$
Kamiokande [5]	νe	$2.80 \pm 0.19 \pm 0.33$
Super-K I [112,114]	νe	$2.38 \pm 0.02 \pm 0.08$
Super-K II [113,114]	νe	$2.41 \pm 0.05^{+0.16}_{-0.15}$
Super-K III [114]	νe	$2.32 \pm 0.04 \pm 0.05$
SNO Phase I [12]	CC	$1.76^{+0.06}_{-0.05} \pm 0.09$
(pure D$_2$0)	νe	$2.39^{+0.24}_{-0.23} \pm 0.12$
	NC	$5.09^{+0.44+0.46}_{-0.43-0.43}$
SNO Phase II [115]	CC	$1.68 \pm 0.06^{+0.08}_{-0.09}$
(NaCl in D$_2$O)	νe	$2.35 \pm 0.22 \pm 0.15$
	NC	$4.94 \pm 0.21^{+0.38}_{-0.34}$
SNO Phase III [116]	CC	$1.67^{+0.05+0.07}_{-0.04-0.08}$
(^{3}He counters)	νe	$1.77^{+0.24+0.09}_{-0.21-0.10}$
	NC	$5.54^{+0.33+0.36}_{-0.31-0.34}$
SNO Phase I+II [117]	NC	$5.140^{+0.160+0.132}_{-0.158-0.117}$
	Φ_B from fit to all reactions	$5.046^{+0.159+0.107}_{-0.152-0.123}$
SNO Phase I+II+III [118]	Φ_B from fit to all reactions	$5.25 \pm 0.16^{+0.11}_{-0.13}$
Borexino [123]	νe	$2.4 \pm 0.4 \pm 0.1$
SSM [BPS08(GS)] [102]	–	$5.94(1 \pm 0.11)$
SSM [SHP11(GS)] [104]	–	$5.58(1 \pm 0.14)$

to 10 MeV.

13.4.2. *Evidence for solar neutrino flavour conversion* :

Solar neutrino experiments achieved remarkable progress in the past ten years, and the solar-neutrino problem, which had remained unsolved for more than 30 years, has been understood as due to neutrino flavour conversion. In 2001, the initial SNO CC result combined with the Super-Kamiokande's high-statistics νe elastic scattering result [124] provided direct evidence for flavour conversion of solar neutrinos [11]. Later, SNO's NC measurements further strengthened this conclusion [12,115,116]. From the salt-phase

Table 13.5: ^{7}Be solar neutrino result from Borexino [120]. The predictions of BPS08(GS) and SHP11(GS) standard solar models are also shown.

	Reaction	^{7}Be ν flux $(10^9 \text{cm}^{-2}\text{s}^{-1})$
Borexino [120]	νe	3.10 ± 0.15
SSM [BPS08(GS)] [102]	–	$5.07(1 \pm 0.06)$
SSM [SHP11(GS)] [104]	–	$5.00(1 \pm 0.07)$

Table 13.6: *pep* solar neutrino result from Borexino [122]. The predictions of BPS08(GS) and SHP11(GS) standard solar models are also shown.

	Reaction	*pep* ν flux $(10^8 \text{cm}^{-2}\text{s}^{-1})$
Borexino [122]	νe	1.0 ± 0.2
SSM [BPS08(GS)] [102]	–	$1.41(1 \pm 0.011)$
SSM [SHP11(GS)] [104]	–	$1.44(1 \pm 0.012)$

measurement [115], the fluxes measured with CC, ES, and NC events were obtained as

$$\phi_{\text{SNO}}^{\text{CC}} = (1.68 \pm 0.06^{+0.08}_{-0.09}) \times 10^6 \text{cm}^{-2}\text{s}^{-1} \ , \tag{13.70}$$

$$\phi_{\text{SNO}}^{\text{ES}} = (2.35 \pm 0.22 \pm 0.15) \times 10^6 \text{cm}^{-2}\text{s}^{-1} \ , \tag{13.71}$$

$$\phi_{\text{SNO}}^{\text{NC}} = (4.94 \pm 0.21^{+0.38}_{-0.34}) \times 10^6 \text{cm}^{-2}\text{s}^{-1} \ , \tag{13.72}$$

where the first errors are statistical and the second errors are systematic. In the case of $\nu_e \to \nu_{\mu,\tau}$ transitions, Eq. (13.72) is a mixing-independent result and therefore tests solar models. It shows good agreement with the ^{8}B solar-neutrino flux predicted by the solar model [101]. Fig. 13.3 shows the salt phase result of $\phi(\nu_{\mu \text{ or } \tau})$ versus the flux of electron neutrinos $\phi(\nu_e)$ with the 68%, 95%, and 99% joint probability contours. The flux of non-ν_e active neutrinos, $\phi(\nu_{\mu \text{ or } \tau})$, can be deduced from these results. It is

$$\phi(\nu_{\mu \text{ or } \tau}) = \left(3.26 \pm 0.25^{+0.40}_{-0.35}\right) \times 10^6 \text{cm}^{-2}\text{s}^{-1}. \tag{13.73}$$

The non-zero $\phi(\nu_{\mu \text{ or } \tau})$ is strong evidence for neutrino flavor conversion. These results are consistent with those expected from the LMA (large mixing angle) solution of solar
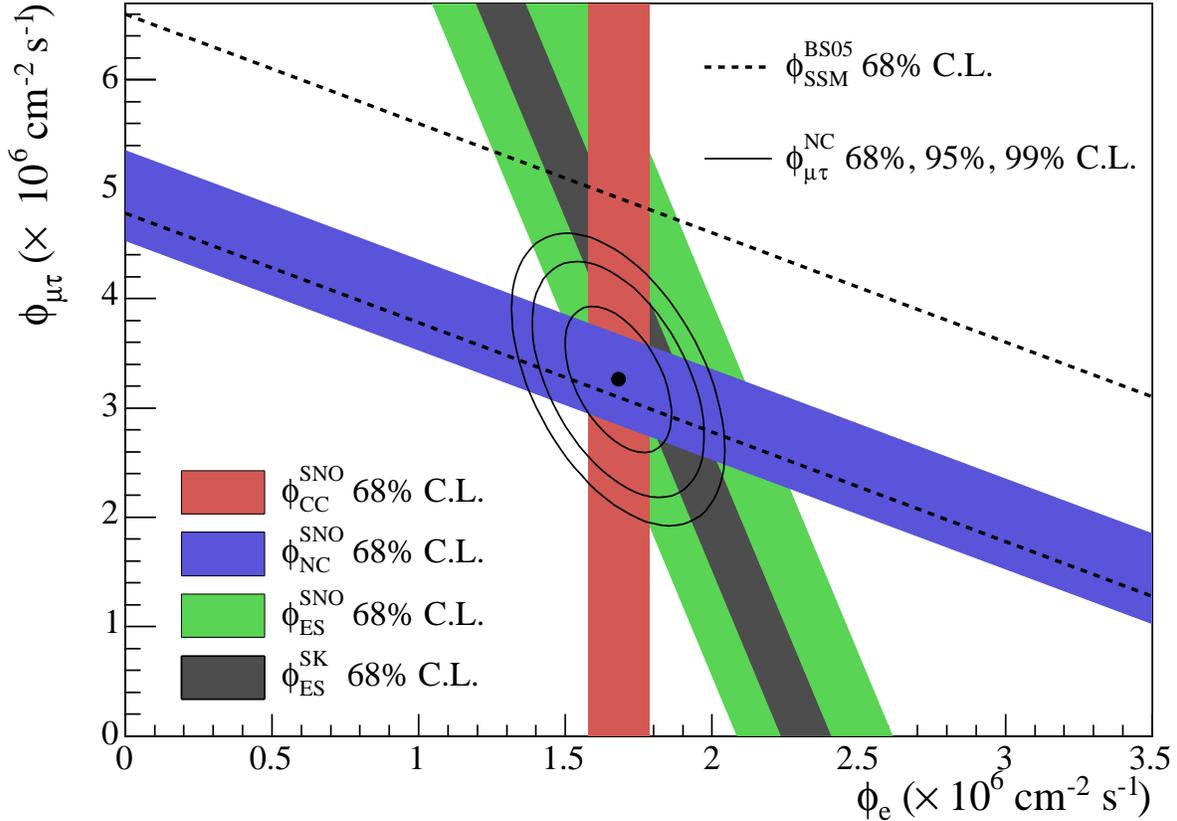
Figure 13.3: Fluxes of ^{8}B solar neutrinos, $\phi(\nu_e)$, and $\phi(\nu_{\mu \text{ or } \tau})$, deduced from the SNO's CC, ES, and NC results of the salt phase measurement [115]. The Super-Kamiokande ES flux is from Ref. 125. The BS05(OP) standard solar model prediction [101] is also shown. The bands represent the 1σ error. The contours show the 68%, 95%, and 99% joint probability for $\phi(\nu_e)$ and $\phi(\nu_{\mu \text{ or } \tau})$. The figure is from Ref. 115.

neutrino oscillation in matter [22,23] with $\Delta m_\odot^2 \sim 5 \times 10^{-5}$ eV^2 and $\tan^2\theta_\odot \sim 0.45$. However, with the SNO data alone, the possibility of other solutions cannot be excluded with sufficient statistical significance.

13.4.3. *KamLAND experiment* :

KamLAND is a 1-kton ultra-pure liquid scintillator detector located at the old Kamiokande's site in Japan. The primary goal of the KamLAND experiment was a long-baseline (flux-weighted average distance of $\sim$ 180 km) neutrino oscillation studies using $\bar{\nu}_e$'s emitted from nuclear power reactors. The reaction $\bar{\nu}_e + p \rightarrow e^+ + n$ is used to detect reactor $\bar{\nu}_e$'s and a delayed coincidence of the positron with a 2.2 MeV γ-ray from neutron capture on a proton is used to reduce the backgrounds. With the reactor $\bar{\nu}_e$'s energy spectrum ($<$ 8 MeV) and a prompt-energy analysis threshold of 2.6 MeV, this experiment has a sensitive Δm^2 range down to $\sim 10^{-5}$ eV^2. Therefore, if the LMA
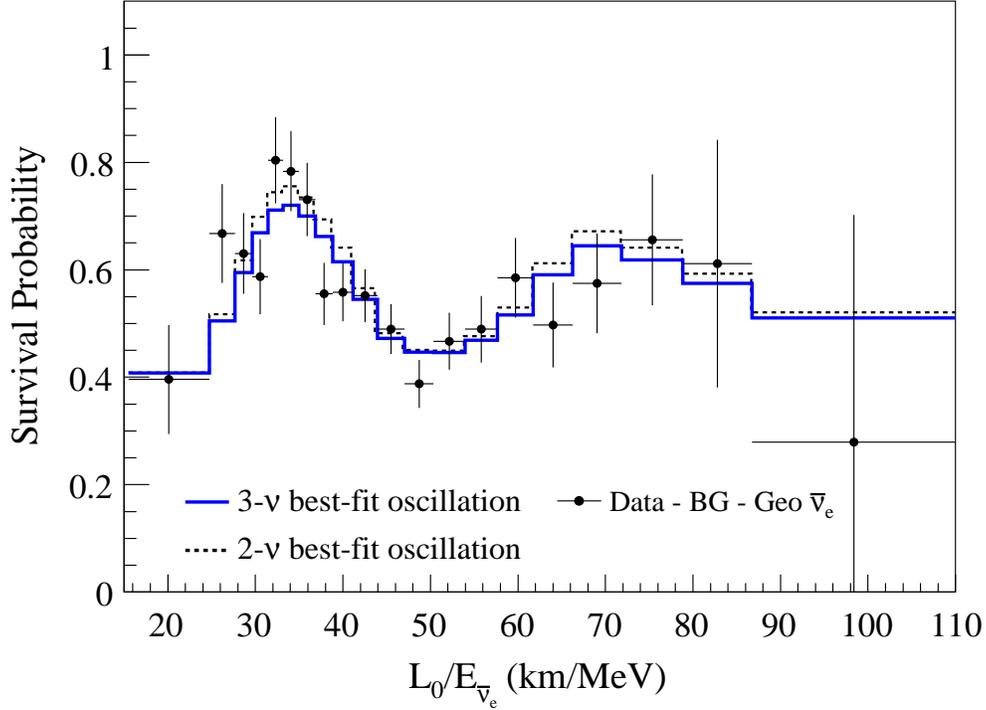
Figure1.4: The ratio of the background and geoneutrino-subtracted $\bar{\nu}_e$ spectrum to the predicted one without oscillations (survival probability) as a function of L_0/E, where $L_0 = 180$ km. The histograms show the expected distributions based on the best-fit parameter values from the two- and three-flavor neutrino oscillation analyses. The figure is from Ref. 128.

solution is the real solution of the solar neutrino problem, KamLAND should observe reactor $\bar{\nu}_e$ disappearance, assuming CPT invariance.

The first KamLAND results [15] with 162 ton·yr exposure were reported in December 2002. The ratio of observed to expected (assuming no $\bar{\nu}_e$ oscillations) number of events was

$$\frac{N_{\text{obs}} - N_{\text{BG}}}{N_{\text{NoOsc}}} = 0.611 \pm 0.085 \pm 0.041 \tag{13.74}$$

with obvious notation. This result showed clear evidence of an event deficit expected from neutrino oscillations. The 95% CL allowed regions are obtained from the oscillation analysis with the observed event rates and positron spectrum shape. A combined global solar + KamLAND analysis showed that the LMA is a unique solution to the solar neutrino problem with $> 5\sigma$ CL [126]. With increased statistics [16,127,128], KamLAND observed not only the distortion of the $\bar{\nu}_e$ spectrum, but also for the first time the periodic feature of the $\bar{\nu}_e$ survival probability expected from neutrino oscillations (see Fig. 13.4).

13.5. Measurements of $|\Delta m_A^2|$ and θ_A

13.5.1. *Atmospheric neutrino results* :

The first compelling evidence for the neutrino oscillation was presented by the Super-Kamiokande Collaboration in 1998 [13] from the observation of atmospheric neutrinos produced by cosmic-ray interactions in the atmosphere. The zenith-angle distributions of the μ-like events which are mostly muon-neutrino and muon antineutrino initiated charged-current interactions, showed a clear deficit compared to the no-oscillation expectation. Note that a water Cherenkov detector cannot measure the charge of the final-state leptons, and therefore neutrino and antineutrino induced events cannot be discriminated. Neutrino events having their vertex in the 22.5 kton fiducial volume in Super-Kamiokande are classified into fully contained (FC) events and partially contained (PC) events. The FC events are required to have no activity in the anti-counter. Single-ring events have only one charged lepton which radiates Cherenkov light in the final state, and particle identification is particularly clean for single-ring FC events. A ring produced by an e-like ($e^\pm$, γ) particle exhibits a more diffuse pattern than that produced by a μ-like ($\mu^\pm$, $\pi^\pm$) particle, since an e-like particle produces an electromagnetic shower and low-energy electrons suffer considerable multiple Coulomb scattering in water. All the PC events were assumed to be μ-like since the PC events comprise a 98% pure charged-current ν_μ sample.

Fig. 13.5 shows the zenith-angle distributions of e-like and μ-like events from the SK-I measurement [129]. $\cos\theta = 1$ corresponds to the downward direction, while $\cos\theta = -1$ corresponds to the upward direction. Events included in these plots are single-ring FC events subdivided into sub-GeV (visible energy < 1.33 GeV) events and multi-GeV (visible energy > 1.33 GeV) events. The zenith-angle distribution of the multi-GeV μ-like events is shown combined with that of the PC events. The final-state leptons in these events have good directional correlation with the parent neutrinos. The dotted histograms show the Monte Carlo expectation for neutrino events. If the produced flux of atmospheric neutrinos of a given flavour remains unchanged at the detector, the data should have similar distributions to the expectation. However, the zenith-angle distribution of the μ-like events shows a strong deviation from the expectation. On the other hand, the zenith-angle distribution of the e-like events is consistent with the expectation. This characteristic feature may be interpreted that muon neutrinos coming from the opposite side of the Earth's atmosphere, having travelled $\sim 10,000$ km, oscillate into other neutrinos and disappeared, while oscillations still do not take place for muon neutrinos coming from above the detector, having travelled from a few to a few tens km. Disappeared muon neutrinos may have oscillated into tau neutrinos because there is no indication of electron neutrino appearance. The atmospheric neutrinos corresponding to the events shown in Fig. 13.5 have $E = 1 \sim 10$ GeV. With $L = 10000$ km, the hypothesis of neutrino oscillations suggests $\Delta m^2 \sim 10^{-3} - 10^{-4}$ eV^2. The solid histograms show the best-fit results of a two-neutrino oscillation analysis with the hypothesis of $\nu_\mu \leftrightarrow \nu_\tau$. For the allowed parameter region, see Fig. 13.6.

Also, a search for a ν_τ appearance signal by using the SK-I atmospheric neutrino data has been made by the Super-Kamiokande Collaboration [131], and no ν_τ appearance
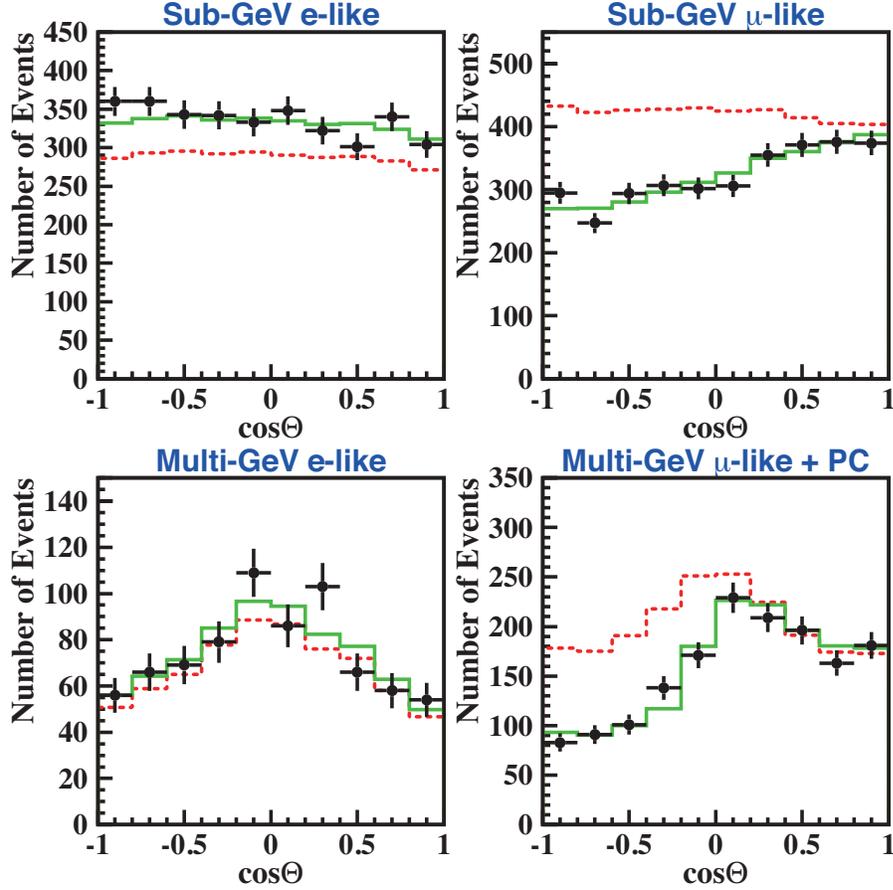
Figure 13.5: The zenith angle distributions for fully contained 1-ring *e*-like and *μ*-like events with visible energy < 1.33 GeV (sub-GeV) and > 1.33 GeV (multi-GeV). For multi-GeV *μ*-like events, a combined distribution with partially contained (PC) events is shown. The dotted histograms show the non-oscillated Monte Carlo events, and the solid histograms show the best-fit expectations for $\nu_\mu \leftrightarrow \nu_\tau$ oscillations. (This figure is provided by the Super-Kamiokande Collab.)

hypothesis is disfavored at 2.4σ.

Although the SK-I atmospheric neutrino observations gave compelling evidence for muon neutrino disappearance which is consistent with two-neutrino oscillation $\nu_\mu \leftrightarrow \nu_\tau$ [131], the question may be asked whether the observed muon neutrino disappearance is really due to neutrino oscillations. First, other exotic explanations such as neutrino decay [132] and quantum decoherence [133] cannot be completely ruled out from the zenith-angle distributions alone. To confirm neutrino oscillation, characteristic sinusoidal behavior of the conversion probability as a function of neutrino energy E for a fixed distance L in the case of long-baseline neutrino oscillation experiments, or as a function of L/E in the case of atmospheric neutrino experiments, should be observed. By selecting events with high L/E resolution, evidence for the dip in the L/E distribution was observed at the right place expected from the interpretation of the SK-I data in terms of $\nu_\mu \leftrightarrow \nu_\tau$ oscillations [14], see Fig. 13.7. This dip cannot be explained by alternative
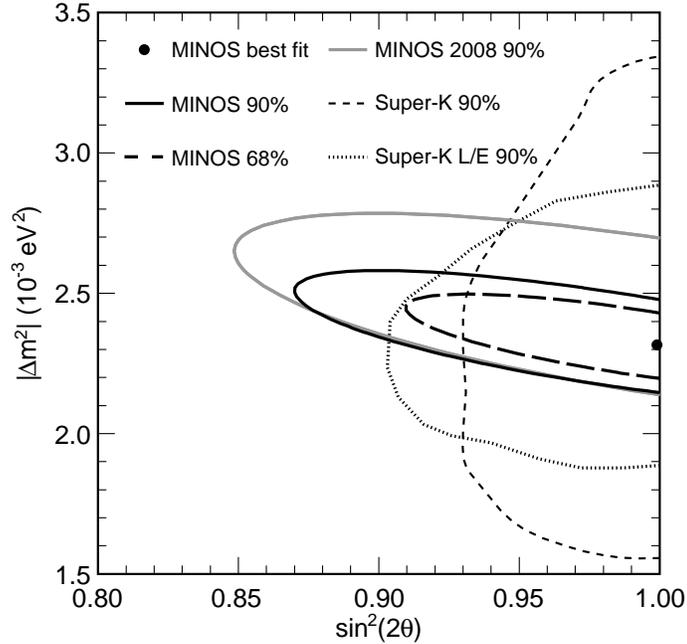
Figure 13.6: Allowed region for the $\nu_\mu \leftrightarrow \nu_\tau$ oscillation parameters from the MINOS results published in 2011. The 68 % and 90 % CL allowed regions are shown together with the Super-Kamiokande and MINOS 2008 90% CL allowed regions. This figure is taken from Ref. 130.

hypotheses of neutrino decay and neutrino decoherence, and they are excluded at more than 3σ in comparison with the neutrino oscillation interpretation. For the constraints obtained from the L/E analysis, see Fig. 13.6.

13.5.2. *Results from accelerator experiments* :

The $\Delta m^2 \geq 2 \times 10^{-3}$ eV^2 region can be explored by accelerator-based long-baseline experiments with typically $E \sim 1$ GeV and $L \sim$ several hundred km. With a fixed baseline distance and a narrower, well understood neutrino spectrum, the value of $|\Delta m^2_{\rm A}|$ and, with higher statistics, also the mixing angle, are potentially better constrained in accelerator experiments than from atmospheric neutrino observations.

The K2K (KEK-to-Kamioka) long-baseline neutrino oscillation experiment [19] is the first accelerator-based experiment with a neutrino path length extending hundreds of kilometers. K2K aimed at confirmation of the neutrino oscillation in ν_μ disappearance in the $|\Delta m^2_{\rm A}| \geq 2 \times 10^{-3}$ eV^2 region. A horn-focused wide-band muon neutrino beam having an average $L/E_\nu \sim 200$ ($L = 250$ km, $\langle E_\nu \rangle \sim 1.3$ GeV), was produced by 12-GeV protons from the KEK-PS and directed to the Super-Kamiokande detector. The spectrum and profile of the neutrino beam were measured by a near neutrino detector system located 300 m downstream from the production target.
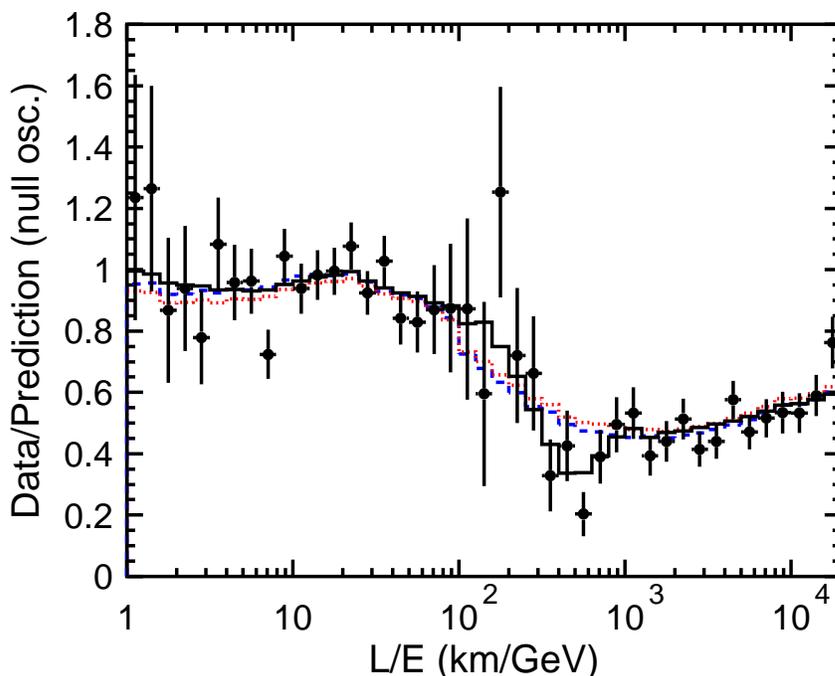
Figure 13.7: Results of the L/E analysis of SK-I atmospheric neutrino data. The points show the ratio of the data to the Monte Carlo prediction without oscillations, as a function of the reconstructed L/E. The error bars are statistical only. The solid line shows the best fit with 2-flavour $\nu_\mu \leftrightarrow \nu_\tau$ oscillations. The dashed and dotted lines show the best fit expectations for neutrino decay and neutrino decoherence hypotheses, respectively. (From Ref. 14.)

The construction of the K2K neutrino beam line and the near detector began before Super-Kamiokande's discovery of atmospheric neutrino oscillations. K2K experiment started data-taking in 1999 and was completed in 2004. The total number of protons on target (POT) for physics analysis amounted to 0.92×10^{20}. The observed number of beam-originated FC events in the 22.5 kton fiducial volume of Super-Kamiokande was 112, compared with an expectation of $158.1^{+9.2}_{-8.6}$ events without oscillation. For 58 1-ring μ-like subset of the data, the neutrino energy was reconstructed from measured muon momentum and angle, assuming CC quasi-elastic kinematics. The measured energy spectrum showed the distortion expected from neutrino oscillations. The probability that the observations are due to a statistical fluctuation instead of neutrino oscillation is 0.0015% or 4.3 σ [19].

MINOS is the second long-baseline neutrino oscillation experiment with near and far detectors. Neutrinos are produced by the NuMI (Neutrinos at the Main Injector) facility using 120 GeV protons from the Fermilab Main Injector. The far detector is a 5.4 kton (total mass) iron-scintillator tracking calorimeter with toroidal magnetic field, located underground in the Soudan mine. The baseline distance is 735 km. The near detector is also an iron-scintillator tracking calorimeter with toroidal magnetic field, with a total mass of 0.98 kton. The neutrino beam is a horn-focused wide-band beam. Its energy spectrum can be varied by moving the target position relative to the first horn and
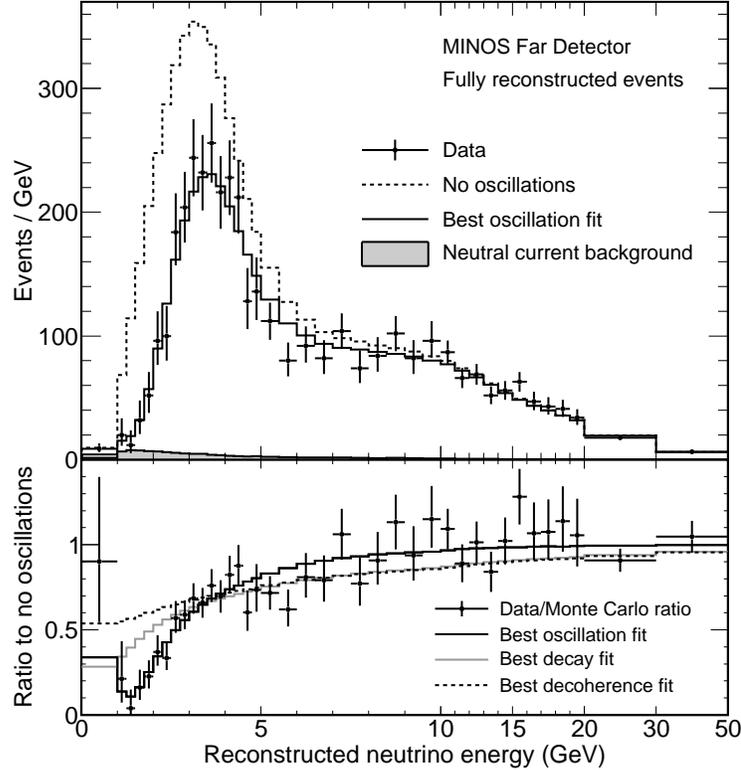
Figure 13.8: The top panel shows the energy spectra of fully reconstructed events in the MINOS far detector classified as CC interactions. The bottom panel shows the background subtracted ratios of data to the no-oscillation hypothesis. The best fit with the hypothesis of $\nu_\mu \to \nu_\tau$ oscillations as well as the best fit to alternative models (neutrino decay and decoherence) is also shown. This figure is taken from Ref. 130.

changing the horn current.

MINOS started the neutrino-beam run in 2005. Earlier ν_μ disappearance results were reported in Ref. 20 with 1.27×10^{20} POT and in Ref. 21 with 3.36×10^{20} POT. The updated results corresponding to a total POT of 7.25×10^{20} have been published recently [130]. Most of the data were taken with a "low-energy" option for the spectrum of the neutrino beam (the flux was enhanced in the 1-5 GeV energy range, peaking at 3 GeV). In the far detector, a total of 1986 fully reconstructed CC events were produced by the NuMI beam, compared to the unoscillated expectation of 2451 events. Fig. 13.8 shows the observed energy spectra and the expected spectra with no oscillation. Fig. 13.6 shows the 68% and 90% CL allowed regions obtained from the $\nu_\mu \to \nu_\tau$ oscillation analysis. The results are compared with the 90% CL allowed regions obtained from the earlier MINOS [21], SK-I zenith-angle dependence [129,79], and the SK-I L/E analysis [14]. The MINOS results constrain the oscillation parameters as $|\Delta m_A^2| = (2.32^{+0.12}_{-0.08}) \times 10^{-3}$ eV^2 and $\sin^2 2\theta_A > 0.90$ at 90% CL. The alternative models to explain the ν_μ disappearance, neutrino decay and quantum decoherence of neutrinos, are disfavored at the 7σ and 9σ, respectively, by the MINOS data (see Fig. 13.8).

In addition to ν_μ disappearance, MINOS first observed muon antineutrino disappearance [134] with the NUMI beam line optimized for $\bar{\nu}_\mu$ production. MINOS recently released $\bar{\nu}_\mu$ disappearance result corresponding to POT $= 2.95 \times 10^{20}$ [135]. With increased statistics, the best-fit oscillation parameters are $|\Delta \bar{m}_A^2| = (2.62^{+0.31}_{-0.28} \pm 0.09) \times 10^{-3}$ eV^2 and $\sin^2 2\bar{\theta}_A = 0.95^{+0.10}_{-0.11} \pm 0.01$, or $\sin^2 2\bar{\theta}_A > 0.75$ at 90% CL. These results are consistent with their neutrino counterparts.

The regions of neutrino parameter space favored or excluded by various neutrino oscillation experiments are shown in Fig. 13.9.

Although the atmospheric neutrino oscillations and accelerator long-baseline ν_μ disappearance data are fully consistent with $\nu_\mu \rightarrow \nu_\tau$ oscillations, appearance of ν_τ remained to be confirmed. For this purpose, a promising method is an accelerator long-baseline experiment using emulsion technique to identify short-lived τ leptons event-by-event. The only experiment of this kind is OPERA with a neutrino source at CERN and a detector at Gran Sasso with the baseline distance of 730 km. The detector is a combination of the "Emulsion Cloud Chamber" and magnetized spectrometer. The CNGS (CERN Neutrinos to Gran Sasso) neutrino beam with $\langle E_\nu \rangle = 17$ GeV is produced by high-energy protons from the CERN SPS. So far, OPERA reported observation of one ν_τ candidate in the hadronic decay channel of τ, corresponding to an exposure of 5.30×10^{19} POT with a target mass of 1290 tons in 2008 and 2009 runs [60,61], with expectation of 1.65 signal events [61].

13.6.   Measurements of θ_{13}

Reactor $\bar{\nu}_e$ disappearance experiments with $L \sim 1$ km, $\langle E \rangle \sim 3$ MeV are sensitive to $\sim E/L \sim 3 \times 10^{-3}$ eV$^2 \sim |\Delta m_A^2|$. At this baseline distance, the reactor $\bar{\nu}_e$ oscillations driven by $\Delta m_\odot^2$ are negligible. Therefore, as can be seen from Eq. (13.22) and Eq. (13.24), θ_{13} can be directly measured. A reactor neutrino oscillation experiment at the Chooz nuclear power station in France [58] was the first experiment of this kind. The detector was located in an underground laboratory with 300 mwe (meter water equivalent) rock overburden, at about 1 km from the neutrino source. It consisted of a central 5-ton target filled with 0.09% gadolinium loaded liquid scintillator, surrounded by an intermediate 17-ton and outer 90-ton regions filled with undoped liquid scintillator. Reactor $\bar{\nu}_e$'s were detected via the reaction $\bar{\nu}_e + p \rightarrow e^+ + n$. Gd-doping was chosen to maximize the neutron capture efficiency. The Chooz experiment [58] found no evidence for $\bar{\nu}_e$ disappearance. The 90% CL upper limit for $|\Delta m_A^2| = 2.0 \times 10^{-3}$ eV^2 is $\sin^2 2\theta_{13} < 0.19$, and for the MINOS 2008 measurement [21] of $|\Delta m_A^2| = 2.43 \times 10^{-3}$ eV it is $\sin^2 2\theta_{13} < 0.15$, both at 90% CL.

In the accelerator neutrino oscillation experiments with conventional neutrino beams, θ_{13} can be measured using $\nu_\mu \rightarrow \nu_e$ appearance. K2K was the first long-baseline experiment to search for ν_e appearance signal due to the $\nu_\mu \rightarrow \nu_e$ oscillations [136]. Based on the dominant term in the probability of $\nu_\mu \rightarrow \nu_e$ oscillations (see Eq. (13.23) and Eq. (13.24)),

$$P(\nu_\mu \rightarrow \nu_e) = \sin^2 2\theta_{13} \cdot \sin^2 \theta_{23} \cdot \sin^2(1.27 \Delta m_A^2 L/E)$$
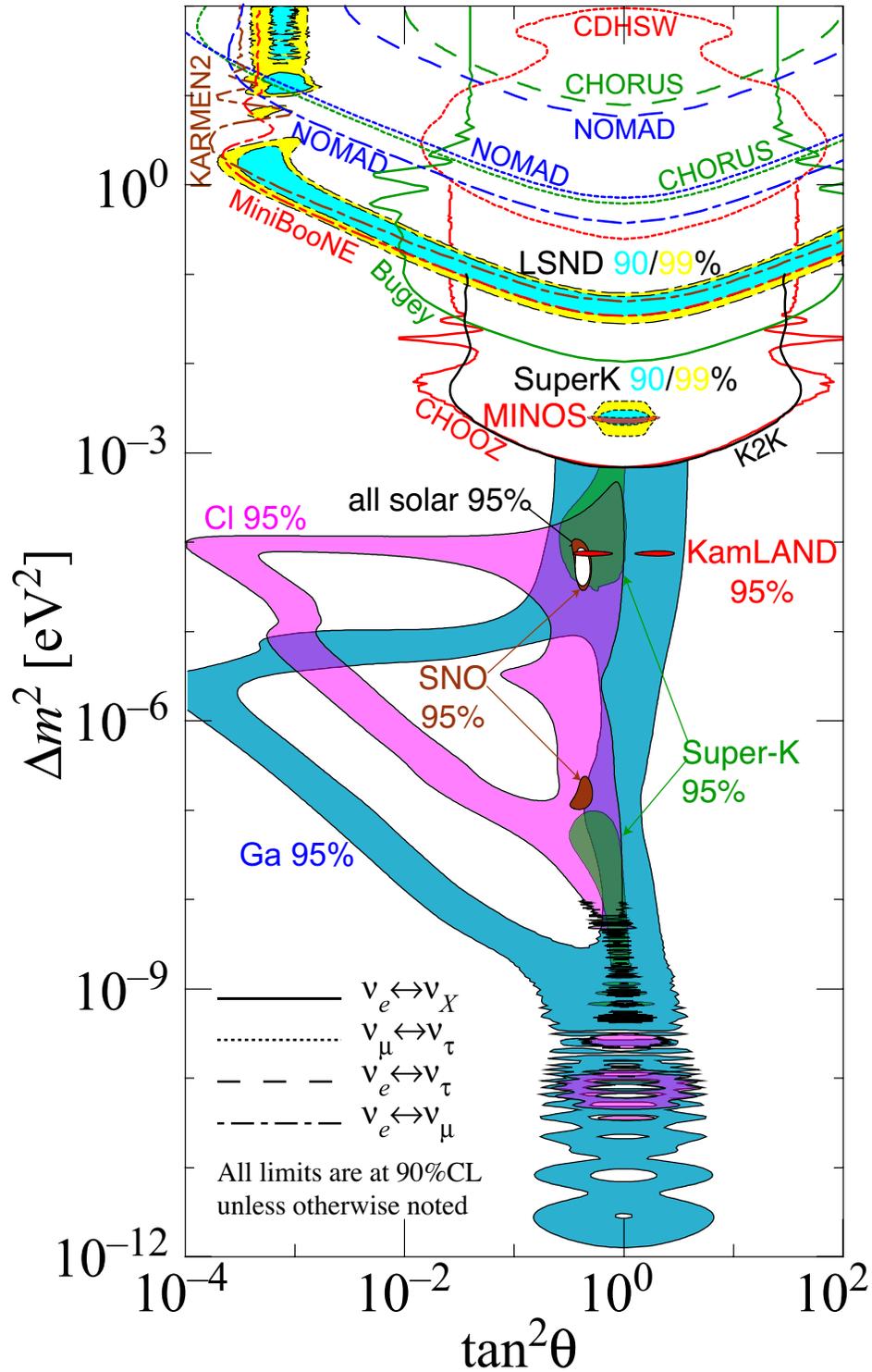
Figure 13.9: The regions of squared-mass splitting and mixing angle favored or excluded by various experiments based on two-flavor neutrino oscillation analyses. The figure was contributed by H. Murayama (University of California, Berkeley, and IPMU, University of Tokyo). References to the data used in the figure can be found at `http://hitoshi.berkeley.edu/neutrino`.

$$\sim \frac{1}{2} \sin^2 2\theta_{13} \sin^2(1.27\Delta m_{\mathrm{A}}^2 L/E). \tag{13.75}$$

K2K set the 90% CL upper limit $\sin^2 2\theta_{13} < 0.26$.

By examining the expression for the probability of $\nu_\mu \to \nu_e$ oscillations in matter (given by Eq. (13.45) in which the sign of the $P_{\sin\delta}$ term is flipped), however, it is understood that subleading terms could have rather large effects and the unknown CP-violating phase δ causes uncertainties in determining the value of θ_{13}. Actually, from the measurement of $\nu_\mu \to \nu_e$ appearance, θ_{13} is given as a function of δ for a given sign of Δm_{A}^2, or of $\Delta m_{32}^2 \cong \Delta m_{31}^2$. (Also, deviations from maximal θ_{23} mixing would cause a further uncertainty.) Therefore, a single experiment with a neutrino beam cannot determine the value of θ_{13}, although it is possible to establish a non-zero θ_{13}. In 2010, MINOS [137] set the limits for $2 \sin^2 \theta_{23} \sin^2 2\theta_{13}$ as a function of δ. At $\delta = 0$, the 90% CL upper limit is 0.12 (0.20) for $\Delta m_{\mathrm{A}}^2 > 0$ ($\Delta m_{\mathrm{A}}^2 < 0$).

In 2011, experimental indications of $\nu_\mu \to \nu_e$ oscillations and a non-zero θ_{13} have been reported by the T2K [24] experiment. Also, MINOS [25] searched for $\nu_\mu \to \nu_e$ appearance and disfavored the $\theta_{13} = 0$ hypothesis at the 89% CL.

The T2K experiment is the first off-axis long-baseline neutrino oscillation experiment. The baseline distance is 295 km between the J-PARC in Tokai, Japan and Super-Kamiokande. A narrow-band ν_μ beam produced by 30 GeV protons from the J-PARC Main Ring is directed 2.5° off-axis to SK. With this configuration, the ν_μ beam is tuned to the first oscillation maximum. With 1.43×10^{20} POT, the T2K [24] Collaboration observed six candidate ν_e events having all characteristics of being due to $\nu_\mu \to \nu_e$ oscillations, while the expectation for $\theta_{13} = 0$ is 1.5 ± 0.3 events. The probability to observe six or more candidate events when 1.5 ± 0.3 events are predicted is 7×10^{-3}, implying a non-zero θ_{13} with statistical significance of 2.5σ. At $\delta = 0$, $\sin^2 2\theta_{23} = 1$ and $|\Delta m_{\mathrm{A}}^2| = 2.4 \times 10^{-3}$ eV^2, this result gives a best fit value of $\sin^2 2\theta_{13} = 0.11$ (0.14) and a 90% CL interval of $0.03\ (0.04) < \sin^2 2\theta_{13} < 0.28\ (0.34)$ for $\Delta m_{\mathrm{A}}^2 > 0$ ($\Delta m_{\mathrm{A}}^2 < 0$).

The MINOS Collaboration [25] also searched for the $\nu_\mu \to \nu_e$ appearance signal. Though dependent on the definition of the signal, typically 62 candidate events are observed with an exposure of 8.2×10^{20} POT, while the expectation for $\theta_{13} = 0$ is $49.6 \pm 7.0 \pm 2.7$ events. At the 90% CL, the MINOS result implies that $2 \sin^2 2\theta_{13} \sin^2 \theta_{23} < 0.12$ (0.20) for $\Delta m_{\mathrm{A}}^2 > 0$ ($\Delta m_{\mathrm{A}}^2 < 0$) and $\delta = 0$, with a best fit value $2 \sin^2 \theta_{23} \sin^2 2\theta_{13} = 0.041^{+0.047}_{-0.031}$ ($0.079^{+0.071}_{-0.053}$). The MINOS data disfavored the $\theta_{13} = 0$ hypothesis at the 89% CL [25].

Recently, the three reactor neutrino experiments Double Chooz [59], Daya Bay [26], and RENO [27] reported their first results on reactor $\bar{\nu}_e$ disappearance. Daya Bay and RENO measured reactor $\bar{\nu}_e$s with near and far detectors. The first results of Double Chooz was obtained with only a far detector, though this experiment is planning to have a near detector in 2012. The $\bar{\nu}_e$ detectors of all the three experiments have similar structures; an antineutrino detector consisting of three layers and an optically independent outer veto detector. The innermost layer of the antineutrino detector is filled with Gd-doped liquid scintillator (LS), which is surrounded by a "γ-catcher" layer filled with Gd-free LS, and outside the γ-catcher is a buffer layer filled with mineral oil. An

outer veto detector is filled with purified water (Daya Bay and RENO) or LS (Double Chooz).

The Daya Bay experiment [26] measured $\bar{\nu}_e$s from the Daya Bay nuclear power complex (six 2.9 GW$_{\text{th}}$ reactors) in China with six functionally identical detectors deployed in two near (470 m and 576 m of flux-weighted baselines) and one far (1648 m) underground halls. With live time of 55 days, the ratio of the observed to expected number of $\bar{\nu}_e$s at the far hall is $R = 0.940 \pm 0.011 \pm 0.004$ and the rate-only analysis yielded

$$\sin^2 2\theta_{13} = 0.092 \pm 0.016 \pm 0.005. \tag{13.76}$$

From this result, θ_{13} is non-zero with a significance of 5.2σ.

The RENO experiment [27] measured $\bar{\nu}_e$s from six 2.8 GW$_{\text{th}}$ reactors at Yonggwang Nuclear Power Plant in Korea with two identical detectors located at 294 m and 1383 m from the reactor array center. With 229 days of running time, the ratio of the observed to expected number of $\bar{\nu}_e$s in the far detector is $R = 0.920 \pm 0.009 \pm 0.014$, and from a rate-only analysis the following result is obtained:

$$\sin^2 2\theta_{13} = 0.113 \pm 0.013 \pm 0.019 \tag{13.77}$$

This result excludes the no-oscillation hypothesis at the 4.9σ level.

The Double Chooz experiment [59] measured $\bar{\nu}_e$s from two 4.25 GW$_{\text{th}}$ reactors with a far detector at 1050 m from the two reactor cores. With 101 days of running, this experiment obtained $\sin^2 2\theta_{13} = 0.086 \pm 0.041 \pm 0.030$, or $0.017 < \sin^2 2\theta_{13} < 0.16$ at the 90% CL, by analyzing the rate and energy spectrum of prompt positrons using the reactor $\bar{\nu}_e$ spectrum of Ref. 36 and Ref. 34 and the Bugey4 rate measurement [138].

Turning to atmospheric and solar neutrino observations, Eq. (13.40) to Eq. (13.43) and Eq. (13.62) indicate that they are sensitive to θ_{13} through sub-leading effects. So far, the SK, SNO, and KamLAND Collaborations presented their own θ_{13} analyses by adding or updating their own data. In the atmospheric neutrino sector, the SK group analyzed its atmospheric neutrino data [79,139], and in the solar neutrino sector, SNO [117], SK [114], and KamLAND [128] analyzed the data from all solar neutrino experiments, with or without the KamLAND data, in terms of 3-neutrino oscillations. In addition, KamLAND [128] made a global analysis of all available neutrino data incorporating the Chooz, atmospheric and accelerator data. All these results are consistent with the recent results from accerelator [24,25] and reactor [59,26,27] experiments.

13.7.   The three neutrino mixing

All existing compelling data on neutrino oscillations can be described assuming 3-flavour neutrino mixing in vacuum. This is the minimal neutrino mixing scheme which can account for the currently available data on the oscillations of the solar (ν_e), atmospheric (ν_μ and $\bar{\nu}_\mu$), reactor ($\bar{\nu}_e$) and accelerator (ν_μ) neutrinos. The (left-handed) fields of the flavour neutrinos ν_e, ν_μ and ν_τ in the expression for the weak charged

lepton current in the CC weak interaction Lagrangian, are linear combinations of the LH components of the fields of three massive neutrinos ν_j:

$$\mathcal{L}_{\text{CC}} = -\frac{g}{\sqrt{2}} \sum_{l=e,\mu,\tau} \overline{l_L}(x)\,\gamma_\alpha\,\nu_{lL}(x)\,W^{\alpha\dagger}(x) + h.c.\,,$$

$$\nu_{l\text{L}}(x) = \sum_{j=1}^{3} U_{lj}\,\nu_{j\text{L}}(x), \tag{13.78}$$

where U is the 3×3 unitary neutrino mixing matrix [17,18]. The mixing matrix U can be parameterized by 3 angles, and, depending on whether the massive neutrinos ν_j are Dirac or Majorana particles, by 1 or 3 CP violation phases [40,41]:

$$U = \begin{bmatrix} c_{12}c_{13} & s_{12}c_{13} & s_{13}e^{-i\delta} \\ -s_{12}c_{23} - c_{12}s_{23}s_{13}e^{i\delta} & c_{12}c_{23} - s_{12}s_{23}s_{13}e^{i\delta} & s_{23}c_{13} \\ s_{12}s_{23} - c_{12}c_{23}s_{13}e^{i\delta} & -c_{12}s_{23} - s_{12}c_{23}s_{13}e^{i\delta} & c_{23}c_{13} \end{bmatrix}$$
$$\times \text{diag}(1,\ e^{i\frac{\alpha_{21}}{2}},\ e^{i\frac{\alpha_{31}}{2}})\ . \tag{13.79}$$

where $c_{ij} = \cos\theta_{ij}$, $s_{ij} = \sin\theta_{ij}$, the angles $\theta_{ij} = [0, \pi/2]$, $\delta = [0, 2\pi]$ is the Dirac CP violation phase and α_{21}, α_{31} are two Majorana CP violation phases. Thus, in the case of massive Dirac neutrinos, the neutrino mixing matrix U is similar, in what concerns the number of mixing angles and CP violation phases, to the CKM quark mixing matrix. The presence of two additional physical CP violation phases in U if ν_j are Majorana particles is a consequence of the special properties of the latter (see, *e.g.*, Refs. [39,40]) .

As we see, the fundamental parameters characterizing the 3-neutrino mixing are: i) the 3 angles θ_{12}, θ_{23}, θ_{13}, ii) depending on the nature of massive neutrinos ν_j - 1 Dirac (δ), or 1 Dirac + 2 Majorana ($\delta, \alpha_{21}, \alpha_{31}$), CP violation phases, and iii) the 3 neutrino masses, m_1, m_2, m_3. Thus, depending on whether the massive neutrinos are Dirac or Majorana particles, this makes 7 or 9 additional parameters in the minimally extended Standard Model of particle interactions with massive neutrinos.

The neutrino oscillation probabilities depend (Section 13.2), in general, on the neutrino energy, E, the source-detector distance L, on the elements of U and, for relativistic neutrinos used in all neutrino experiments performed so far, on $\Delta m_{ij}^2 \equiv (m_i^2 - m_j^2)$, $i \neq j$. In the case of 3-neutrino mixing there are only two independent neutrino mass squared differences, say $\Delta m_{21}^2 \neq 0$ and $\Delta m_{31}^2 \neq 0$. The numbering of massive neutrinos ν_j is arbitrary. It proves convenient from the point of view of relating the mixing angles θ_{12}, θ_{23} and θ_{13} to observables, to identify $|\Delta m_{21}^2|$ with the smaller of the two neutrino mass squared differences, which, as it follows from the data, is responsible for the solar ν_e and, the observed by KamLAND, reactor $\bar{\nu}_e$ oscillations. We will number (just for convenience) the massive neutrinos in such a way that $m_1 < m_2$, so that $\Delta m_{21}^2 > 0$. With these choices made, there are two possibilities: either $m_1 < m_2 < m_3$, or $m_3 < m_1 < m_2$. Then the larger neutrino mass square difference $|\Delta m_{31}^2|$ or $|\Delta m_{32}^2|$, can be associated with the experimentally observed oscillations of the atmospheric ν_μ and $\bar{\nu}_\mu$ and accelerator

ν_μ. The effects of Δm^2_{31} or Δm^2_{32} in the oscillations of solar ν_e, and of Δm^2_{21} in the oscillations of atmospheric ν_μ and $\bar{\nu}_\mu$ and of accelerator ν_μ, are relatively small and subdominant as a consequence of the facts that i) L, E and L/E in the experiments with solar ν_e and with atmospheric ν_μ and $\bar{\nu}_\mu$ or accelerator ν_μ, are very different, ii) the conditions of production and propagation (on the way to the detector) of the solar ν_e and of the atmospheric ν_μ and $\bar{\nu}_\mu$ or accelerator ν_μ, are very different, and iii) $|\Delta m^2_{21}|$ and $|\Delta m^2_{31}|$ ($|\Delta m^2_{32}|$) in the case of $m_1 < m_2 < m_3$ ($m_3 < m_1 < m_2$), as it follows from the data, differ by approximately a factor of 30, $|\Delta m^2_{21}| \ll |\Delta m^2_{31(32)}|$, $|\Delta m^2_{21}|/|\Delta m^2_{31(32)}| \cong 0.03$. This implies that in both cases of $m_1 < m_2 < m_3$ and $m_3 < m_1 < m_2$ we have $\Delta m^2_{32} \cong \Delta m^2_{31}$ with $|\Delta m^2_{31} - \Delta m^2_{32}| = |\Delta m^2_{21}| \ll |\Delta m^2_{31,32}|$.

It follows from the results of the Chooz experiment with reactor $\bar{\nu}_e$ [58] and from the more recent data discussed in the preceding subsection that, in the convention we use, in which $0 < \Delta m^2_{21} < |\Delta m^2_{31(32)}|$, the element $|U_{e3}|=\sin\theta_{13}$ of the neutrino mixing matrix U, as the results of the Daya Bay and RENO experiments show, is small. This makes it possible to identify the angles θ_{12} and θ_{23} as the neutrino mixing angles associated with the solar ν_e and the dominant atmospheric ν_μ (and $\bar{\nu}_\mu$) oscillations, respectively. The angles θ_{12} and θ_{23} are often called "solar" and "atmospheric" neutrino mixing angles, and are often denoted as $\theta_{12} = \theta_\odot$ and $\theta_{23} = \theta_A$ (or θ_{atm}) while Δm^2_{21} and Δm^2_{31} are often referred to as the "solar" and "atmospheric" neutrino mass squared differences and are often denoted as $\Delta m^2_{21} \equiv \Delta m^2_\odot$, $\Delta m^2_{31} \equiv \Delta m^2_A$ (or Δm^2_{atm}).

The solar neutrino data tell us that $\Delta m^2_{21} \cos 2\theta_{12} > 0$. In the convention employed by us we have $\Delta m^2_{21} > 0$. Correspondingly, in this convention one must have $\cos 2\theta_{12} > 0$.

Global analyses [140,141] of the existing neutrino oscillation data, including the T2K [24] and MINOS [25]   (but not the Daya Bay [26] and RENO [27])   results, allowed us to determine the parameters which drive the solar neutrino and the dominant atmospheric neutrino oscillations, $\Delta m^2_\odot = \Delta m^2_{21}$, θ_{12}, and $|\Delta m^2_A| = |\Delta m^2_{31}| \cong |\Delta m^2_{32}|$, θ_{23}, with a relatively good precision, and to establish that the angle $\theta_{13} \neq 0$ at $\gtrsim 99.73\%$ CL. The Daya Bay and RENO experiments provided a rather precise determination of the angle θ_{13}. Analyses of the global neutrino oscillation data, in which the Daya Bay and RENO results on θ_{13} are also included, are lacking at present. Therefore we present in Table 13.7 the best fit values and the 99.73% CL allowed ranges of Δm^2_{21}, $\sin^2\theta_{12}$, $|\Delta m^2_{31(32)}|$, $\sin^2\theta_{23}$ and $\sin^2\theta_{13}$, found in Ref. 140 as well as the PDG average [142] of the results of the three recent reactor experiments [26,27,59].   Since the PDG average of $\sin^2\theta_{13}$ is very close to that obtained in the global analysis in Ref. 140, and since the other oscillation parameter ranges are almost uncorrelated from θ_{13}, we do not expect that the inclusion of the Daya Bay and RENO data will change significantly the results (neither the central values nor the errors) for Δm^2_{21}, $\sin^2\theta_{12}$, $|\Delta m^2_{31(32)}|$ and $\sin^2\theta_{23}$ obtained in Ref. 140. Obviously, the uncertainty in the value of $\sin^2\theta_{13}$ will shrink considerably. We note also that the results from Ref. 140 quoted in Table 13.7 are derived by marginalizing over $\text{sgn}(\Delta m^2_{31}) = \pm 1$ and over $\cos\delta = \pm 1$ and that the values (the values in brackets) of $\sin^2\theta_{12}$ and $\sin^2\theta_{13}$ are obtained in Ref. 140 using the reactor $\bar{\nu}_e$ fluxes from Ref. 35 (from Ref. 34).

Table 13.7: The best-fit values and 3σ allowed ranges of the 3-neutrino oscillation parameters, derived from a global fit of the current neutrino oscillation data, including the T2K and MINOS (but not the Daya Bay and RENO) results (from [140]) . The PDG average of the results of the three recent reactor experiments [26,27,59] is given in the last line [142]. The values (values in brackets) of $\sin^2\theta_{12}$ and $\sin^2\theta_{13}$ are obtained using the "old" [35] ("new" [34]) reactor $\bar{\nu}_e$ fluxes in the analysis.

Parameter	best-fit ($\pm 1\sigma$)	3σ
$\Delta m^2_{\odot}$ [10^{-5} eV ^{2}]	$7.58^{+0.22}_{-0.26}$	$6.99 - 8.18$
$\|\Delta m^2_A\|$ [10^{-3} eV ^{2}]	$2.35^{+0.12}_{-0.09}$	$2.06 - 2.67$
$\sin^2\theta_{12}$	$0.306\ (0.312)^{+0.018}_{-0.015}$	$0.259\ (0.265) - 0.359\ (0.364)$
$\sin^2\theta_{23}$	$0.42^{+0.08}_{-0.03}$	$0.34 - 0.64$
$\sin^2\theta_{13}$ [140]	$0.021\ (0.025)^{+0.007}_{-0.008}$	$0.001\ (0.005) - 0.044\ (0.050)$
$\sin^2\theta_{13}$ [142]	0.0251 ± 0.0034	$0.015 - 0.036$

A combined analysis of the data on θ_{13} from the T2K, MINOS, Double Chooz, Daya Bay and RENO experiments was performed in Ref. 145. The authors find that $\theta_{13} \neq 0$ at 7.7σ:

$$\sin^2 2\theta_{13} = 0.096 \pm 0.013\ (\pm 0.040)\ \text{at}\ 1\sigma\ (3\sigma) \tag{13.80}$$

In this analysis the positive or negative sign of Δm^2_A was used as input and the values of $\sin^2 2\theta_{23}$ and $|\Delta m^2_A|$ were varied imposing Gaussian priors based on the results of the atmospheric neutrino [139] and MINOS [130] experiments. The value of $\sin^2 2\theta_{13}$ thus obtained showed a statistically insignificant dependence on the Dirac phase δ.

It follows from the results given in Table 13.7 that $\theta_{23} \cong \pi/4$, $\theta_{12} \cong \pi/5.4$ and that $\theta_{13} \cong \pi/20$. Correspondingly, the pattern of neutrino mixing is drastically different from the pattern of quark mixing.

Note also that Δm^2_{21}, $\sin^2\theta_{12}$, $|\Delta m^2_{31(32)}|$, $\sin^2\theta_{23}$ and $\sin^2\theta_{13}$ are determined from the data with a 1σ uncertainty ($= 1/6$ of the 3σ range) of approximately 2.6%, 5.4%, 4.3%, 12% and absolute error 0.42×10^{-2}, respectively.

The existing SK atmospheric neutrino, K2K and MINOS data do not allow to determine the sign of $\Delta m^2_{31(32)}$. Maximal solar neutrino mixing, *i.e.*, $\theta_{12} = \pi/4$, is ruled out at more than 6σ by the data. Correspondingly, one has $\cos 2\theta_{12} \geq 0.27$ (at 99.73% CL).

At present no experimental information on the Dirac and Majorana CP violation phases in the neutrino mixing matrix is available. Thus, the status of CP symmetry in the lepton sector is unknown. With $\theta_{13} \neq 0$, the Dirac phase δ can generate CP violation effects in neutrino oscillations [40,52,53]. The magnitude of CP violation in $\nu_l \to \nu_{l'}$ and

$\bar{\nu}_l \to \bar{\nu}_{l'}$ oscillations, $l \neq l' = e, \mu, \tau$, is determined, as we have seen, by the rephasing invariant J_{CP} (see Eq. (13.19)), which in the "standard" parametrisation of the neutrino mixing matrix (Eq. (13.79)) has the form:

$$J_{CP} \equiv \mathrm{Im}\,(U_{\mu 3}\,U_{e3}^*\,U_{e2}\,U_{\mu 2}^*) = \frac{1}{8}\,\cos\theta_{13}\,\sin 2\theta_{12}\,\sin 2\theta_{23}\,\sin 2\theta_{13}\,\sin\delta\,. \qquad (13.81)$$

Thus, given the fact that $\sin 2\theta_{12}$, $\sin 2\theta_{23}$ and $\sin 2\theta_{13}$ have been determined experimentally with a relatively good precision, the size of CP violation effects in neutrino oscillations depends essentially only on the magnitude of the currently unknown value of the Dirac phase δ. The current data implies $|J_{CP}| \lesssim 0.045$, where we have used the 3σ ranges of $\sin^2\theta_{12}$, $\sin^2\theta_{23}$ and $\sin^2\theta_{13}$ given in Table 13.7 and Eq. (13.76), respectively.

As we have indicated, the existing data do not allow one to determine the sign of $\Delta m_{\mathrm{A}}^2 = \Delta m_{31(2)}^2$. In the case of 3-neutrino mixing, the two possible signs of $\Delta m_{31(2)}^2$ correspond to two types of neutrino mass spectrum. In the widely used conventions of numbering the neutrinos with definite mass in the two cases, the two spectra read:

   – i) spectrum with normal ordering:

$$m_1 < m_2 < m_3,\ \Delta m_{\mathrm{A}}^2 = \Delta m_{31}^2 > 0,$$

$$\Delta m_{\odot}^2 \ \equiv \Delta m_{21}^2 > 0,\ m_{2(3)} = (m_1^2 + \Delta m_{21(31)}^2)^{\frac{1}{2}};$$

   – ii) spectrum with inverted ordering (IO):

$$m_3 < m_1 < m_2,\ \Delta m_{\mathrm{A}}^2 = \Delta m_{32}^2 < 0,\ \Delta m_{\odot}^2 \ \equiv \Delta m_{21}^2 > 0,$$

$$m_2 = (m_3^2 + \Delta m_{23}^2)^{\frac{1}{2}},\ m_1 = (m_3^2 + \Delta m_{23}^2 - \Delta m_{21}^2)^{\frac{1}{2}}.$$

Depending on the values of the lightest neutrino mass [143], $\min(m_j)$, the neutrino mass spectrum can also be:

   – *Normal Hierarchical (NH)*:

$$m_1 \ll m_2 < m_3,\ m_2 \cong (\Delta m_{\odot}^2\ )^{\frac{1}{2}} \cong 0.0086\ \mathrm{eV},$$

$$m_3 \cong |\Delta m_{\mathrm{A}}^2|^{\frac{1}{2}} \cong 0.048\ \mathrm{eV};\ \mathrm{or}$$

   – *Inverted Hierarchical (IH)*:

$$m_3 \ll m_1 < m_2,\ \mathrm{with}\ m_{1,2} \cong |\Delta m_{\mathrm{A}}^2|^{\frac{1}{2}} \cong 0.048\ \mathrm{eV};\ \mathrm{or}$$

   – *Quasi-Degenerate (QD)*:

$$m_1 \cong m_2 \cong m_3 \cong m_0,\ m_j^2 \gg |\Delta m_{\mathrm{A}}^2|,\ m_0 \gtrsim 0.10\ \mathrm{eV}.$$

All three types of spectrum are compatible with the existing constraints on the absolute scale of neutrino masses m_j. Information about the latter can be obtained, *e.g.*, by measuring the spectrum of electrons near the end point in $^3\mathrm{H}$ β-decay experiments [146–149] and from cosmological and astrophysical data. The most stringent upper bounds on the $\bar{\nu}_e$ mass were obtained in the Troitzk [147,148] experiment:

$$m_{\bar{\nu}_e} < 2.05\ \mathrm{eV} \quad \mathrm{at}\ 95\%\ \mathrm{CL}. \qquad (13.82)$$

We have $m_{\bar{\nu}_e} \cong m_{1,2,3}$ in the case of QD spectrum. The KATRIN experiment [149] is planned to reach sensitivity of $m_{\bar{\nu}_e} \sim 0.20$ eV, *i.e.*, it will probe the region of the QD spectrum.

The Cosmic Microwave Background (CMB) data of the WMAP experiment, combined with supernovae data and data on galaxy clustering can be used to obtain an upper limit on the sum of neutrinos masses (see review on Cosmological Parameters [150] and, *e.g.*, Ref. 151). Depending on the model complexity and the input data used one obtains [151]: $\sum_j m_j \lesssim (0.3 - 1.3)$ eV, 95% CL.

It follows from these data that neutrino masses are much smaller than the masses of charged leptons and quarks. If we take as an indicative upper limit $m_j \lesssim 0.5$ eV, we have $m_j/m_{l,q} \lesssim 10^{-6}$, $l = e, \mu, \tau$, $q = d, s, b, u, c, t$. It is natural to suppose that the remarkable smallness of neutrino masses is related to the existence of a new fundamental mass scale in particle physics, and thus to new physics beyond that predicted by the Standard Model.

13.7.1.   *The see-saw mechanism and the baryon asymmetry of the Universe* :

A natural explanation of the smallness of neutrino masses is provided by the (type I) see-saw mechanism of neutrino mass generation [3]. An integral part of this rather simple mechanism [152] are the RH neutrinos ν_{lR} (RH neutrino fields $\nu_{lR}(x)$). The latter are assumed to possess a Majorana mass term as well as Yukawa type coupling $\mathcal{L}_Y(x)$ with the Standard Model lepton and Higgs doublets, $\psi_{lL}(x)$ and $\Phi(x)$, respectively, $(\psi_{lL}(x))^T = (\nu_{lL}^T(x) \quad l_L^T(x))$, $l = e, \mu, \tau$, $(\Phi(x))^T = (\Phi^{(0)} \quad \Phi^{(-)})$. In the basis in which the Majorana mass matrix of RH neutrinos is diagonal, we have:

$$\mathcal{L}_{Y,M}(x) = \left(\lambda_{il} \, \overline{N_{iR}}(x) \, \Phi^\dagger(x) \, \psi_{lL}(x) + \text{h.c.} \right) - \frac{1}{2} \, M_i \, \overline{N_i}(x) \, N_i(x) , \qquad (13.83)$$

where λ_{il} is the matrix of neutrino Yukawa couplings and N_i ($N_i(x)$) is the heavy RH Majorana neutrino (field) possessing a mass $M_i > 0$. When the electroweak symmetry is broken spontaneously, the neutrino Yukawa coupling generates a Dirac mass term: $m_{il}^D \, \overline{N_{iR}}(x) \, \nu_{lL}(x) + \text{h.c.}$, with $m^D = v\lambda$, $v = 174$ GeV being the Higgs doublet v.e.v. In the case when the elements of m^D are much smaller than M_k, $|m_{il}^D| \ll M_k$, $i, k = 1, 2, 3$, $l = e, \mu, \tau$, the interplay between the Dirac mass term and the mass term of the heavy (RH) Majorana neutrinos N_i generates an effective Majorana mass (term) for the LH flavour neutrinos [3]: $m_{l'l}^{LL} \cong -(m^D)_{l'j}^T M_j^{-1} m_{jl}^D$. In grand unified theories, m^D is typically of the order of the charged fermion masses. In $SO(10)$ theories, for instance, m^D coincides with the up-quark mass matrix. Taking indicatively $m^{LL} \sim 0.1$ eV, $m^D \sim 100$ GeV, one finds $M \sim 10^{14}$ GeV, which is close to the scale of unification of the electroweak and strong interactions, $M_{GUT} \cong 2 \times 10^{16}$ GeV. In GUT theories with RH neutrinos one finds that indeed the heavy Majorana neutrinos N_j naturally obtain masses which are by few to several orders of magnitude smaller than M_{GUT}. Thus, the enormous disparity between the neutrino and charged fermion masses is explained in this approach by the huge difference between effectively the electroweak symmetry breaking scale and M_{GUT}.

An additional attractive feature of the see-saw scenario is that the generation and smallness of neutrino masses is related via the leptogenesis mechanism [2] to the

generation of the baryon asymmetry of the Universe. The Yukawa coupling in Eq. (13.83), in general, is not CP conserving. Due to this CP-nonconserving coupling the heavy Majorana neutrinos undergo, *e.g.*, the decays $N_j \to l^+ + \Phi^{(-)}$, $N_j \to l^- + \Phi^{(+)}$, which have different rates: $\Gamma(N_j \to l^+ + \Phi^{(-)}) \neq \Gamma(N_j \to l^- + \Phi^{(+)})$. When these decays occur in the Early Universe at temperatures somewhat below the mass of, say, N_1, so that the latter are out of equilibrium with the rest of the particles present at that epoch, CP violating asymmetries in the individual lepton charges L_l, and in the total lepton charge L, of the Universe are generated. These lepton asymmetries are converted into a baryon asymmetry by $(B - L)$ conserving, but $(B + L)$ violating, sphaleron processes, which exist in the Standard Model and are effective at temperatures $T \sim (100 - 10^{12})$ GeV. If the heavy neutrinos N_j have hierarchical spectrum, $M_1 \ll M_2 \ll M_3$, the observed baryon asymmetry can be reproduced provided the mass of the lightest one satisfies $M_1 \gtrsim 10^9$ GeV [153]. Thus, in this scenario, the neutrino masses and mixing and the baryon asymmetry have the same origin - the neutrino Yukawa couplings and the existence of (at least two) heavy Majorana neutrinos. Moreover, quantitative studies based on recent advances in leptogenesis theory [154] have shown that the Dirac and/or Majorana phases in the neutrino mixing matrix U can provide the CP violation, necessary in leptogenesis for the generation of the observed baryon asymmetry of the Universe [155]. This implies, in particular, that if the CP symmetry is established not to hold in the lepton sector due to U, at least some fraction (if not all) of the observed baryon asymmetry might be due to the Dirac and/or Majorana CP violation present in the neutrino mixing.

13.7.2.   *The nature of massive neutrinos* :

The experiments studying flavour neutrino oscillations cannot provide information on the nature - Dirac or Majorana, of massive neutrinos [40,54]. Establishing whether the neutrinos with definite mass ν_j are Dirac fermions possessing distinct antiparticles, or Majorana fermions, i.e. spin 1/2 particles that are identical with their antiparticles, is of fundamental importance for understanding the origin of ν-masses and mixing and the underlying symmetries of particle interactions (see *e.g.*, Ref. 66). The neutrinos with definite mass ν_j will be Dirac fermions if the particle interactions conserve some additive lepton number, *e.g.*, the total lepton charge $L = L_e + L_\mu + L_\tau$. If no lepton charge is conserved, ν_j will be Majorana fermions (see *e.g.*, Ref. 39). The massive neutrinos are predicted to be of Majorana nature by the see-saw mechanism of neutrino mass generation [3]. The observed patterns of neutrino mixing and of neutrino mass squared differences can be related to Majorana massive neutrinos and the existence of an approximate symmetry in the lepton sector corresponding, *e.g.*, to the conservation of the lepton charge $L' = L_e - L_\mu - L_\tau$ [156]. Determining the nature of massive neutrinos ν_j is one of the fundamental and most challenging problems in the future studies of neutrino mixing.

The Majorana nature of massive neutrinos ν_j manifests itself in the existence of processes in which the total lepton charge L changes by two units: $K^+ \to \pi^- + \mu^+ + \mu^+$, $\mu^- + (A, Z) \to \mu^+ + (A, Z - 2)$, *etc.* Extensive studies have shown that the only feasible experiments having the potential of establishing that the massive neutrinos are Majorana particles are at present the experiments searching for $(\beta\beta)_{0\nu}$-decay:
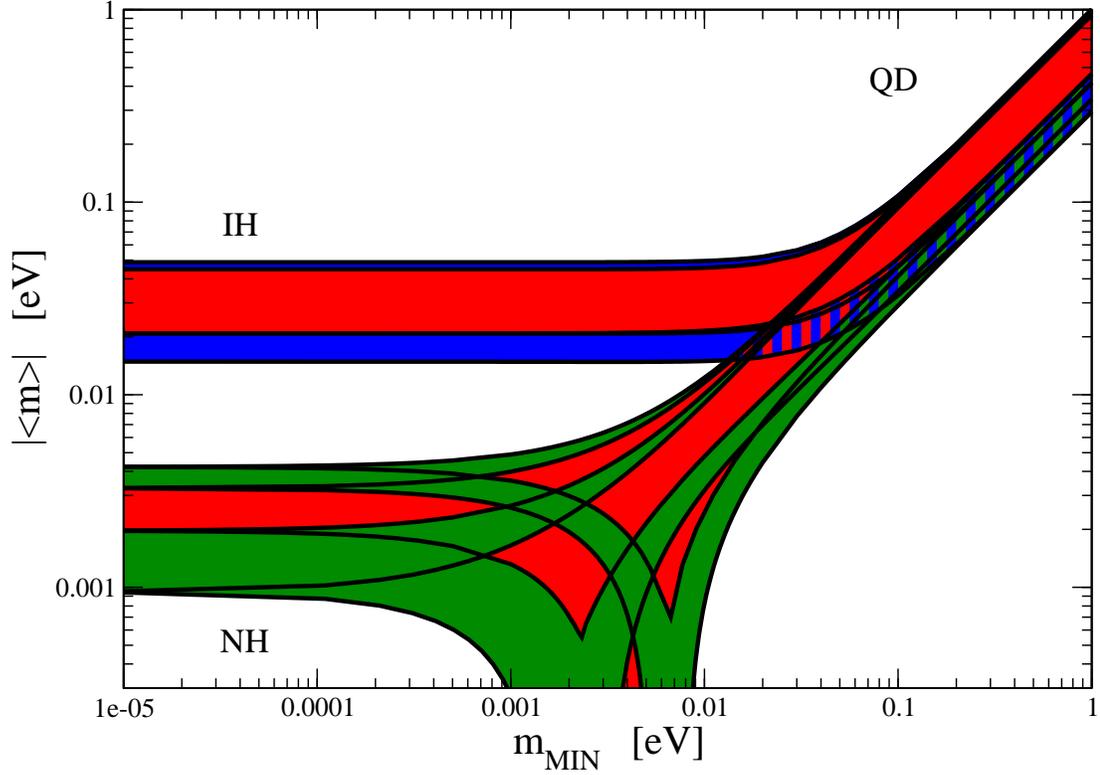
Figure 13.10: The effective Majorana mass $|<m>|$ (including a 2σ uncertainty), as a function of $\min(m_j)$ for $\sin^2\theta_{13} = 0.0236 \pm 0.0042$ [26] and $\delta = 0$. The figure is obtained using also the best fit values and 1σ errors of Δm_{21}^2, $\sin^2\theta_{12}$, and $|\Delta m_{31}^2| \cong |\Delta m_{32}^2|$ from Ref. 140 (given in Table 13.7). For $\sin^2\theta_{12}$ the results found with the "old" reactor $\bar{\nu}_e$ fluxes [35] were employed. The phases $\alpha_{21,31}$ are varied in the interval $[0,\pi]$. The predictions for the NH, IH and QD spectra are indicated. The red regions correspond to at least one of the phases $\alpha_{21,31}$ and $(\alpha_{31} - \alpha_{21})$ having a CP violating value, while the blue and green areas correspond to $\alpha_{21,31}$ possessing CP conserving values. (Update by S. Pascoli of a figure from the last article quoted in Ref. 160.)

$(A, Z) \to (A, Z + 2) + e^- + e^-$ (see *e.g.*, Ref. 157). The observation of $(\beta\beta)_{0\nu}$-decay and the measurement of the corresponding half-life with sufficient accuracy, would not only be a proof that the total lepton charge is not conserved, but might also provide unique information on the i) type of neutrino mass spectrum (see, *e.g.*, Ref. 158), ii) Majorana phases in U [144,159] and iii) the absolute scale of neutrino masses (for details see Ref. 157 to Ref. 160 and references quoted therein).

Under the assumptions of 3-ν mixing, of massive neutrinos ν_j being Majorana particles, and of $(\beta\beta)_{0\nu}$-decay generated only by the (V-A) charged current weak interaction via the exchange of the three Majorana neutrinos ν_j having masses $m_j \lesssim$ few MeV, the $(\beta\beta)_{0\nu}$-decay amplitude has the form (see, *e.g.*, Ref. 39 and Ref. 157): $A(\beta\beta)_{0\nu} \cong <m> M$, where M is the corresponding nuclear matrix element which does

not depend on the neutrino mixing parameters, and

$$|<m>| = \left| m_1 U_{e1}^2 + m_2 U_{e2}^2 + m_3 U_{e3}^2 \right|$$
$$= \left| \left(m_1 c_{12}^2 + m_2 s_{12}^2 e^{i\alpha_{21}} \right) c_{13}^2 + m_3 s_{13}^2 e^{i(\alpha_{31}-2\delta)} \right|, \tag{13.84}$$

is the effective Majorana mass in $(\beta\beta)_{0\nu}$-decay. In the case of CP-invariance one has [42], $\eta_{21} \equiv e^{i\alpha_{21}} = \pm 1$, $\eta_{31} \equiv e^{i\alpha_{31}} = \pm 1$, $e^{-i2\delta} = 1$. The three neutrino masses $m_{1,2,3}$ can be expressed in terms of the two measured Δm_{jk}^2 and, *e.g.*, $\min(m_j)$. Thus, given the neutrino oscillation parameters Δm_{21}^2, $\sin^2\theta_{12}$, Δm_{31}^2 and $\sin^2\theta_{13}$, $|<m>|$ is a function of the lightest neutrino mass $\min(m_j)$, the Majorana (and Dirac) CP violation phases in U and of the type of neutrino mass spectrum. In the case of NH, IH and QD spectrum we have (see, *e.g.*, Ref. 144 and Ref. 160):

$$|<m>| \cong \left| \sqrt{\Delta m_{21}^2} s_{12}^2 c_{13}^2 + \sqrt{\Delta m_{31}^2} s_{13}^2 e^{i(\alpha_{31}-\alpha_{21}-2\delta)} \right|, \quad \text{NH}, \tag{13.85}$$

$$|<m>| \cong \tilde{m} \left(1 - \sin^2 2\theta_{12} \sin^2 \frac{\alpha_{21}}{2} \right)^{\frac{1}{2}}, \quad \text{IH (IO) and QD}, \tag{13.86}$$

where $\tilde{m} \equiv \sqrt{\Delta m_{23}^2 + m_3^2}$ and $\tilde{m} \equiv m_0$ for IH (IO) and QD spectrum, respectively. In Eq. (13.86) we have exploited the fact that $\sin^2\theta_{13} \ll \cos 2\theta_{12}$. The CP conserving values of the Majorana phases $(\alpha_{31} - \alpha_{21})$ and α_{21} determine the intervals of possible values of $|<m>|$, corresponding to the different types of neutrino mass spectrum. Using the 3σ ranges of the allowed values of the neutrino oscillation parameters from Table 13.7 and Eq. (13.76) one finds that: i) 2.3×10^{-4} eV $\lesssim |<m>| \lesssim 5.0 \times 10^{-3}$ eV in the case of NH spectrum; ii) $\sqrt{\Delta m_{23}^2} \cos 2\theta_{12} \lesssim |<m>| \lesssim \sqrt{\Delta m_{23}^2}$, or 1.3×10^{-2} eV $\lesssim |<m>| \lesssim 5.2 \times 10^{-2}$ eV in the case of IH spectrum; iii) $m_0 \cos 2\theta_{12} \lesssim |<m>| \lesssim m_0$, or 2.8×10^{-2} eV $\lesssim |<m>| \lesssim m_0$ eV, $m_0 \gtrsim 0.10$ eV, in the case of QD spectrum. The difference in the ranges of $|<m>|$ in the cases of NH, IH and QD spectrum opens up the possibility to get information about the type of neutrino mass spectrum from a measurement of $|<m>|$ [158]. The predicted $(\beta\beta)_{0\nu}$-decay effective Majorana mass $|<m>|$ as a function of the lightest neutrino mass $\min(m_j)$ is shown in Fig. 13.10.

13.8. Outlook

After the spectacular experimental progress made in the studies of neutrino oscillations, further understanding of the pattern of neutrino masses and neutrino mixing, of their origins and of the status of CP symmetry in the lepton sector requires an extensive and challenging program of research. The main goals of such a research program, outlined in the 2010 PDG edition of the Review of Particle Physics, included:

- Determining the nature - Dirac or Majorana, of massive neutrinos ν_j. This is of fundamental importance for making progress in our understanding of the origin of

neutrino masses and mixing and of the symmetries governing the lepton sector of particle interactions.

- Determination of the sign of Δm_A^2 (Δm_{31}^2) and of the type of neutrino mass spectrum.

- Determining or obtaining significant constraints on the absolute scale of neutrino masses.

- Measurement of, or improving by at least a factor of (5 - 10) the existing upper limit on, the small neutrino mixing angle θ_{13}. Together with the Dirac CP-violating phase, the angle θ_{13} determines the magnitude of CP-violation effects in neutrino oscillations.

- Determining the status of CP symmetry in the lepton sector.

- High precision measurement of Δm_{21}^2, θ_{12}, and $|\Delta m_{31}^2|$, θ_{23}.

- Understanding at a fundamental level the mechanism giving rise to neutrino masses and mixing and to L_l-non-conservation. This includes understanding the origin of the patterns of ν-mixing and ν-masses suggested by the data. Are the observed patterns of ν-mixing and of $\Delta m_{21,31}^2$ related to the existence of a new fundamental symmetry of particle interactions? Is there any relation between quark mixing and neutrino mixing, *e.g.*, does the relation $\theta_{12} + \theta_c = \pi/4$, where θ_c is the Cabibbo angle, hold? What is the physical origin of CP violation phases in the neutrino mixing matrix U? Is there any relation (correlation) between the (values of) CP violation phases and mixing angles in U? Progress in the theory of neutrino mixing might also lead to a better understanding of the mechanism of generation of baryon asymmetry of the Universe.

The successful realization of this research program, which would be a formidable task and would require many years, already began during the last two years with the results of the T2K and MINOS experiments on the value of θ_{13}, of the global analyses of the neutrino oscillation data, which showed that $\theta_{13} \neq 0$ at 3σ, and with the subsequent rather precise measurements of the value of $\sin^2 2\theta_{13}$ in the Daya Bay and RENO experiments. Averaging the results of the three recent reactor experiments with the standard PDG method, one obtains $\sin^2 2\theta_{13} = 0.098 \pm 0.013$ [142]. These results on θ_{13} have far reaching implications. The measured relatively large value of θ_{13} opens up the possibilities, in particular,

i) for searching for CP violation effects in neutrino oscillation experiments with high intensity accelerator neutrino beams, like T2K, NOνA, etc. NOνA [63], an off-axis ν_e appearance experiment using the NuMI beam, is under construction and expected to be complete in 2014. The sensitivities of T2K and NOνA on CP violation in neutrino oscillations are discussed in, *e.g.*, Ref. 162.

ii) for determining the sign of Δm_{32}^2, and thus the type of neutrino mass spectrum in the long baseline neutrino oscillation experiments at accelerators, in the experiments studying the oscillations of atmospheric neutrinos (see, *e.g.*, Ref. 82), as well as in experiments with reactor antineutrinos [161]. A value of $\sin \theta_{13} \gtrsim 0.09$ is a necessary condition for a successful "flavoured" leptogenesis with hierarchical heavy Majorana neutrinos when the CP violation required for the generation of the matter-antimatter

asymmetry of the Universe is provided entirely by the Dirac CP violating phase in the neutrino mixing matrix [155].

With the measurement of θ_{13}, the first steps on the long "road" leading to a comprehensive understanding of the patterns of neutrino masses and mixing, of their origin and implications, were made.

References:
   1. B. Pontecorvo, Zh. Eksp. Teor. Fiz. **53**, 1717 (1967) [Sov. Phys. JETP **26**, 984 (1968)].
   2. M. Fukugita and T. Yanagida, Phys. Lett. **B174**, 45 (1986); V.A. Kuzmin, V.A. Rubakov, and M.E. Shaposhnikov, Phys. Lett. **B155**, 36 (1985).
   3. P. Minkowski, Phys. Lett. **B67**, 421 (1977); see also: M. Gell-Mann, P. Ramond, and R. Slansky in *Supergravity*, p. 315, edited by F. Nieuwenhuizen and D. Friedman, North Holland, Amsterdam, 1979; T. Yanagida, *Proc. of the Workshop on Unified Theories and the Baryon Number of the Universe*, edited by O. Sawada and A. Sugamoto, KEK, Japan 1979; R.N. Mohapatra and G. Senjanović, Phys. Rev. Lett. **44**, 912 (1980).
   4. B.T. Cleveland *et al.*, Astrophys. J. **496**, 505 (1988).
   5. Y. Fukuda *et al.*, [Super-Kamiokande Collab.], Phys. Rev. Lett. **77**, 1683 (1996).
   6. J.N. Abdurashitov *et al.*, [SAGE Collab.], Phys. Rev. **C80**, 015807 (2009).
   7. P. Anselmann *et al.*, [GALLEX Collab.], Phys. Lett. **B285**, 376 (1992).
   8. W. Hampel *et al.*, [GALLEX Collab.], Phys. Lett. **B447**, 127 (1999).
   9. M. Altmann *et al.*, [GNO Collab.], Phys. Lett. **B616**, 174 (2005).
   10. S. Fukuda *et al.*, [Super-Kamiokande Collab.], Phys. Lett. **B539**, 179 (2002).
   11. Q.R. Ahmad *et al.*, [SNO Collab.], Phys. Rev. Lett. **87**, 071301 (2001).
   12. Q.R. Ahmad *et al.*, [SNO Collab.], Phys. Rev. Lett. **89**, 011301 (2002).
   13. Y. Fukuda *et al.*, [Super-Kamiokande Collab.], Phys. Rev. Lett. **81**, 1562 (1998).
   14. Y. Ashie *et al.*, [Super-Kamiokande Collab.], Phys. Rev. Lett. **93**, 101801 (2004).
   15. K. Eguchi *et al.*, [KamLAND Collab.], Phys. Rev. Lett. **90**, 021802 (2003).
   16. T. Araki *et al.*, [KamLAND Collab.], Phys. Rev. Lett. **94**, 081801 (2005).
   17. B. Pontecorvo, Zh. Eksp. Teor. Fiz. **33**, 549 (1957) and **34**, 247 (1958).
   18. Z. Maki, M. Nakagawa, and S. Sakata, Prog. Theor. Phys. **28**, 870 (1962).
   19. M.H. Ahn *et al.*, [K2K Collab.], Phys. Rev. **D74**, 072003 (2006).
   20. D.G. Michael *et al.*, [MINOS Collab.], Phys. Rev. Lett. **97**, 191801 (2006).
   21. P. Adamson *et al.*, [MINOS Collab.], Phys. Rev. Lett. **101**, 131802 (2008).
   22. L. Wolfenstein, Phys. Rev. **D17**, 2369 (1978); *Proc. of the 8th International Conference on Neutrino Physics and Astrophysics - "Neutrino'78"* (ed. E.C. Fowler, Purdue University Press, West Lafayette, 1978), p. C3.
   23. S.P. Mikheev and A.Y. Smirnov, Sov. J. Nucl. Phys. **42**, 913 (1985); Nuovo Cimento **9C**, 17 (1986).
   24. K. Abe *et al.*, [T2K Collab.], Phys. Rev. Lett. **107**, 041801 (2011).
   25. P. Adamson *et al.*, [MINOS Collab.], Phys. Rev. Lett. **107**, 181802 (2011).
   26. F.P. An *et al.*, [Daya Bay Collab.], Phys. Rev. Lett. **108**, 171803 (2012).

27. J.K. Ahn *et al.*, [RENO Collab.], Phys. Rev. Lett. **108**, 191802 (2012).

28. A. Aguilar *et al.*, [LSND Collab.], Phys. Rev. **D64**, 112007 (2001).

29. A.A. Aguilar-Arevalo *et al.*, [MiniBooNE Collab.], Phys. Rev. Lett. **105**, 181801 (2010).

30. D. Karlen in RPP2010.

31. A.A. Aguilar-Arevalo *et al.*, [MiniBooNE Collab.], Phys. Rev. Lett. **98**, 231801 (2007), and Phys. Rev. Lett. **102**, 101802 (2009).

32. J. Kopp, M. Maltoni and T. Schwetz, Phys. Rev. Lett. **107**, 091801 (2011), and references quoted therein.

33. G. Mention *et al.*, Phys. Rev. **D83**, 073006 (2011).

34. T.A. Mueller *et al.*, Phys. Rev. **C83**, 054615 (2011).

35. K. Schreckenbach *et al.*, Phys. Lett. **B160**, 325 (1985).

36. P. Huber, Phys. Rev. **C84**, 024617 (2011).

37. E. Majorana, Nuovo Cimento **5**, 171 (1937).

38. Majorana particles, in contrast to Dirac fermions, are their own antiparticles. An electrically charged particle (like the electron) cannot coincide with its antiparticle (the positron) which carries the opposite non-zero electric charge.

39. S.M. Bilenky and S.T. Petcov, Rev. Mod. Phys. **59**, 671 (1987).

40. S.M. Bilenky, J. Hosek, and S.T. Petcov, Phys. Lett. **B94**, 495 (1980).

41. J. Schechter and J.W.F. Valle, Phys. Rev. **D22**, 2227 (1980); M. Doi *et al.*, Phys. Lett. **B102**, 323 (1981).

42. L. Wolfenstein, Phys. Lett. **B107**, 77 (1981); S.M. Bilenky, N.P. Nedelcheva, and S.T. Petcov, Nucl. Phys. **B247**, 61 (1984); B. Kayser, Phys. Rev. **D30**, 1023 (1984).

43. S. Nussinov, Phys. Lett. **B63**, 201 (1976); B. Kayser, Phys. Rev. **D24**, 110 (1981); J. Rich, Phys. Rev. **D48**, 4318 (1993); H. Lipkin, Phys. Lett. **B348**, 604 (1995); W. Grimus and P. Stockinger, Phys. Rev. **D54**, 3414 (1996); L. Stodolski, Phys. Rev. **D58**, 036006 (1998); W. Grimus, P. Stockinger, and S. Mohanty, Phys. Rev. **D59**, 013011 (1999); L.B. Okun, Surv. High Energy Physics **15**, 75 (2000); J.-M. Levy, `hep-ph/0004221` and `arXiv:0901.0408`; A.D. Dolgov, Phys. Reports **370**, 333 (2002); C. Giunti, Phys. Scripta **67**, 29 (2003) and Phys. Lett. **B17**, 103 (2004); M. Beuthe, Phys. Reports **375**, 105 (2003); H. Lipkin, Phys. Lett. **B642**, 366 (2006); S.M. Bilenky, F. von Feilitzsch, and W. Potzel, J. Phys. **G34**, 987 (2007); C. Giunti and C.W. Kim, *Fundamentals of Neutrino Physics and Astrophysics* (Oxford University Press, Oxford, 2007); E.Kh. Akhmedov, J. Kopp, and M. Lindner, JHEP **0805**, 005 (2008); E.Kh. Akhmedov and A.Yu. Smirnov, Phys. Atom. Nucl. **72**, 1363 (2009).

44. For the subtleties involved in the step leading from Eq. (13.1) to Eq. (13.5) see, *e.g.*, Ref. 45.

45. A.G. Cohen, S.L. Glashow, and Z. Ligeti, Phys. Lett. **B678**, 191 (2009).

46. The neutrino masses do not exceed approximately 1 eV, $m_j \lesssim 1$, while in neutrino oscillation experiments neutrinos with energy $E \gtrsim 100$ keV are detected.

47. S.M. Bilenky and B. Pontecorvo, Phys. Reports **41**, 225 (1978).

48. In Eq. (13.9) we have neglected the possible instability of neutrinos ν_j. In most theoretical models with nonzero neutrino masses and neutrino mixing, the predicted half life-time of neutrinos with mass of 1 eV exceeds the age of the Universe, see, *e.g.*, S.T. Petcov, Yad. Fiz. **25**, 641 (1977), (E) *ibid.*, **25** (1977) 1336 [Sov. J. Nucl. Phys. **25**, 340 (1977), (E) *ibid.*, **25**, (1977), 698], and Phys. Lett. **B115**, 401 (1982); W. Marciano and A.I. Sanda, Phys. Lett. **B67**, 303 (1977); P. Pal and L. Wolfenstein, Phys. Rev. **D25**, 766 (1982).

49. L.B. Okun (2000), J.-M. Levy (2000) and H. Lipkin (2006) quoted in Ref. 43 and Ref. 45.

50. The articles by L. Stodolsky (1998) and H. Lipkin (1995) quoted in Ref. 43.

51. V. Gribov and B. Pontecorvo, Phys. Lett. **B28**, 493 (1969).

52. N. Cabibbo, Phys. Lett. **B72**, 333 (1978).

53. V. Barger *et al.*, Phys. Rev. Lett. **45**, 2084 (1980).

54. P. Langacker *et al.*, Nucl. Phys. **B282**, 589 (1987).

55. P.I. Krastev and S.T. Petcov, Phys. Lett. **B205**, 84 (1988).

56. C. Jarlskog, Z. Phys. **C29**, 491 (1985).

57. A. De Rujula *et al.*, Nucl. Phys. **B168**, 54 (1980).

58. M. Apollonio *et al.*, [Chooze Collab.], Phys. Lett. **B466**, 415 (1999); Eur. Phys. J. **C27**, 331 (2003).

59. Y. Abe *et al.*, [Double Chooz Collab.], Phys. Rev. Lett. **108**, 131801 (2012).

60. N. Agafonova *et al.*, [OPERA Collab.], Phys. Lett. **B691**, 138 (2010).

61. N. Agafonova *et al.*, [OPERA Collab.], `arXiv:1107.2594`.

62. S. Goswami *et al.*, Nucl. Phys. (Proc. Supp.) **B143**, 121 (2005).

63. D.S. Ayres *et al.* [NOνA Collab.], `hep-ex/0503053`.

64. These processes are important, however, for the supernova neutrinos see, *e.g.*, G. Raffelt, *Proc. International School of Physics "Enrico Fermi", CLII Course "Neutrino Physics"*, 23 July-2 August 2002, Varenna, Italy [`hep-ph/0208024`]), and articles quoted therein.

65. We standardly assume that the weak interaction of the flavour neutrinos ν_l and antineutrinos $\bar{\nu}_l$ is described by the Standard Model (for alternatives see, *e.g.*, Ref. 22; M.M. Guzzo *et al.*, Phys. Lett. **B260**, 154 (1991); E. Roulet, Phys. Rev. **D44**, R935 (1991) and Ref. 66).

66. R. Mohapatra *et al.*, Rept. on Prog. in Phys. **70**, 1757 (2007); A. Bandyopadhyay *et al.*, Rept. on Prog. in Phys. **72**, 106201 (2009).

67. V. Barger *et al.*, Phys. Rev. **D22**, 2718 (1980).

68. P. Langacker, J.P. Leveille, and J. Sheiman, Phys. Rev. **D27**, 1228 (1983).

69. The difference between the ν_μ and ν_τ indices of refraction arises at one-loop level and can be relevant for the $\nu_\mu - \nu_\tau$ oscillations in very dense media, like the core of supernovae, *etc.*; see F.J. Botella, C.S. Lim, and W.J. Marciano, Phys. Rev. **D35**, 896 (1987).

70. The relevant formulae for the oscillations between the ν_e and a sterile neutrino ν_s, $\nu_e \leftrightarrow \nu_s$, can be obtained from those derived for the case of $\nu_e \leftrightarrow \nu_{\mu(\tau)}$ oscillations by Refs. [54,68] replacing N_e with $(N_e - 1/2N_n)$, N_n being the neutron number density in matter.

71. T.K. Kuo and J. Pantaleone, Phys. Lett. **B198**, 406 (1987).
72. A.D. Dziewonski and D.L. Anderson, Physics of the Earth and Planetary Interiors **25**, 297 (1981).
73. The first studies of the effects of Earth matter on the oscillations of neutrinos were performed numerically in Refs. [67,74] and in E.D. Carlson, Phys. Rev. **D34**, 1454 (1986); A. Dar *et al.*, *ibid.*, **D35**, 3607 (1988); in Ref. 55 and in G. Auriemma *et al.*, *ibid.*, **D37**, 665 (1988).
74. A.Yu. Smirnov and S.P. Mikheev, *Proc. of the VIth Moriond Workshop* (eds. O. Fackler, J. Tran Thanh Van, Frontières, Gif-sur-Yvette, 1986), p. 355.
75. S.T. Petcov, Phys. Lett. **B434**, 321 (1998), (E) *ibid.* **B444**, 584 (1998); see also: Nucl. Phys. (Proc. Supp.) **B77**, 93 (1999) and `hep-ph/9811205`.
76. M.V. Chizhov, M. Maris, and S.T. Petcov, `hep-ph/9810501`.
77. E.Kh. Akhmedov *et al.*, Nucl. Phys. **B542**, 3 (1999).
78. S.T. Petcov, Phys. Lett. **B214**, 259 (1988).
79. J. Hosaka *et al.*, [Super-Kamiokande Collab.], Phys. Rev. **D74**, 032002 (2006).
80. E.Kh. Akhmedov, Nucl. Phys. **B538**, 25 (1999).
81. M.V. Chizhov and S.T. Petcov, Phys. Rev. Lett. **83**, 1096 (1999) and Phys. Rev. Lett. **85**, 3979 (2000); Phys. Rev. **D63**, 073003 (2001).
82. J. Bernabéu, S. Palomares-Ruiz, and S.T. Petcov, Nucl. Phys. **B669**, 255 (2003); S.T. Petcov and T. Schwetz, Nucl. Phys. **B740**, 1 (2006); R. Gandhi *et al.*, Phys. Rev. **D76**, 073012 (2007); E.Kh. Akhmedov, M. Maltoni, and A.Yu. Smirnov, JHEP **0705**, 077 (2007).
83. The mantle-core enhancement maxima, *e.g.*, in $P_m^{2\nu}(\nu_\mu \to \nu_\mu)$, appeared in some of the early numerical calculations, but with incorrect interpretation (see, *e.g.*, the articles quoted in Ref. 73).
84. M. Freund, Phys. Rev. **D64**, 053003 (2001).
85. M.C. Gonzalez-Garcia and Y. Nir, Rev. Mod. Phys. **75**, 345 (2003); S.M. Bilenky, W. Grimus, and C. Giunti, Prog. in Part. Nucl. Phys. **43**, 1 (1999).
86. J.N. Bahcall, *Neutrino Astrophysics*, Cambridge University Press, Cambridge, 1989; J.N. Bahcall and M. Pinsonneault, Phys. Rev. Lett. **92**, 121301 (2004).
87. J.N. Bahcall, A.M. Serenelli, and S. Basu, Astrophys. J. Supp. **165**, 400 (2006).
88. A. Messiah, *Proc. of the VIth Moriond Workshop* (eds. O. Fackler, J. Tran Thanh Van, Frontières, Gif-sur-Yvette, 1986), p. 373.
89. S.J. Parke, Phys. Rev. Lett. **57**, 1275 (1986).
90. S.T. Petcov, Phys. Lett. **B200**, 373 (1988).
91. P.I. Krastev and S.T. Petcov, Phys. Lett. **B207**, 64 (1988); M. Bruggen, W.C. Haxton, and Y.-Z. Quian, Phys. Rev. **D51**, 4028 (1995).
92. T. Kaneko, Prog. Theor. Phys. **78**, 532 (1987); S. Toshev, Phys. Lett. **B196**, 170 (1987); M. Ito, T. Kaneko, and M. Nakagawa, Prog. Theor. Phys. **79**, 13 (1988), (E) *ibid.*, **79**, 555 (1988).
93. S.T. Petcov, Phys. Lett. **B406**, 355 (1997).
94. C. Cohen-Tannoudji, B. Diu, and F. Laloe, *Quantum Mechanics*, Vol. 1 (Hermann, Paris, and John Wiley & Sons, New York, 1977).

95. S.T. Petcov, Phys. Lett. **B214**, 139 (1988); E. Lisi *et al.*, Phys. Rev. **D63**, 093002 (2000); A. Friedland, Phys. Rev. **D64**, 013008 (2001).

96. S.T. Petcov and J. Rich, Phys. Lett. **B224**, 401 (1989).

97. An expression for the "jump" probability P' for N_e varying linearly along the neutrino path was derived in W.C. Haxton, Phys. Rev. Lett. **57**, 1271 (1986) and in Ref. 89 on the basis of the old Landau-Zener result: L.D. Landau, Phys. Z. USSR **1**, 426 (1932), C. Zener, Proc. R. Soc. A **137**, 696 (1932). An analytic description of the solar ν_e transitions based on the Landau-Zener jump probability was proposed in Ref. 89 and in W.C. Haxton, Phys. Rev. **D35**, 2352 (1987). The precision limitations of this description, which is less accurate than that based on the exponential density approximation, were discussed in S.T. Petcov, Phys. Lett. **B191**, 299 (1987) and in Ref. 91.

98. A. de Gouvea, A. Friedland, and H. Murayama, JHEP **0103**, 009 (2001).

99. C.-S. Lim, Report BNL 52079, 1987; S.P. Mikheev and A.Y. Smirnov, Phys. Lett. **B200**, 560 (1988).

100. G.L. Fogli *et al.*, Phys. Lett. **B583**, 149 (2004).

101. J.N. Bahcall, A.M. Serenelli, and S. Basu, Astrophys. J. **621**, L85 (2005).

102. C. Peña-Garay and A.M. Serenelli, `arXiv:0811.2424`.

103. L.C. Stonehill, J.A. Formaggio, and R.G.H. Robertson, Phys. Rev. **C69**, 015801 (2004).

104. A.M. Serenelli, W.C. Haxton, and C. Peña-Garay, Astrophys. J. **743**, 24 (2011).

105. B. Pontecorvo, Chalk River Lab. report PD-205, 1946.

106. D. Davis, Jr., D.S. Harmer, and K.C. Hoffman, Phys. Rev. Lett. **20**, 1205 (1968).

107. F. Kaether *et al.*, Phys. Lett. **B685**, 47 (2010). These authors reanalyzed a complete set of the GALLEX data with a method providing a better background reduction than that adopted in Ref. 8.

108. A.I. Abazov *et al.*, [SAGE Collab.], Phys. Rev. Lett. **67**, 3332 (1991).

109. J.N. Abdurashitov *et al.*, [SAGE Collab.], Phys. Lett. **B328**, 234 (1994).

110. K.S. Hirata *et al.*, [Kamiokande Collab.], Phys. Rev. Lett. **63**, 16 (1989).

111. Y. Fukuda *et al.*, [Super-Kamiokande Collab.], Phys. Rev. Lett. **81**, 1158 (1998).

112. J. Hosaka *et al.*, [Super-Kamiokande Collab.], Phys. Rev. **D73**, 112001 (2006).

113. J.P. Cravens *et al.*, [Super-Kamiokande Collab.], Phys. Rev. **D78**, 032002 (2008).

114. K. Abe *et al.*, [Super-Kamiokande Collab.], Phys. Rev. **D83**, 052010 (2011).

115. B. Aharmim *et al.*, [SNO Collab.], Phys. Rev. **C72**, 055502 (2005).

116. B. Aharmim *et al.*, [SNO Collab.], Phys. Rev. Lett. **101**, 111301 (2008).

117. B. Aharmim *et al.*, [SNO Collab.], Phys. Rev. **C81**, 055504 (2010).

118. B. Aharmim *et al.*, [SNO Collab.], `arXiv:1109.0763`.

119. C. Arpesella *et al.*, [Borexino Collab.], Phys. Lett. **B658**, 101 (2008); Phys. Rev. Lett. **101**, 091302 (2008).

120. G. Bellini *et al.*, [Borexino Collab.], Phys. Rev. Lett. **107**, 141302 (2011).

121. G. Bellini *et al.*, [Borexino Collab.], Phys. Lett. **B707**, 22 (2012).

122. G. Bellini *et al.*, [Borexino Collab.], Phys. Rev. Lett. **108**, 051302 (2012).

123. G. Bellini *et al.*, [Borexino Collab.], Phys. Rev. **D82**, 033006 (2010).

124. Y. Fukuda *et al.*, [Super-Kamiokande Collab.], Phys. Rev. Lett. **86**, 5651 (2001).

125. Y. Fukuda *et al.*, [Super-Kamiokande Collab.], Phys. Lett. **B539**, 179 (2002).
126. G. L. Fogli *et al.*, Phys. Rev. **D67**, 073002 (2003); M. Maltoni, T. Schwetz, and J.W. Valle, Phys. Rev. **D67**, 093003 (2003); A. Bandyopadhyay *et al.*, Phys. Lett. **B559**, 121 (2003); J.N. Bahcall, M.C. Gonzalez-Garcia, and C. Peña-Garay, JHEP **0302**, 009 (2003); P.C. de Holanda and A.Y. Smirnov, JCAP **0302**, 001 (2003).
127. S. Abe *et al.*, [KamLAND Collab.], Phys. Rev. Lett. **100**, 221803 (2008).
128. A. Gando *et al.*, [KamLAND Collab.], Phys. Rev. **D83**, 052002 (2011).
129. Y. Ashie *et al.*, [Super-Kamiokande Collab.], Phys. Rev. **D71**, 112005 (2005).
130. P. Adamson *et al.*, [MINOS Collab.], Phys. Rev. Lett. **106**, 181801 (2011).
131. K. Abe *et al.*, [Super-Kamiokande Collab.], Phys. Rev. Lett. **97**, 171801 (2006).
132. V. Barger *et al.*, Phys. Rev. Lett. **82**, 2640 (1999).
133. E. Lisi *et al.*, Phys. Rev. Lett. **85**, 1166 (2000).
134. P. Adamson *et al.*, [MINOS Collab.], Phys. Rev. Lett. **107**, 021801 (2011).
135. P. Adamson *et al.*, [MINOS Collab.], Phys. Rev. Lett. **108**, 191801 (2012).
136. S. Yamamoto *et al.*, [K2K Collab.], Phys. Rev. Lett. **96**, 181801 (2006).
137. P. Adamson *et al.*, [MINOS Collab.], Phys. Rev. **D82**, 051102 (2010).
138. Y. Declais *et al.*, Phys. Lett. **B338**, 383 (1994).
139. R. Wendell *et al.*, [Super-Kamiokande Collab.], Phys. Rev. **D81**, 092004 (2010).
140. G.L. Fogli *et al.*, Phys. Rev. **D84**, 053007 (2011).
141. T. Schwetz, M Tórtola, and J.W.F. Valle, New J. Phys. **13**, 109401 (2011).
142. Neutrino Mixing section in the Lepton Particle Listings, RPP2012.
143. In the convention we use, the neutrino masses are not ordered in magnitude according to their index number: $\Delta m_{31}^2 < 0$ corresponds to $m_3 < m_1 < m_2$. We can also number the massive neutrinos in such a way that one always has $m_1 < m_2 < m_3$, see, *e.g.*, Ref. 144.
144. S.M. Bilenky, S. Pascoli, and S.T. Petcov, Phys. Rev. **D64**, 053010 (2001), and *ibid.*, 113003.
145. P.A.N. Machado *et al.*, JHEP **1205**, 023 (2012).
146. F. Perrin, Comptes Rendus **197**, 868 (1933); E. Fermi, Nuovo Cim. **11**, 1 (1934).
147. V.N. Aseev *et al.*, Phys. Rev. **D84**, 112003 (2011).
148. V. Lobashev *et al.*, Nucl. Phys. **A719**, 153c, (2003).
149. K. Eitel *et al.*, Nucl. Phys. (Proc. Supp.) **B143**, 197 (2005).
150. O. Lahav and A.R. Liddle in RPP2010.
151. K.N. Abazajian *et al.*, Astopart. Phys. **35**, 177 (2011).
152. For alternative mechanisms of neutrino mass generation see, *e.g.*, the first article in Ref. 66 and references quoted therein.
153. S. Davidson and A. Ibarra, Phys. Lett. **B535**, 25 (2002).
154. A. Abada *et al.*, JCAP **0604**, 004 (2006); E. Nardi *et al.*, JHEP **0601**, 164 (2006).
155. S. Pascoli, S.T. Petcov, and A. Riotto, Phys. Rev. **D75**, 083511 (2007) and Nucl. Phys. **B774**, 1 (2007); E. Molinaro and S.T. Petcov, Phys. Lett. **B671**, 60 (2009).
156. S.T. Petcov, Phys. Lett. **B110**, 245 (1982); R. Barbieri *et al.*, JHEP **9812**, 017 (1998); P.H. Frampton, S.T. Petcov, and W. Rodejohann, Nucl. Phys. **B687**, 31 (2004).

157. A. Morales and J. Morales, Nucl. Phys. (Proc. Supp.) **B114**, 141 (2003); C. Aalseth *et al.*, `hep-ph/0412300`; S.R. Elliott and P. Vogel, Ann. Rev. Nucl. Part. Sci. **52**, 115 (2002).

158. S. Pascoli and S.T. Petcov, Phys. Lett. **B544**, 239 (2002); see also: S. Pascoli, S.T. Petcov, and L. Wolfenstein, Phys. Lett. **B524**, 319 (2002).

159. S.M. Bilenky *et al.*, Phys. Rev. **D54**, 4432 (1996).

160. S.M. Bilenky *et al.*, Phys. Lett. **B465**, 193 (1999); F. Vissani, JHEP **9906**, 022 (1999); K. Matsuda *et al.*, Phys. Rev. **D62**, 093001 (2000); K. Czakon *et al.*, `hep-ph/0003161`; H.V. Klapdor-Kleingrothaus, H. Päs and A.Yu. Smirnov, Phys. Rev. **D63**, 073005 (2001); S. Pascoli, S.T. Petcov and W. Rodejohann, Phys. Lett. **B549**, 177 (2002), and *ibid.* **B558**, 141 (2003); H. Murayama and Peña-Garay, Phys. Rev. **D69**, 031301 (2004); S. Pascoli, S.T. Petcov, and T. Schwetz, Nucl. Phys. **B734**, 24 (2006); M. Lindner, A. Merle, and W. Rodejohann, Phys. Rev. **D73**, 053005 (2006); A. Faessler *et al.*, Phys. Rev. **D79**, 053001 (2009); S. Pascoli and S.T. Petcov, Phys. Rev. **D77**, 113003 (2008); W. Rodejohann, Int. J. Mod. Phys. E **20**, 1833 (2011).

161. S.T. Petcov and M. Piai, Phys. Lett. **B533**, 94 (2002); S. Choubey, S.T. Petcov and M. Piai, Phys. Rev. **D68**, 113006 (2003); J. Learned *et al.*, Phys. Rev. **D78**, 071302 (2008); L. Zhan *et al.*, Phys. Rev. **D78**, 111103 (2008) and Phys. Rev. **D79**, 073007 (2009); P. Ghoshal and S.T. Petcov, JHEP **1103**, 058 (2011).

162. J. Bernabeu *et al.*, `arXiv:1005.3146`.